XYLENE TRANSFORMATION OVER Y ZEOLITE IN A FLUIDIZED-BED REACTOR

BY

AbdulJelil Iliyas

A Thesis Presented to the

DEANSHIP OF GRADUATE STUDIES

KING FAHD UNIVERSITY OF PETROLEUM & MINERALS

DHAHRAN, SAUDI ARABIA

In Partial Fulfillment of the
Requirements for the Degree of

MASTER OF SCIENCE

In

CHEMICAL ENGINEERING

May, 2004

KING FAHD UNIVERSITY OF PETROLEUM & MINERALS

DHAHRAN 31261, SAUDI ARABIA

DEANSHIP OF GRADUATE STUDIES

This thesis, written by AbdulJelil Iliyas under the direction of his thesis advisor and approved by his thesis committee, has been presented to and accepted by the Dean of Graduate Studies, in partial fulfillment of the requirement for the degree of MASTER OF SCIENCE IN CHEMICAL ENGINEERING.

Thesis Committee

Dr. Sulaiman Al-Khattaf
(Thesis Advisor)

Dr. Adnan Al-Amer
(Co-Advisor)

Dr. Kevin Loughlin
(Member)

Dr. Nadhir Al-Baghli
(Member)

Dr. Raafat Alnaizy
(Member)

Prof. Mohamed B. Amin
(Department Chairman)

Prof. Osama Ahmed Jannadi
(Dean of Graduate Studies)

7-6-2004
Date

Dedicated to

My Loving Parents

ACKNOWLEDGMENTS

In the Name of Allah the Most Gracious and the Most Merciful

I am grateful to Almighty Allah for given me the opportunity to pursue my M.S degree and the capability to complete this work successfully.

With deep sense of gratitude and appreciations, I would like to thank my thesis advisor, Dr. Sulaiman Al-Khattaf, for his guidance and encouragement. Indeed, his great enthusiasm and innovative thinking were great inspiration for me, which helped me to complete this thesis within a short period of time.

I also appreciate the cooperation and valuable advice rendered to me by my co-advisor, Dr. Adnan Al-Amer. Similarly, the great help and guidance offered by my committee members; Dr. Nadhir Al-Baghli, Dr. Kevin Loughlin, and Dr. Raafat Alnaizy, is deeply appreciated.

I am indebted to Prof. Tomoyuki Inui for his conscientious effort in reviewing some of the papers written from this work. I am specially thankful to Mr. Mariano Gica of Catalysis Research Laboratory for his helpful collaboration regarding the experimental work. I also wish to express my thanks to Mr. Romeo for his technical advice on the riser simulator.

I greatly acknowledged the assistance extended to me by Mr. Musaed Al-Ghamdi, Mr. Kurshid Alam, and Mr. Abdulrasheed of Research Institute, KFUPM on the characterization of the catalysts used for this work. I also wish to thank Mr. Abbas Al-

Ghamdi of Catalysis Research Department of ARAMCO for measuring coke and BET surface area of the catalysts.

The financial support provided by King Fahd University of Petroleum & Minerals under the Project 255 is highly appreciated. Also, I would like to acknowledge all faculty, staff members, and colleagues at Chemical Engineering Department, KFUPM for their cooperation and support throughout the period of my M.S program.

Finally and with deep sense of affection, I offer my sincere thanks to my wife for typing part of this thesis, and for her encouragement, support, and prayers.

TABLE OF CONTENTS

LIST OF TABLES

LIST OF FIGURES

THESIS ABSTRACT

NAME: ABDUL JELIL ILIYAS

TITLE OF STUDY: XYLENE TRANSFORMATION OVER Y-ZEOLITE IN A FLUIDIZED-BED REACTOR

MAJOR FIELD: CHEMICAL ENGINEERING

DATE OF DEGREE: MAY, 2004

The kinetics of vapor-phase transformation of xylenes is investigated over a USY zeolite catalyst using a fluidized-bed reactor. The reaction rate constants and activation energies are estimated from simplified kinetic models based on the isomerization of the pure xylene isomers. The proposed model is tested with Time-On-Stream (TOS) and Reactant Converted (RC) decay models. The results obtained from both models indicate that the mutual interconversion of p- and o-xylenes is quite difficult as compared to intramolecular 1, 2-methyl shifts.

A systematic study on the influence of reaction conditions (temperature, time, and reactant type) on the selectivity of xylene transformation is also carried out over USY zeolite. Initial product selectivity revealed that both isomerization and disproportionation of xylenes are primary reactions. Higher conversion is observed with p-xylene reactant as compared to m- and o-xylene.

m-Xylene transformation is further studied on as-prepared H-Y and a series of dealuminated Y zeolite catalysts. The moderately dealuminated Y zeolite catalyst at 710°C for 3 h showed relatively high activity as compared to the other catalysts. Paring

reaction is proposed as an alternative reaction pathway, in addition to the well-known isomerization and disproportionation pathways. A higher coke deposition is found for the transformation of m-xylene over the parent H-Y as compared to the highly dealuminated USY zeolite. The formation of benzene and C_2 - C_4 gases are found to be proportional to the zeolite acid concentration.

خلاصة البحث

الإسـم : عبدالجليل الياس
العنـوان : تفاعلات مركبات الزايلين على زيولايت Y بواسطة المفاعل المتطاير
الـدرجة : الماجستير
التخصص: هندسة كيميائية
التاريـخ : ربيع الآخر 1425هـ

يقوم البحث الحالي على دراسة هندسة تحويل مركبات الزايلين باستخدام مادة الزيولايت نوع Y الحفازه وذلك بواسطة المفاعل المتطاير، وتم استنباط ثوابت التفاعل وطاقات التفاعل المحركة من نمذجة بسيطة لتفاعلات الزايلين كلاً على حدى، وتم اختبار النموذج المقترح بواسطة نموذجين مختلفين وهما (TOS) و (RC)، وقد تبين من نتائج هذين النموذجين أن تحويل بارازايلين إلى أرثوزايلين والعكس من الصعوبة بمكان مقارنة بنقل مجموعة (CH_3) من مكان 1 إلى مكان 2 المجاور.

وقد تم إعداد دراسة كاملة على تأثير الحرارة زمن التفاعل ونوع المركب على تفاعلات الزايلين في نفس ظروف التفاعل والحفازات، وبالنظر إلى المركبات الناتجة من هذه التفاعلات فقد تبين أن كلى isomerization و disproportionation هي تفاعلات أوليه وأن البارازيلين قد تبين أنه أكثر مركبات الزايلين تفاعلية.

وتم إعداد دراسة أخرى لمركب ميتازايلين على عدة أنواع من زيولايت Y ، وتبين أن عينة الزيولايت التي تم انتزاع قسم بسيط من مادة الالومينا بواسطة بخار الماء عند $710\ C^o$ لمدة 3 ساعات تمتلك أكثر فاعلية لتحويل هذا المركب إلى مركبات أخرى مقارنة بالعينات الأخرى.

وتتميز هذه الدراسة بتقديم ما يسمى "تفاعل بيرنغ" بالإضافة إلى التفاعلين الشهيرين isomerization و disproportionation ، واثبتت التجارب المعملية أن المادة الحفازه من نوع زيولايت Y الغير منزوعة الالومينا لديها قدره كبيرة على إنتاج مادة الفحم والبنزين والغازات مقارنة بالعينات الأخرى وذلك لامتلاك هذه المادة الحفازه إلى حامضيه أعلى من العينات الأخرى.

درجة الماجستير في العلوم
جامعة الملك فهد للبترول والمعادن
ربيع الآخر 1425هـ

CHAPTER 1

1 Introduction

1.1 Background

Xylenes are the second most important aromatic product in terms of world consumption for chemical manufacture, ranking behind benzene and ahead of toluene. The three isomers; o-, m-, and p-xylene represent the major uses of isolated mixed xylenes, and account for most of the consumption. Most of the separated isomers are oxidized to their corresponding dibasic aromatic acid or anhydride (phthalic anhydride, isophthalic acid and terephthalic acid). These are largely used in the manufacture of polymeric materials [1].

The production value of mixed xylenes worldwide in 1999 is estimated to have been just under $5 billion. The largest producing regions based on capacity are Asia (47%) and North America (29%). By 2004, Asia's capacity share is expected to increase to 52%. The Middle East is adding capacity to produce aromatics from liquefied petroleum gas and to isolate the isomers and participate more fully in this segment of the petrochemical business. The kingdom of Saudi Arabia is becoming a producer of these important chemicals in the world. In the year 2000, the Arabian Industrial Fibers Co., an affiliate of Saudi Basic Industries Corporation (SABIC) produced around 330,000 ton/year p-xylene, and 45,000 ton/year o-xylene using the cyclar process from liquidified petroleum gas feedstock [2].

World consumption of mixed xylenes was about 24 million metric tons in 1999, and is expected to grow at a rate of 6.2% to 32.5 million metric tons in 2004. Consumption of o-xylene was 2.7 million metric tons, and is expected to grow at a rate of 4.8% to 2004. Consumption of p-xylene was 15 million metric tons in 1 999 and will grow at a rate of about 5.9% to 2004 [1].

Xylenes are mainly obtained from catalytic reforming and cracking units in the refinery with other C_6, C_7, and C_8 aromatics. Among the three xylene isomers, p-xylene is the most important. The production rate and the market demand for the three xylene isomers are shown in Figure 1.1. It is shown in this figure that m-xylene has the highest production rate, although it is the least demanded isomer. Furthermore, the equilibrium mixture obtained from catalytic reformers has a higher ratio of the meta isomer. Table 1.1 shows the thermodynamic composition of the C_8 aromatics at three temperatures [3]. Since the amount of p-xylene obtained directly from the reaction mixtures cannot meet market requirement, the surplus m-xylene and o-xylene are further isomerized to p-xylene to balance the market demand [4].

The transformation of m-xylene to p- and o-xylene has gain an important position in the petrochemical industry. This is because it is one of the processes in which the introduction of zeolites as catalysts has represented a clear technological improvement. Practically the largest petrochemical application of zeolites is in the ZSM-5-catalyzed xylene transformation processes [5]. Moreover, since after the commercialization of this process, the demand for p-xylene continues to grow, and drive the search for improved xylene isomerization processes.

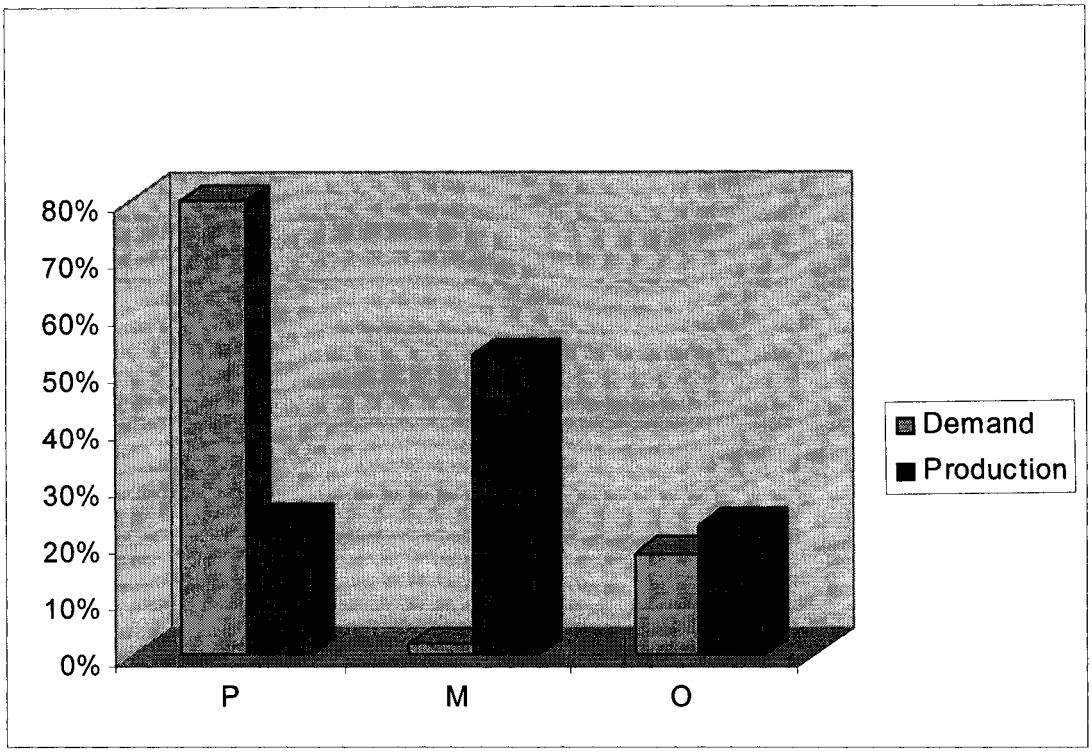

Figure 1.1 Worldwide production rate and demand of xylenes

Table 1.1 Thermodynamic equilibrium compositions of C_8 aromatics

	Composition		
Aromatic wt %	200°C	300 °C	500 °C
p-Xylene	21.8	21.1	18.9
o-Xylene	20.6	21.6	23.0
m-Xylene	53.5	51.1	47.1
Ethylbenzene	4.1	6.2	11.0

Besides its technological interest, the transformation of m-xylene has been abundantly described in the literature because it provides information on the geometry of the zeolite channels, and also because it is considered as an appropriate reaction to give information on the acidic properties of solids [6].

1.2 Structure and Properties of Xylenes

Xylenes are dimethylbenzenes homologues with the molecular formula C_8H_{10}, which differ in the positions of the two-methyl groups on the benzene ring. The structure of each of the xylene isomers are shown in Figure 1.2

Because of their similar structure, the three xylenes exhibit similar properties. The distillation characteristics of the C_8 aromatic compounds are of considerable importance. o-Xylene is more readily separated from m-xylene because of a 5°C difference in boiling point. The difference in freezing point between p-xylene and the other C_8 aromatic compounds is utilized for p-xylene separation. The properties of the xylenes and ethylbenzene are summarized in Table 1.2 [7].

The free energies of formation of the various isomers are such that m-xylene is most abundant isomer in the equilibrium mixture. Although, the xylene isomers have identical molecular weights, but they still differ somewhat in their polarity, since the bond between the methyl group and the aromatic ring is polar. With p-xylene, the two dipolar bonds oppose each other and the net dipole moment is zero. However, in o-xylene the dipolar bonds are aligned in nearly the same direction and the net dipole moment is greatest [7].

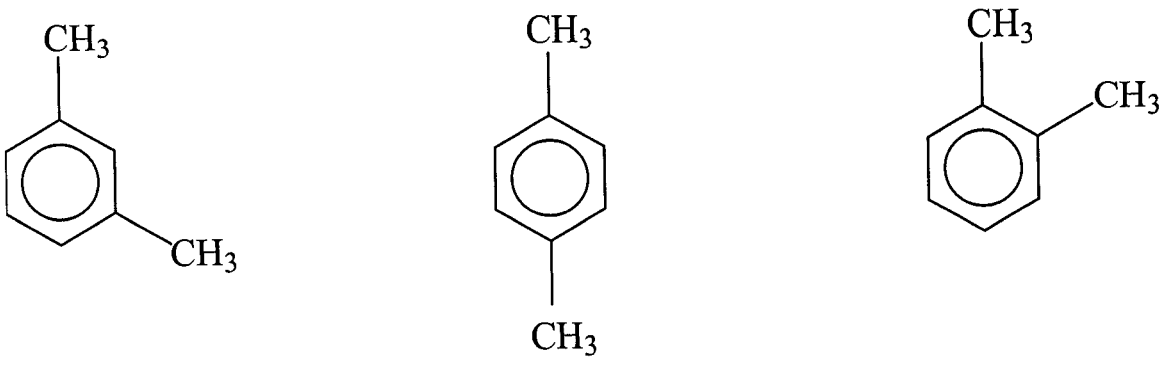

m-xylene p-xylene o-xylene

Figure 1.2 Structure of the three xylene isomers

Table 1.2 Properties of xylenes and ethylbenzene

	o-Xylene	m-Xylene	p-Xylene	Ethylbenzene
Amount in equilibrium at 1000K	23	43	19	15
Boiling point, K	417.3	412.6	411.8	409.6
Freezing point, K	248.1	225.4	286.6	178.4
Change in boiling point with change in pressure, 10^{-40} K/Pa	3.73	3.68	3.69	3.68
Dipole moment, 10^{-28} C/molecule	2.1	1.2	0	-
Polarizability, 10^{-31} m^3	141	141.8	142	-
Dielectric constant	2.26	2.24	2.23	2.24
Surface tension at 293 K, mJ/m^2	30.03	28.63	28.31	29.04
Molecular weight	106.16	106.16	106.16	106.16
Density at 293 K, mg/m^3	0.8802	0.8642	0.8610	0.8670
Density at critical point, mg/m^3	0.28	0.27	0.29	0.29
Latent heat of vaporization at boiling point, kJ/kg	347	343	340	339

1.3 Chemistry of Xylene Transformation

Xylenes undergo two major reactions over acid catalysts; isomerization (Reaction 1) and disproportionation (Reaction 2) as shown in Figure 1.3. Isomerization is a mono-molecular reaction involving the transformation of benzenium ions intermediates through the shift of methyl group along the aromatic ring. Depending on the xylene used as reactant, isomerization may proceed via sequence reaction scheme involving 1, 2 methyl shifts, or as will be shown in this work, via apparent direct interconversion between p- and o-xylene depicted Figure 1.4. The other two xylene isomers are the primary products of isomerization reaction. In addition, isomerization reaction is known to require only one acid site for its catalysis.

On the other hand, disproportionation of xylenes produces toluene and trimethyl-benzene isomers in a more complex reaction mechanism. Unlike isomerization, disproportionation is a bimolecular reaction involving two molecules of xylenes aligned to each other on pairs of adjacent acid sites. As a result, at least two acid sites are necessary for catalyzing disproportionation reaction. Moreover, both the isomerization and disproportionation reactions have been reported to be catalyzed by Brönsted acid sites. Apart from these two, other reactions, such as dealkylation, transalkylation, ring cracking, and paring reactions have been reported during xylene transformation over acid catalyst. However, the theory of these reactions is somewhat less understood, in comparison to isomerization and disproportionation reactions. As a result, only a few research works can be found devoting attention to these other reaction pathways.

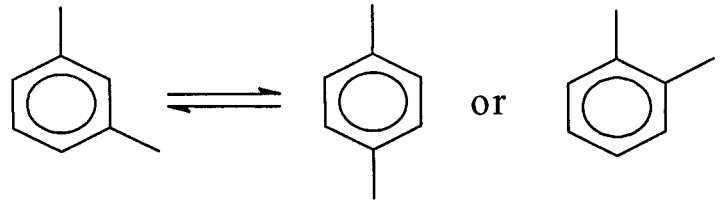

Reaction 1: Isomerization (I)

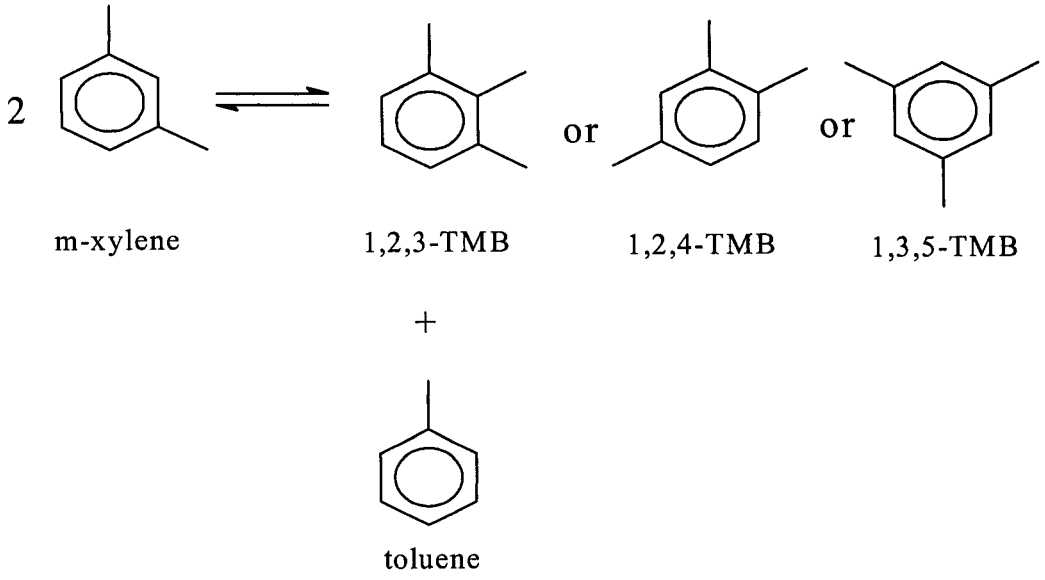

Reaction 2: Disproportionation (D)

Figure 1.3 Isomerization and disproportionation reactions of xylenes

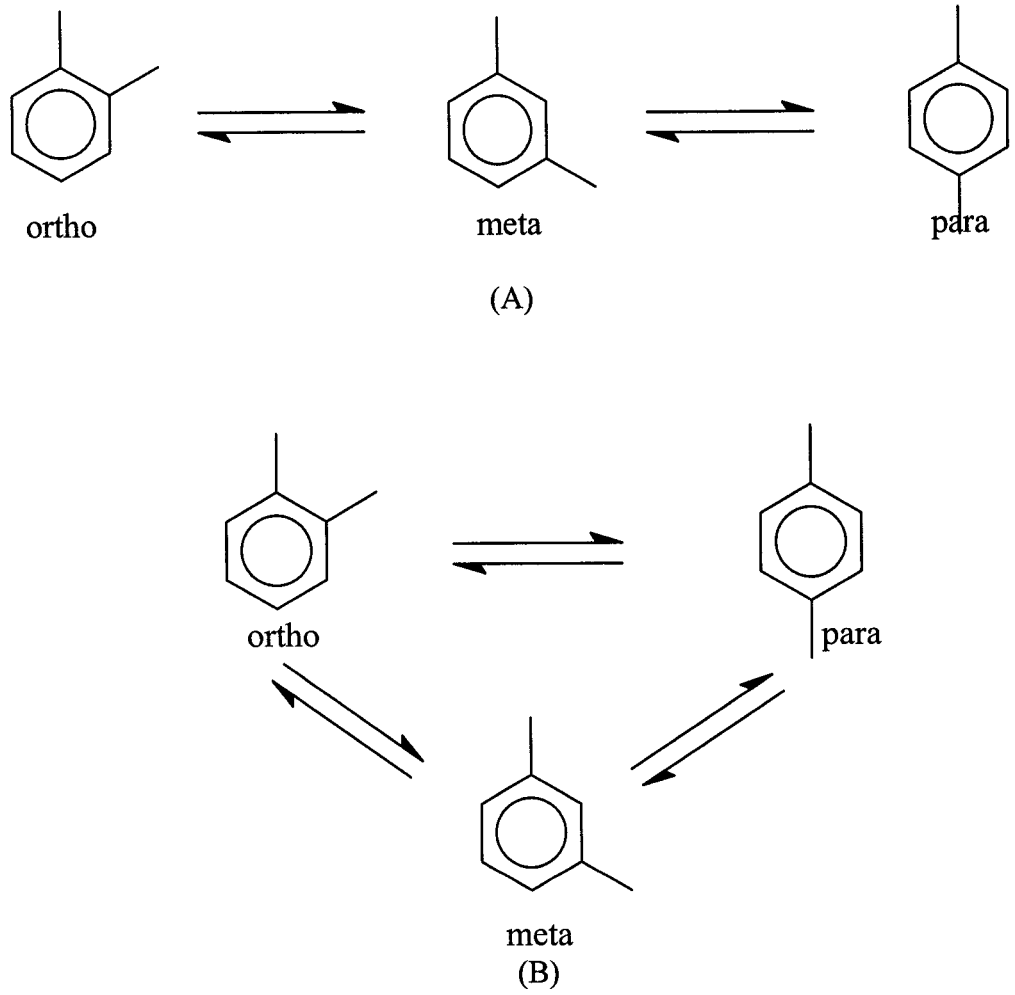

Figure 1.4 Reactions schemes of xylene isomerization. (A) Sequence reaction scheme (B) Triangular reaction scheme

1.4 Structure of Zeolites

1.4.1 General

Zeolites are a group of hydrated aluminosilicates of the alkali or alkaline earth metals (principally sodium, potassium, magnesium and calcium). They have three-dimensional crystalline frameworks of tetrahedral silica or alumina anions strongly bonded at all corners. The zeolite structure contain (-Si-O-Al-) linkages that form surface pores of uniform diameter and enclose regular internal cavities with channels of discrete sizes and shapes, depending on the chemical composition and crystal structure of the specific zeolite involved. The enclosed cavities contain both the metal cations and water molecules. The cations are loosely bound to the lattice, and thus engage in ion exchange. The water molecules can also be reversibly driven off in most zeolites [8].

The fundamental building block of all zeolites is a tetrahedron of four oxygen anions surrounding a small silicon or aluminium ion. These tetrahedral are arranged so that each of the four oxygen ion is shared in turn with another silica or aluminium tetrahedron (Figure 1.5). The silica and alumina tetrahedral are combined into more complicated secondary building units (SBUs) as shown in Figure 1.6. The SBUs join to form structurally and chemically important zeolite channels known as oxygen windows that pass through the zeolite. It is the pore system in the zeolites that gives rise to their interesting properties. The pores can pass through the zeolite in 1, 2 or 3 directions, vary in size and in the case of ZSM-5 (Figure 1.6), can also be sinusoidal [8].

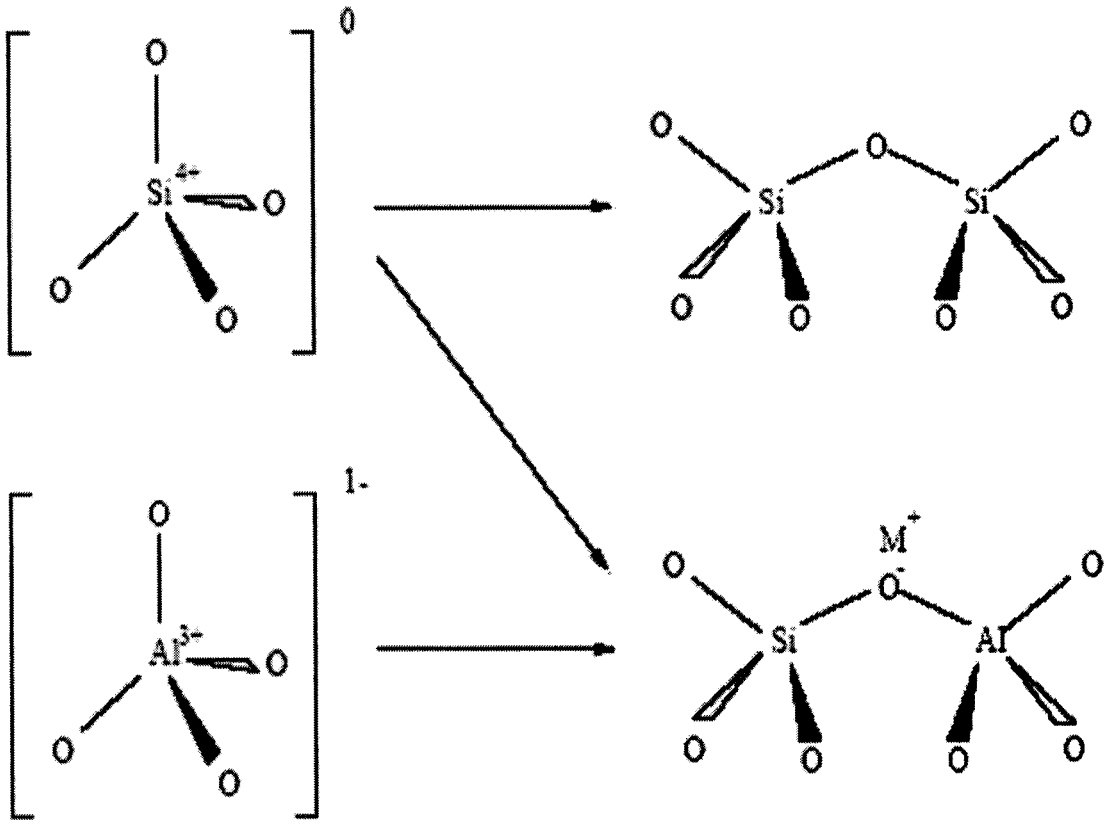

Figure 1.5 Primary building blocks of zeolites.

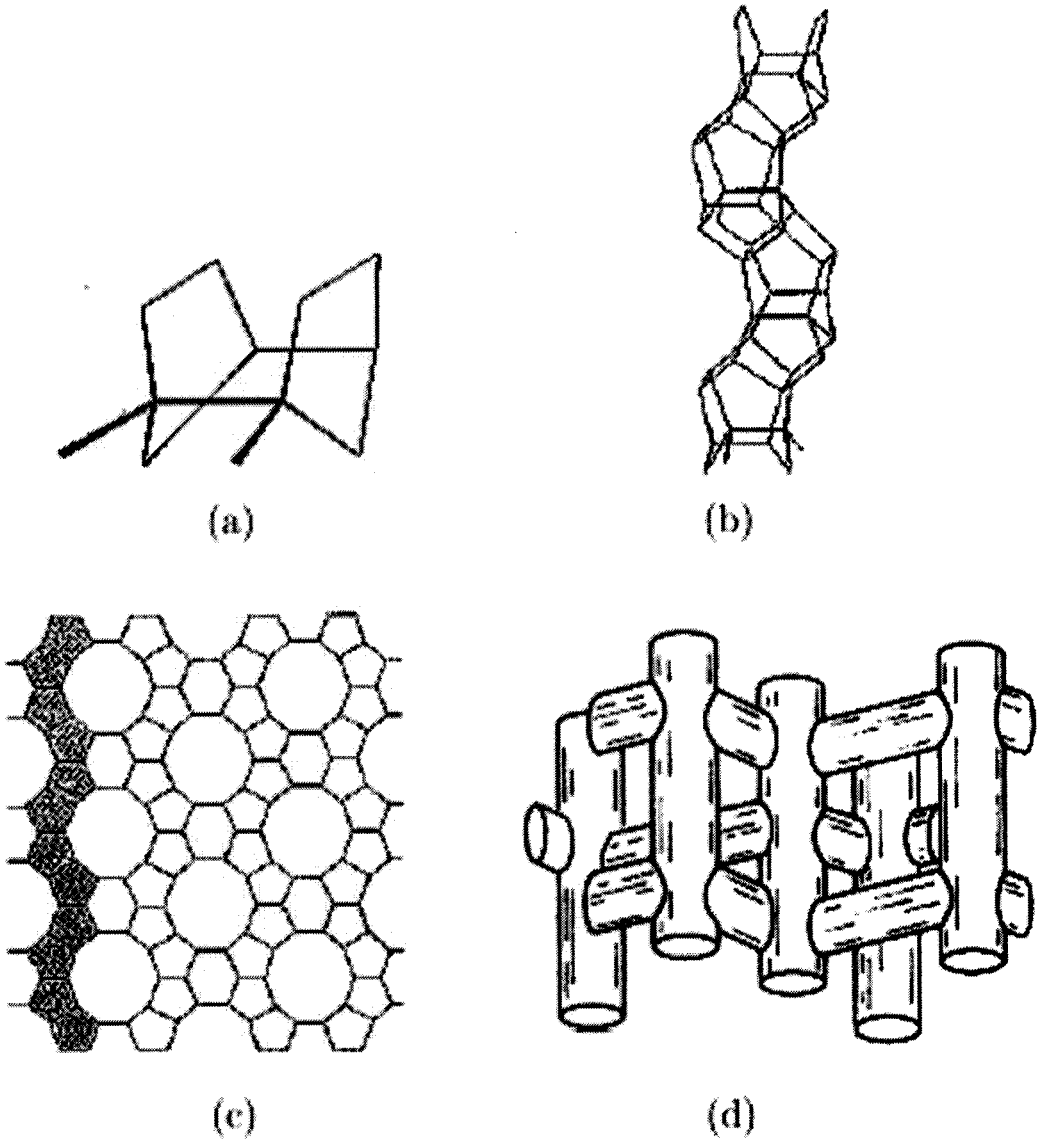

Figure 1.6 (a)Secondary building unit (SBU) of silicalite (b) chains formed by linking the SBUs (c) schematic of silicalite layers formed by side-linking the chains and (d) schematic of the three-dimensional intra-crystalline pore structure of silicalite or ZSM-5.

1.4.2 Y-Zeolite

The Zeolites finding the largest scale application in catalysis belong to the family of Faujasites, including Zeolite X and Y. Having 7.4 Å apertures (12-membered oxygen rings) and a three dimensional pore structure, they admit even hydrocarbon molecules larger than naphthalene. The sodalite cages in Faujasites are arranged in an array with greater spacing than in Zeolite A. Each sodalite cage is connected to four other sodalite cages; each connecting unit is six bridging oxygen ions linking the hexagonal faces of two sodalite units, as shown by the unit cell in Figure 1.7 [8].

1.4.3 Acidity of Zeolites

The acidity of zeolites is a result of the protons that are required to maintain electrical neutrality in the structure. The number and strength of the acid sites are related to the zeolite framework, in so far as Brönsted acid sites are associated to the presence of framework aluminum atoms. The number of these aluminum atoms can be varied and adjusted to specific needs either by synthesis or by post-treatments [9].

Zeolites with low aluminum contents can be prepared by many procedures. Among these is the process known as dealumination. Dealumination can be effected through the use of steam, chelating agents, or by treatment with silicon tetrachloride. However, the most common procedure is hydrothermal treatment at elevated temperatures under controlled atmosphere (steaming), which yields more siliceous framework [10].

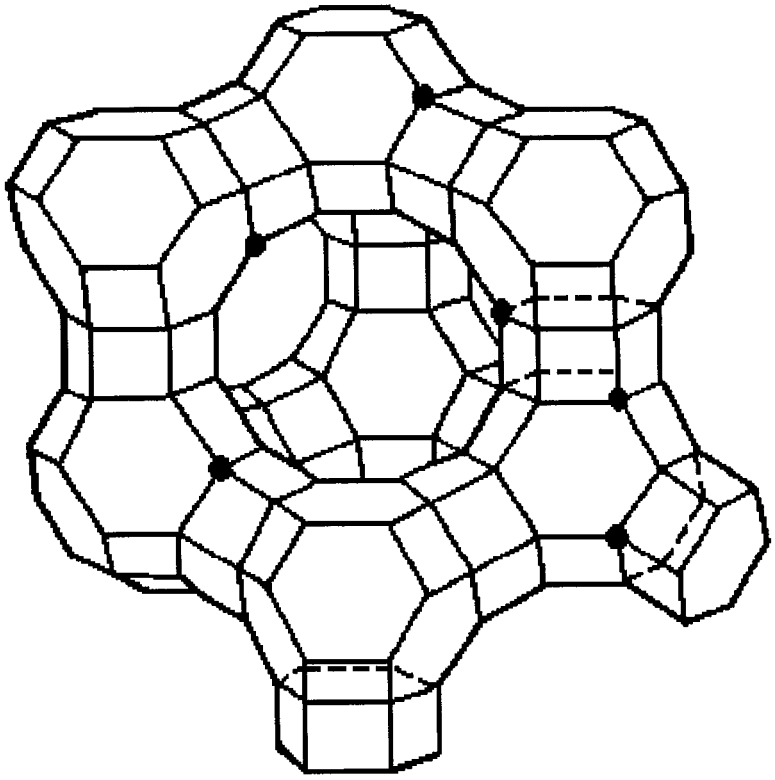

Figure 1.7 Unit cell of Y-zeolite

1.4.4 Zeolites Deactivation

Deactivation of zeolites is mainly due to the formation of carbonaceous products ("coke"), which occurs during hydrocarbon acid-catalyzed reactions. Coke is an ill-defined material which is not desorbed from the catalyst upon purging with a suitable fluid. Coke consists of polyaromatic condensed-ring structure, which is close to the graphite structure [11]. Coke produces a decrease in catalytic activity of zeolites by two mechanisms: active site suppression or pore blocking. Both deactivation modes can occur simultaneously, although one of the two mechanisms is usually predominant [12].

The loss of sorption capacity of coked catalysts has been used to determine the mode of zeolite deactivation. When coke deposition takes place by simple pore filling, the ratio between the volume occupied by coke (V_c) and the volume not accessible to the adsorbate (V_{na}) should be around 1.0. In contrast, when coke deposition leads to a blockage of the channels and intersections in which there are no coke deposits, a (V_c/V_{na}) ratio lower than 1.0 is expected. On the other hand, if coke is deposited on the external zeolite surface, blocking the entrances to the internal structure, a very low value of V_c/V_{na} is obtained [12].

1.5 Scope and Objectives of the Thesis

The present thesis work describes the results of an experimental and kinetic investigation of xylene transformations over Y-zeolites in a fluidized-bed reactor. As this will be the first reported research work for the transformation of xylenes using this type of reactor, emphasis was placed in developing detailed kinetic models with different reaction schemes, under the short reaction time peculiar to the reactor system used for the

study. The objectives of the thesis can be summarized as follows:

1. To investigate the transformation of xylenes in a reactor that simulates the operation of commercial FCC units.
2. To develop a comprehensive kinetic model for the overall reaction.
3. To estimate the numerous kinetic parameters for the overall reaction network of xylene transformation.
4. To compare the transformation of each xylene isomers
5. To study the effect of Y-zeolite acidity alteration on m-xylene transformation reactions.

The results of the thesis are presented in three refereed papers [13, 14, 15] and a submitted paper [16].

1.6 References

[1] Davenport B., "Xylenes", Chemical Economics Handbook, SRI Consulting, (2001).

[2] Al-Khattaf, S., and Al-Amer, A., Catalytic Isomerization of Xylene in a Fluidized Bed Reactor" Research proposal submitted to Research Institute KFUPM Saudi Arabia, (2002).

[3] Matar S., Hatch L.F., "Chemistry of Petrochemical Processes", 2nd Ed. Butterworth and Heinemann, USA, p289 (2001).

[4] Tsai, T., Liu, S., and Wang, I., Disproportionation and Transalkylation of Alkylbezenes over Zeolite Catalysts. Applied Catalysis A. 181, 355 (1991).

[5] Bhatia S., "Zeolite Catalysts: Principles and Applications" CRC Press, Inc., Boca Raton, Florida, (1990).

[6] Molina, R., Schutz, A., Poncelet, G., Transformation of m-Xylene over Al-Pillared Clays and Ultrastable Zeolite Y. J. Catal., 145 (1994), 79.

[7] Khaleeq M., "Adsorption of xylenes on BA-X Zeolite Pellets". M.S Thesis, King Fahd University of Petroleum & Minerals, Dhahran Saudi Arabia, January, (1984).

[8] Dimitrios K., "Disproportionation of Toluene over USY Zeolite Catalysts". Research Report, Department of Chemical Engineering, University College London, U.K (2002).

[9] Seddigi Z. S., "Characterization of the Acidic Properties of Zeolites and their Catalytic Behavior in the Synthesis of MTBE". M.S Thesis, King Fahd University of Petroleum & Minerals, Dhahran Saudi Arabia, May, (1994).

[10] Sulikowski B., Datka J., Gill B., Ptaszynski, J., Klinowski J., Acidity and Catalytic Properties of Realuminated Zeolite Y. J. Phys. Chem. B 101 (1997), 6929.

[11] Al-Khattaf S., "Diffusion and Reaction of Hydrocarbon in FCC Catalysts" Ph.D. Dissertation, University of Western Ontario, London, Canada, (2001).

[12] de Lucas A., Canizares P., Duran A., Carrero A., Coke Formation, Location, Nature and Regeneration on Dealuminated HZSM-5 Type Zeolites. Appl. Catal. A: General 156 (1997), 299.

[13] Iliyas A., Al-Khattaf S., m-Xylene Isomerization over USY Zeolite in a Riser Simulator: A Simplified Kinetic Model. Chem. Eng. J., in press (2003).

[14] Iliyas A., Al-Khattaf S., Xylene Isomerization over USY Zeolite in a Riser Simulator: A Comprehensive Kinetic Model. Ind. Eng. Chem. Res., 43 (2004), 1349.

[15] Iliyas A., Al-Khattaf S., Xylene Transformation over USY Zeolite: An Experimental and Kinetic Study. Accepted in Appl. Catal. A; General (2004).

[16] Al-Khattaf S., Iliyas A., Al-Amer A., Inui T., The Effect of Y-Zeolite Acidity on m-Xylene Transformation Reactions. Submitted to Appl. Catal. A: General, April, (2004).

CHAPTER 2

2 Literature Review

2.1 Background

The transformation of xylenes is generally carried out in the presence of an acid catalyst. The reaction can occur in both the liquid and vapor phase. The liquid phase isomerization using acid-halide catalysts (homogeneous reaction) suffers from conversion and recovery problems. On the other hand, the vapor phase isomerization on heterogeneous acids avoids the problems of homogenous catalysts. However, high temperature is required, which leads to coke formation, thereby affecting the yield of the desired products. Addition of hydrogen to the xylene feed reduces coke formation, suppresses side reactions and increases the rate of xylene isomerization [1].

In recent years, most of the xylene transformation studies have been carried out on various types of zeolite catalysts. Some of the zeolite catalysts (e.g ZSM-5) showed considerable improvements over the amorphous catalysts as far as activity and selectivity are concerned. In addition metal dispersed on zeolite catalysts have been employed to obtain a higher yield and selectivity of products [1].

2.2 Xylene Transformation over Y-Zeolite

The work of Lanewala and Bolton, 1969 [2] on the transformation of the three xylene isomers over Y-zeolite in a fixed-bed reactor, remains one of the pioneering

research studies with regard to this reaction. A higher isomerization and disproportionation rate was observed with p-xylene as compared to the other two isomers. They established that a linear relationship exits between the percent approach of xylenes to their equilibrium values and the extent of disproportionation. They are also the first group to propose a bimolecular reaction mechanism for isomerization pathway.

Chatterjee and Ganguli, 1985 [3] studied the transformation of o-xylene over 20 different catalysts based on a large variety of multicationic (mono to trivalent) Y-zeolite. Catalysts containing La^{3+} and Ni^{2+} showed maximum activity. Activities caused by the presence of divalent ions were reported to follow the sequence: Ni > Co > Zn > Mg > Ca. All the catalysts showed very high selectivity for m-xylene isomer, but relative improvement in p-xylene yield was obtained with catalysts containing La^{3+} and Ni^{2+}. T/TMBs mole ratio was found to be time-dependent. This phenomenon was attributed to the relatively strong adsorption of the TMBs on the zeolite surface, and their slow desorption with time.

Molina et al., 1994 [4] carried out m-xylene transformation over Al-pillared beidellite (AIPB), montmorillonite (AIPM) and ultrastable Y-zeolite (USY). They observed that the activity of the catalyst follows the sequence USY > AIPB > AIPM. They attributed the higher activity of the USY catalyst as compared to the pillared clays to its higher content of strong acid sites, and also to its greater micropore volume. In addition, the higher activity of AIPB compared to AIPM was interpreted in terms of framework substitution differences between the two clays. It was concluded that during the deactivation of the catalyst, stronger Brönsted sites are preferentially poisoned, resulting in their faster initial deactivation.

Yang et al., 1996 [5] studied the transformation of m-xylene over ultrastable Y-zeolite, mixed physically with NiS/AL_20_3 in a hydrogen atmosphere. The improved activity of the mixed catalyst as compared to USY was attributed to the effect of hydrogen spillover. It was proposed that active hydrogen species generated by the dissociation of gaseous hydrogen on NiS migrates to the surface of USY zeolite. This results in the protonation of the aromatic ring on the USY. Thus, promoting the desorption of carbenium ion as intermediates of m-xylene transformation at Brönsted acid site, and hence increase the turnover frequency of the reaction.

In a parallel study, Morin et al., 1996 [6] carried out the transformation of pure xylenes, pure trimethyl benzenes (TMBs), and a mixture of m-xylene and 1,2,4 trimethylbenzene over HY-zeolite. Based on the obtained experimental results, it was reported that trimethylbenzenes (TMBs) isomerization was 4 to 10 times faster than xylene isomerization. In addition, it was observed that the addition of m-xylene to 1,2,4-trimethylbenzene result in a significant increase of o-xylene. Thus, their result confirmed a previous proposal made by Lanewala and Bolton, 1969 [2] that an ortho-selective bimolecular isomerization is possible over Y-zeolite.

In 1997, Sulikowski et al. [8] carried out a comparative study on the acidity and catalytic properties of fresh HY-zeolite, H-USY-zeolite obtained by steam dealumination, and H-Real-USY-zeolite realuminated by KOH treatment using m-xylene transformation as the test reaction. It was observed that the acidity of the catalysts is in the following sequence: HY $\approx$ H-Real-USY > H-USY. Regardless of the lower concentration of acid centers in the H-Real-USY as compared to HY catalyst, both gives a similar conversion. This was explained by the number of protons accessible for reacting molecules, which is

25 % higher in H-Real-USY than the parent HY catalyst. As a result, a higher acid strength of the catalytically active hydroxyl group was found in the H-Real-USY catalyst. On the other hand, the lower activity of the H-USY catalyst was attributed to the significant decrease in the catalytically active 3640cm^{-1} hydroxyl group. Moreover, the higher isomerization/disproportionation (I/D) ratio with H-USY catalyst was explained to be due to the presence of extra-framework aluminum species, which decrease the void space available for the bulky bimolecular disproportionation transition state.

In a different study, Morin et al., 1998a [9] studied m-xylene transformation over a series of commercial Y zeolite prepared by steaming and acid washing. They found that great difference exist between catalytic properties of the catalysts. In particular, the less steam dealuminated samples present very strong protonic sites resulting from the interaction between framework protonic sites and extraframework aluminum species. While the more steam dealuminated samples have very weak sites corresponding to adjacent OH groups. In contrast, samples dealuminated with $SiCl_4$ did not exhibit the above behavior. Moreover, contrary to the trend reported in some previous studies, they observed an increase in disproportionation/isomerization (D/I) ratio with decreasing acid site density. This was attributed to the corresponding decrease in acid strength with decreasing acid density under the conditions of their study.

Pamin et al., 2000 [10] studied the effect of immobilization of 12-Tungstophosphoric (PW_{12}) on dealuminated Y-zeolite during m-xylene transformation. It was observed that the deposition of $H_3PW_{12}O_{40}$ on Y-zeolite results in a drastic increase in disproportionation selectivity, while simultaneously suppressing isomerization selectivity. Their results were explained by the fact that disproportionation of m-xylene

proceeds on sites with higher strength. This could be due to the fact that a higher concentration of sites per unit area of the support was obtained when more acid was supported in the zeolite mesopore systems. This situation favored the disproportionation of m-xylene, being a bimolecular reaction as compared to unimolecular isomerization reaction.

2.2.1 Coke Formation

In an attempt to study the influence of coke deposits products selectivity during xylene transformation, Morin et al., 1998b [11] carried out m-xylene transformation at 623K over a series of commercial HY-zeolites, with framework Si/Al ratios between 4 and 100. They observed that the stronger the acid sites the faster their deactivation by coke deposit, however, the higher the selectivity for monomolecular over the bimolecular isomerization. Thus, it was observed that deactivation causes a significant increase in D/I ratio, and significant decrease in P/O ratio. These selectivity changes were related to a greater selectivity of the strong acid sites in favor of the classical monomolecular mode of isomerization, at the expense of disproportionation. These results led them to the conclusion that the rapid transformation into coke of diphenylmethane intermediates of disproportionation and of bimolecular isomerization on strong acid sites could be used to explain the low selectivity of these sites for both reactions.

The ageing of coke formed during m-xylene transformation at 250°C over a USHY zeolite was investigated under nitrogen flow by Crerqueira et al., 2001 [12]. This ageing treatment causes a decrease in the zeolite coke content and an increase in the size and aromaticity of coke molecules. Pyridine adsorption followed by IR spectroscopy, were used to study the coked samples before and after ageing. It was observed that ageing

causes a significant decrease in the concentrations of protonic and Lewis acid sites able to retain pyridine adsorbed at 150°C. The deactivating effect of coke was also found to be more pronounced after than before ageing. A change in the mode of deactivation from site poisoning to pore blockage was proposed to explain these observations.

In a more recent work, Crerqueira et al., 2002 [13] also investigated the influence of coke deposits during the transformation of m- xylene over USHY-zeolite at 523 and 723 K. A rapid deactivation was found for the reaction at both temperatures, owing to the rapid formation of carbonation compound inside the zeolite micropore (coke). Based on this study, it was concluded that coke molecules during m-xylene transformation results from the transformation of diarylmethane derivatives, which are intermediates of transmethylation reactions, through cylization, isomerization, and hydrogen transfer steps. This result in initial deactivation due to poisoning of the protonic sites, but at longer time on steam, a different mode of deactivation i.e. due to pore blockage by coke deposit was found.

2.3 Xylene Transformation over ZSM-5 Zeolite

As mentioned earlier, the transformation of xylenes has been carried out on a variety of acid catalysts including mordenite, faujasite and ZSM-5. However, the highest selectivity of p-xylene is obtained when modified ZSM-5 zeolites are used. Furthermore, large crystal ZSM-5 with their long diffusion has been found to increase p-xylene selectivity [14]. In addition, different reagents have been successfully used as modifiers of ZSM-5 in order to increase the selectivity of p-xylene. These modifiers include compounds of phosphorus, magnesium, silicon and antimony [15].

Shashikala et al., 1991 [16] used HZSM-35 for m-xylene isomerization in a

differential reactor. It was reported that although ZSM-35 showed exceptionally high para selectivity, it undergoes rapid deactivation due to coking. However, when 10 % HZSM-5 was added it prevents deactivation to a large extent, at the same time retaining high p-xylene selectivity. While in a different study Araujo et al., 2001 [17] carried out the same reaction in a fixed-bed reactor using a solid acid silico-aluminium phosphate type (SAPO-11), mixed with HZSM-5 zeolite. They reported that this composite catalyst promotes better p-xylene selectivity with lower activation energy as compared with pure HZSM-5 due to its improved adsorption properties, and lower acidity.

Kurnschner et al., 1990 [15] took a different approach in their effort to achieve p-xylene selectivity during the transformation of m-xylene. Instead of modifying ZSM-5 by chemical treatment, they were able to carry out controlled hydrothermal treatment of HZSM-5 at 500°C resulting in the transformation of framework into non-framework alumina. They found that the presence of non-framework alumina enhanced p-xylene selectivity in the catalytic disproportionation of toluene and in the isomerization of m-xylene. This conclusion is supportive of what was reported in the literature by Yashima and co-workers, 1981 [18] that p-xylene is produced with high selectivity when HZSM-5 is steamed at 1223 K. They also reported that the rate of isomerization during xylene transformation is more than three orders of magnitude higher than the rate of disproportionation. On the other hand, the number of acid sites on the outer surface of the zeolite catalyst is more than one order of magnitude lower than the number of acid sites inside the pores. This means that p-xylene formed within the channels can undergo secondary isomerization on the outer surface, and owing to its high rate, it therefore overcomes the drawback of small number of outer surface sites. As a result, employing

short contact time for the reaction will prevent the undesired secondary isomerization of p-xylene on the outer surface of the catalyst and hence enhance its selectivity.

On the other hand, Kaeding et al., 1981 [14] have suggested that the selective formation of p-xylene is enhanced by decreasing the zeolite pore size. Thus, it was proposed that loading HZSM-5 with oxides of P, Mg, or B increases the p-xylene selectivity. Another method to control the diffusivity of xylenes inside the zeolite structure is to use large crystal size, which has been found to produce higher p-xylene than using the small zeolite crystals [19].

2.4 Xylene Transformation over H-Mordenite

The transformation of the three xylene isomers was carried out over Pt and Re supported on H-Mordenite catalyst by Aboul-Gheit et al., 1993 [20] using a pulse catalytic microreactor. Higher ratios of p-xylene in the production of the xylene isomer mixture relative to the corresponding thermodynamic equilibrium values were obtained, whereas the ratios of m-xylene were low and those of o-xylene were very low. However, relatively high dealkylation products (toluene and benzene) were obtained at higher temperatures. On the other hand, disproportionation products (trimethylbenzenes) were not detected in the reaction products.

Hong et al., 1994 [21] studied the transformation of o-xylene on seven dealuminated H-mordenites containing different amounts of framework and nonframework aluminum, which were prepared by steaming or calcining NH_4-mordenite. It was observed that the initial rates of isomerization divided by the number of available Brönsted sites are proportional to the number of available Lewis sites. Their result

suggests a synergistic enhancement of the acidity by the interaction between Brönsted and Lewis acid centers.

Benazzi et al., 1995 [22] reported a study on the transformation of o-xylene-ethylbenzene mixture on bifunctional catalysts constituted of Pt/Al_2O_3, H-Mordenite, and H-MFI zeolites. The preferential dealumination of the crystallite outer surface of the H-Mordenite and MFI catalysts was effected by treatment with ammonium hexa-fluorosilicate solutions. The activity of the treated H-Mordenite catalyst is lower than that of non-treated catalysts but their isomerization selectivity is increased because of the inhibition of disproportionation and transalkylation reactions. The decrease in activity was explained by a partial blockage of the channels which could be caused by a silica deposit at the entrance of Mordenite pores during the treatment. The inhibition of disproportionation and transalkylation is due to the decrease in acidity of the outer surface caused by its selective dealumination. On the other hand, the treatment of H-MFI with ammonium hexafluorosilicate causes a significant increase in the rates of ethylbenzene and o-xylene transformation which was attributed to a decrease in the rate of coke formation on the outer surface of the crystallites. Furthermore, there is a decrease in the selectivity of xylenes disproportionation which involves bulky diphenylmethane intermediates, but no change in the selectivity of ethylbenzene disproportionation.

2.5 Xylene Transformation over Beta Zeolite

Perez-Pariente et al., 1991 [23] conducted an investigation of the transformation of m-xylene over Beta zeolites with Si/Al ratios in the range of 11 to 42. The obtained P/O ratio over the catalyst is in agreement with the presence of twelve-membered rings.

Moreover, the high initial selectivity of 1,3,5-TMB indicates that Beta zeolite does not suppress the formation of this bulky TMB isomer. Furthermore, the high values of D/I ratio observed with this zeolite was rationalized by steric suppression of disproportionation pathway in the narrow sinusoidal channels of zeolite β. The highest value of D/I ratio was observed with the samples with Si/Al ratio between 14 and 15. The occurrence of this maximum was explained by the synergetic effect between extraframework and the Brönsted acid sites.

Rakshe et al., 1999 [24] prepared a large pore, Zr-containing aluminosilicate with Beta zeolite structure. The FTIR studies of adsorbed pyridine, evacuated at different temperatures showed an increase in Lewis as well as Brönsted acidity of the samples as compared to other catalysts having similar Al contents. The catalytic activity of the samples was demonstrated in the isomerization of m-xylene at atmospheric pressure in a fixed bed reactor. The additional acidity of the catalyst was correlated with a marginal increase in the isomerization activity as well as selectivity to the isomerization products rather than the disproportionation products, particularly at <500 K.

Mavrodinova et al., 2001 [25] studied the catalytic performance of NH_4-Beta zeolite containing varying amounts of indium with m-xylene transformation. The In cations, regarded as coordinatively unsaturated species possessing Lewis acidity, substantially changed the catalyst stability and selectivity in this reaction under inert atmosphere. An acceleration of the side reactions, disproportionation and coking, was observed with the In-modification, and a mechanism of hydride ion abstraction and faster benzylic cation formation was proposed. In presence of H, these reactions are strongly

suppressed at the expense of the main reaction of isomerization. On the completely In-exchanged Beta zeolite, a partial bimolecular mechanism of isomerization was suggested.

2.6 Xylene Transformation over MCM-22

Laforge et al., 2003 [26] extended the transformation of xylenes to a different zeolite, so-called MCM-22 zeolite with intermediate behavior between those of 12-MR (large pore) and 10-MR (average pore) zeolites. Based on the distribution of the desorbed products, mechanisms were proposed for the formation of the various products and the location of the reactions was followed. The high value of P/O ratio (ca. 4.0) obtained indicates shape selectivity over the catalyst. As a result, it was speculated that isomerization occurs in the supercages or in the sinusoidal channels with significant limitations in the desorption of the bulkier ortho isomer through the narrow apertures of these pores. Furthermore, the higher value of toluene/TMBs mole ratio above one under the conditions of their study, was attributed to the strong limitation of the desorption of TMBs from the internal microspore of MCM-22. Moreover, it was proposed that TMBs undergoes various reactions leading to ethyltoluene (via paring reaction), C_2-C_4 gases (via oligomerization and cracking reactions), toluene, and coke. Deactivation was found to cause a small decrease in isomerization and suppresses disproportionation and secondary TMB transformations.

Recently, Laforge et al., 2004 [27] reported a study on the effect of selective pre-coking on the activity and selectivity of MCM-22 during m-xylene transformation. Among the methods used to selectively deactivate the acid sites of the supercages or of the external hemicages includes: n-heptane cracking at 450°C, dealumination with ammonium hexafluorosilicate, reaction with 1,1,1,3,3,3-hexamethyldisilazane, poisoning

with 2,6- or 2,4-dimethylquinoline and treatment with 2,4-dimethylquinoline. However, only the treatment with 2,4-dimethylquinoline was found to be suitable. Thus, this method was employed to estimate the relative contributions of the protonic sites located in the supercages, the external hemicages, and the sinusoidal channels to be 42, 22 and 36% respectively for m-xylene transformation. Furthermore, it was suggested that in the large supercages with small apertures of MCM-22, isomerization gives P/O ratio of 3.5, while in the large external hemicages, m-xylene is essentially transformed into a quasi-equimolar mixture of p- and o-xylenes.

2.7 Transformation of Xylenes over Different Catalysts

Martens et al., 1988 [19] studied the conversion of m-xylene over various acid zeolites with 10- or 12-membered rings, such as ZSM-5, ZSM-12, ZSM-48, OFF, MOR, FAU, Ω, β, and L zeolites. The P/O ratio in the isomerization of m-xylene is found to be always high for 10-membered ring zeolites with crystals >1 mm. The moderate selectivity for p-xylene formation in some zeolites with 12-membered rings was suggested to be due to transition-state shape selectivity. On the other hand, the D/I ratio is found to be very low for 10-membered ring zeolites, which allows them to be distinguished easily from the 12-membered ring zeolites with much higher value of D/I ratio. Furthermore, in the group of 12-membered ring zeolites, the D/I ratio could not be correlated at all with the effective size of the intracrystralline cavities. Moreover, this ratio was reported to be influenced by the strong isolated acid sites, which are present in cavities that allow the formation of at least one of the possible bimolecular transition-state complexes for disproportionation. The obtained distribution of trimethylbenzene isomers reflects important features of the shape of the pores, the presence and the

position of larger spaces in lobes, cages, or intersections adjacent to the 12-membered ring channels of large-pore zeolites.

The catalytic properties of zeolite β in the transformation of m-xylene, and the methylation and disproportionation of toluene were measured and compared with those of other zeolites like ZSM-5, ZSM-23, ZSM-48, and ZSM-50 by Ratnasamy et al., 1989 [28]. Unlike the other zeolites, zeolite β did not exhibit product shape selectivity. Moreover, it suppresses the formation of the bulky 1,3,5-isomer among trimethylbenzenes leading to high concentration of 1,2,4-isomer having the minimum cross section. The D/I ratio in the reactions of m-xylene over these zeolites followed the order: zeolite β > ZSM-50 > ZSM-5 > ZSM-48 > ZSM-23 > ZSM-22. A comparison of zeolite β with ZSM-5 in the xylene isomerization process using industrial feedstock revealed similar trends. The observed shape-selective properties of zeolite β in these reactions of aromatic hydrocarbons were explained in terms of its 12-membered three-dimensional pore structure.

Morin et al., 1997 [29] studied m-transformation over MCM-41 mesoporous aluminosilicates, and FAU zeolites. It was reported that while over silica alumina and the non-shape selective zeolite catalysts, m-xylene isomerizes at similar rates into o- and p-xylenes as expected from the classical intramolecular mechanism. However, over MCM-41 mesoporous aluminosilicates, o-xylene is preferably formed (O/P $\approx$ 2.5). A bimolecular pathway involving m-xylene disproportionation followed by transalkylation between trimethylbenzenes and m-xylene was suggested to be responsible for this preferential isomerization into o-xylene. In agreement with this proposal, the addition of methylcyclohexane to the reactant causes an identical decrease in the rates of

isomerization and disproportionation, while over silica alumina the xylene isomerization which occurs through the classical intramolecular mechanism is not affected. This particular behavior of MCM-41 aluminosilicates was attributed to their unidirectional mesopore structure (shape selectivity effect) rather than their weak acidity.

Jones et al., 1999a [30] investigated the reactions of m-xylene over a series of unidimensional, high-silica zeolites. It was determined that zeolites with a unidimensional pore structure have unique reaction selectivity when compared to multidimensional zeolites of the same pore size. Unlike multidimensional zeolites with 12 member ring (MR) pores that give a P/O ratio of 1, zeolites with unidimensional pores bounded by 14 MRs or large 12 MRs give a P/O <1 due to the influence of a bimolecular isomerization mechanism between a xylene and trimethylbenzene. The unidimensional, parallel pore zeolites (UTD-1, SSZ-31, CIT-5, SSZ-24, ZSM-12, ZSM-48) gave products with the lowest P/O ratio for the given pore size. Multidimensional zeolites and unidimensional zeolites with internal cavities larger than the pore openings all gave higher P/O selectivities. It was shown that at lower flow rates, where external diffusion becomes important, P/O selectivity can be lowered due to an increased amount of bimolecular isomerization occurring at or near the catalyst external surface. It was concluded that under suitable conditions, the reactions of m-xylene can give information enabling the characterization of medium, large and extra-large pore zeolites.

In the second part of the work, Jones et al., 1999b [31] reported the influence of aluminum population in structures of modified SSZ-33 mol. sieves (CON topology) on the reactions of m-xylene. Borosilicate, SSZ-33 was transformed into the aluminosilicate form by a low-temperature hydrothermal treatment. Aluminosilicate, SSZ-33 samples

with different Al populations behaved similarly in the reactions of m-xylene, suggesting that the intracrystralline pore space acts as an ensemble of cages connected by 10- and 12-member rings (MR) rather than intersecting 10-MR and 12-MR channels. In addition, at low m-xylene flow rates, SSZ-33 samples with high Si/Al ratios showed an increased amount of transalkylation and the P/O and I/D selectivities are lower. Reaction over external-surface deactivated SSZ-33 at low flow rates results in unaltered P/O ratios. In contrast, reaction over SSZ-33 which contains only Al at or near the surface has a greatly decreased P/O ratio. The loss in P/O and I/D selectivity at low flow rates was attributed to the occurrence of ortho-selective bimolecular isomerization at or near the catalyst external surface.

2.8 Reaction Mechanism of Xylene Transformation

When the transformation of xylene was performed as a test reaction for distinguishing between medium and large pore zeolites, it was assumed that the alkyl isomerization takes places through a monomolecular mechanism involving a 1, 2-methyl shifts. On the other hand, a possible transalkylation of the methyl group leading to toluene and TMBs is a bimolecular reaction. The isomerization of xylene can, in principle, proceed via two different mechanisms. Either a monomolecular mechanism via 1, 2-methyl shifts along the benzene ring, or a bimolecular mechanism, consisting of two steps, can take place. In the first step, two xylenes molecules react via a diphenylmethane like intermediates giving TMB and toluene. In the second step, TMB reacts with another xylene molecule resulting in the formation of another TMB and xylene isomers, respectively. As there is a significant difference in the steric requirement for the formation of such reaction intermediates, it can be envisage that the zeolite channel

dimensions and architecture will play a major role in this reaction. A review paper of the mechanism of isomerization over acidic solid catalysts was published by Guisnet et al., 2000 [32]. The authors suggested that the bimolecular mechanism becomes predominant when the catalyst has only weak acid sites localized in the large cavities (zeolite-Y) or in long intersecting channels (MCM-41).

To distinguish monomolecular and bimolecular mechanism in xylene transformation, Corma and Sastre, 1991 [33] used a mixture of deuterated and undeuterated p-xylene. They tested a series of zeolites, namely, Mordenite, Faujasite and Beta structural types. Figure 2.1 shows a scheme of monomolecular and bimolecular xylene isomerization with the mixture of deuterated and undeuterated xylenes. For the monomolecular mechanism (1,2-methyl shift), all the xylene products should have a molecular weight of 106 (normal xylenes) and 112 (deuterated xylenes).

For the bimolecular mechanism, proceeding via the formation of bulk diphenylmethane-like intermediates, xylene isomers would exhibits both monomolecular weights of 106 and 112 and also a value of 109 for one deuterated and undeuterated methyl group. The results demonstrated that the bimolecular mechanism proceeds readily in the three-dimensional system of faujasite channels. The bimolecular mechanism is significantly less important in one-dimensional mordenite and practically does not occur in zeolite Beta for low levels [33]. These results indicated that the bimolecular mechanism of xylene isomerization is controlled by restricted transition state selectivity. This is consistent with xylene isomerization over ZSM-5, where no TMBs were found among the reaction products, which confirms the monomolecular mechanism due to the severe steric hindrance imposed by the medium-sized pores of ZSM-5 zeolites [34].

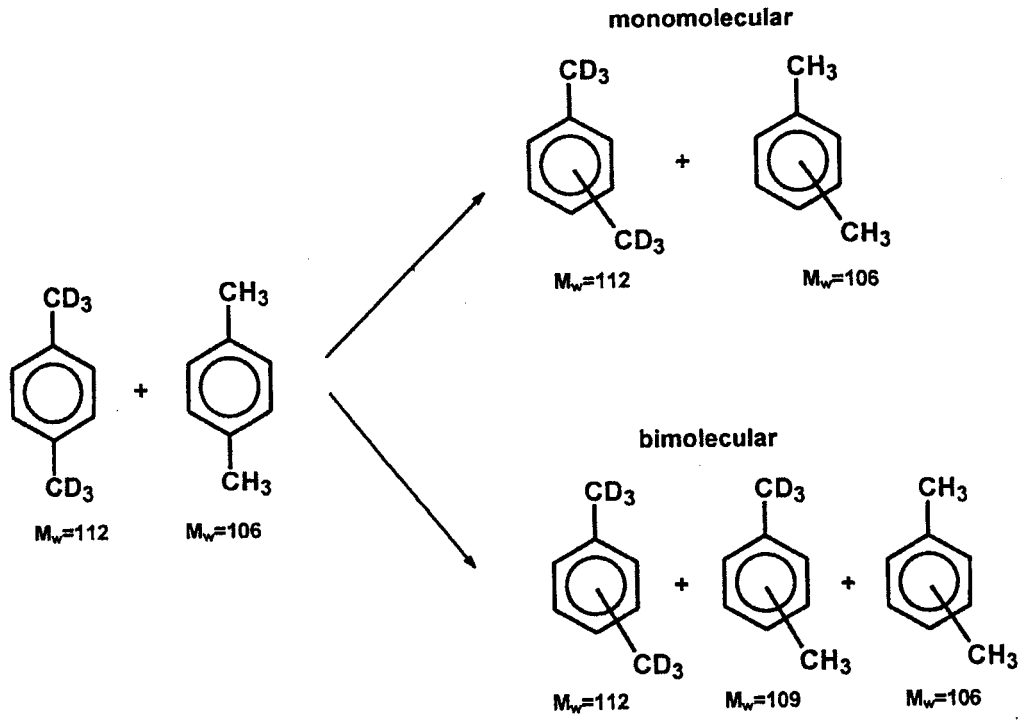

Figure 2.1 Distribution of deuterated and non-deuterated methyl group for monomolecular and bimolecular isomerization of xylene

In a different study, Morin et al., 1996 [6] proposed a simple method for determining the relative significance of unimolecular and bimolecular mechanisms during xylene transformation over HY-zeolite. The P/O ratio of the bimolecular process was found to be completely different from that of monomolecular process (0.275 instead of 1.18). Based on this result, it was estimated that the percentage of bimolecular isomerization constitute 20 % of the overall isomerization process. Their result agrees with those reported by Corma and Sastre, 1991 [33].

2.9 Kinetics of Xylene Transformation

The kinetics of xylene transformation over solid acids has gained considerable interest over the years. This is as a result of the significant contribution of such studies towards understanding the mechanism of the reaction over acid catalysts. The parameters obtained from such studies are often used in evaluating the relative magnitudes of the different reaction paths and the ease of interconversion between the three isomers. It can also be employed in designing commercial-scale reactors from experimental studies conducted in the laboratories.

To understand the kinetic behavior of xylene transformation reaction on the catalyst, the knowledge of detailed kinetic parameters must be required. Many researchers have approached this subject theoretically and experimentally. Amongst the techniques employed in the literature to obtain the kinetic parameters of the xylene transformation process include: analytical methods such as Wei-Prater method [35, 36], Laplace transform [37, 38], and finite integral transform [39]. Curve fitting method, such as Himmelblau method [40, 41], and least square method [42, 43] has also been applied. However, in most of these studies, the complexity of the reaction and the interplay of

diffusion and chemical reaction which causes different reaction paths have often posed great obstacles.

2.9.1 Y-Zeolite

Only a few kinetic study of m-xylene transformation over Y-zeolite has been reported in the open literatures. Most of the kinetic works in this regard has been performed over ZSM-5. This may be due to the fact that most of the currently working xylene transformations plants are conducted over this catalyst. However, as later shown in this work, kinetic study of xylene transformation over Y-zeolite particularly in a fluidized-bed reactor is also practically relevant. This is because C_8 aromatic compounds including the three xylene isomers are obtained from the catalytic reforming/cracking units in the refinery, in which FCC catalysts such as USY-zeolite are employed for the these operations. Thus, studying the kinetic of xylene transformation over USY- zeolite catalysts, while employing a system that simulates the operation of commercial riser-type FCC units (riser simulator) may give an idea of the behavior of the C_8 aromatics during the reforming/cracking operations, prior to their separation and subsequent isomerization.

Gajewski and Sulikowski, 1978 [44] studied the kinetics of m-xylene transformation over dealuminated Y zeolites by the pulse method. The apparent activation energy for the overall xylene isomerization reaction was estimated to be 30 ± 2 kcal/mol. Both the strength of Brönsted acid sites and their efficiency were suggested to be responsible for the high activity of Al-deficient zeolites in m-xylene conversion.

Corma et al., 1993 [45] studied the catalytic adsorption properties of a series of dealuminated zeolites using m-xylene disproportionation as test reaction. On the basis of the estimated kinetic and adsorption parameters, they reported that the transalkylation of

dealuminated Y-zeolite follows a Langmuir-Hinshelwood mechanism. Furthermore, they observed that the activity and selectivity of dealuminated Y zeolites can be related, not only to classical HF and LF hydroxyl groups, but also to presence of very strong acid sites associated with the presence of extra frame work aluminum species.

Gendy, 1998 [42] performed a steady-state simulation model for xylene transformation over HY-Zeolite in a fixed bed reactor. Both the Liquid and vapor phase reactions were considered. The main reactions considered in the model were the isomerization reactions (using both the sequence and triangular scheme) and the disproportionation of xylenes to toluene and trimethylbenzene. The method of least squares was employed to obtain the kinetic parameters including the deactivation constants. The model predicts the concentration and temperature profiles for a given input of operating conditions. The obtained simulation results revealed the similarity in the reactor behavior if it operates either isothermally or adiabatically with respect to the distribution of the reaction products and catalyst deactivation. The study also indicated that performing the reaction in the liquid phase is more favorable than in the vapor phase due to better selectivity, relative productivity, efficiency and approach to equilibrium.

2.9.2 ZSM-5 Zeolite

Cappellazzo et al., 1991 [43] investigated the kinetics of xylene transformation in the liquid phase over a ZSM-5 catalyst using a fixed-bed reactor within the temperature range of 523-573 K. The presence of shape selectivity toward p-xylene was examined and classified by comparison with that of other catalysts previously investigated in the literature. Two effective kinetic models based on the triangular and sequence reaction schemes were employed to estimate the kinetic parameters of the complex reaction. Both

models explicitly account for shape selectivity towards p-xylene and compare fairly well with the obtained experimental data.

A pulse microreactor-chromatograph technique was used to study xylene transformation reaction over HZSM-5 zeolite catalyst by Li et al., 1992 [39]. A mathematical modeling including the diffusion, adsorption, and reaction taking place in the system was performed by a dynamic analytical method. The estimated activation energies based on triangular reaction network indicated that the transformation of m-xylene to o- or p-xylene, o-xylene to m- or p-xylene, and p-xylene to toluene were controlled by reaction, and the conversion of p-xylene to m- or o-xylene was in the transition regime of diffusion and reaction in the intracrystralline zeolite channels. The pulse microreactor-chromatograph and associated modeling techniques were shown to be effective tools in investigating the complex reaction system.

On the other hand, Beschmann et al., 1993 [46] showed that the rate of isomerization of xylenes to an equilibrium mixture of isomers over ZSM-5 zeolite is roughly proportional to the extent of the (external) surface of the zeolite crystals. Also, it was reported that the rates of the different reactions in the triangular scheme of isomerization is nearly independent of crystal size. Their result was rationalized by the interaction of reaction and diffusion in the volume of the crystals. Moreover, it was observed that p-xylene prevails increasingly in the products when crystal size, temperature or Al content in the zeolite increase; essentially pure p-xylene can be obtained in the limit with unmodified H-ZSM-5 as catalyst. The study was conducted in a gradientless batch-reactor at 573 and 723 K.

Liang et al., 1995 [47] developed theoretical model incorporating diffusion and reaction which takes place via the adsorbed state for highly p-xylene selective catalysts (ZSM-5). Based upon the measured values of diffusivities, adsorption equilibrium constants and reaction rate constants, the modified model was used to explain and predict the high para-selectivities in toluene disproportionation and xylene transformation. The agreement between theoretical model and experimental is good.

Li et al., 1996 [48] carried out another kinetic study of xylene transformation over HZSM-5, MgO-HZSM-5, and CaO-HZSM-5 zeolites using the dynamic modeling method. The rate constants, activation energies, and activation entropies for each step in the triangular reaction network on the catalysts were obtained. Their results indicated that strong acidity can favor the conversion of m- and o-xylene, while the isomerization of p-xylene not only takes place on strong acidic sites, but also on the weaker acidic sites. The estimated parameters also indicated that under a loading amount of MgO or CaO in a mol ratio to framework aluminum equal to 1:1, the influence of steric encumbrance caused by the introduction of MgO or CaO is less as compared with the changes of the surface acidity.

2.9.3 H-Mordenite

A study of the kinetics for the liquid phase isomerization of o-xylene over H-mordenite was made at 505 K by Hopper and Shigemura, 1973 [40]. High activity is indicated by the 80 % achievement of p-xylene equilibrium at 505 K. Over 99 % selectivity of isomerization reaction was reported with H-mordenite as indicated by no C_9+ aromatics and less than 0.5 mole % benzene in the product. Catalyst deactivation was also significant. Reaction rate constants are reported for a first-order reversible

triangular model among the xylene isomers with catalyst deactivation incorporated into the model. A significant conclusion was reached regarding the difficulty of direct interconversion of p- and o-xylene in a 1,3 methyl migrations under the condition of their work. This conclusion was based on the estimated higher activation energies for this reaction path as compared to all others.

Sreedharan and Bhatia, 1987 [1] studied the kinetics of vapor phase transformation of m-xylene over a Ni-Mordenite catalyst. The catalyst was prepared by an impregnation technique and the reaction was carried out in a hydrogen atmosphere using a fixed-bed flow reactor. A sequence reaction scheme with no interconversion between o- and p-isomers was proposed for modeling the reaction. The kinetic data were analyzed on the basis of Langmuir-Hinshelwood kinetics with statistical data interpretation. The rate-controlling step in the overall kinetics of the reaction was found to be the dual-site surface reaction model. The activation energy values of 73.07 and 63.87 kJ mol^{-1} were obtained for p- and o-xylene formation, respectively.

2.9.4 Amorphous Silica-Alumina Catalysts

Silvestri and Prater, 1964 [49] are the first to apply the theoretical method of Wei and Prater to study the kinetics of xylene transformation over a silica-alumina catalyst. It was concluded that despite the perturbation, it is still possible to employ the methods of Wei and Prater to study the isomerization subsystem of the total reaction system and for the determination of the relative rate constants for the isomerization reactions in a triangular scheme. Approximate values were also obtained for the six second-order relative rate constants for the disproportionation subsystem through the use of standard techniques.

Hanson and Engel, 1967 [36] performed the transformation of the three xylene isomers over a amorphous silica-alumina catalyst in a differential tubular reactor at 700-900°F and 0-100 psig. Their result showed that m-xylene isomerizes reversibly to o- and p-xylene, but the direct interconversion of o-xylene to m-xylene does not occur (sequence reaction scheme). Furthermore, it was proposed that the isomerization reactions are first order and, by using the Hougen-Watson technique established that it follow a single-site reaction model. The overall activation energy for the isomerization of m- to p-xylene and m- to o-xylene was found to be essentially the same at average value of 25,500 cal/gmole.

The kinetics of the vapor phase catalytic isomerization of m- to o- and p-xylenes at 460-700°F, and over wide range of space velocities, was investigated by Bhattacharya et al., 1975 [50]. The obtained xylene isomer distribution was in agreement with calculated equilibrium values. At 5-10 mm pressure, disproportionation reactions were found to be suppressed. Furthermore, the reaction was reported to obey first-order kinetics, with similar activation energies for the isomerization of m- to p-xylene and m- to o-xylene.

In 1989, Bhatia et al. [51] developed a steady-state simulation model of the xylene isomerization catalytic reactor, using a 0.5% Pt on SiO_2-Al_2O_3 catalyst from the Octafining II process. The main isomerization reactions along with other side reactions such as hydrogenolysis and disproportionation of xylene, and ethylbenzene isomerization were considered in the model. The mathematic model predicted the concentration, temperature, and pressure profiles of an industrial fixed-bed catalytic reactor for a given feed input and operating conditions. The simulated results of an adiabatic reactor model were in good agreement with existing plant data. A sensitivity analysis of the model are

performed to predict the optimum operating conditions of the reactor.

2.9.5 Comparative Kinetic Studies

Collins et al., 1983 [35] compared the transformation of xylenes over LaY and ZSM-5 zeolite in a plug-flow reactor. The catalysts were observed to differ in terms of the isomerization reaction. Zeolite LaY catalyst causes isomerization by intramolecular 1,2 shifts. On the other hand, isomerization with the smaller pore zeolite, ZSM-5 proceeds with apparent direct interconversion between p- and o-xylene in a triangular reaction scheme. Moreover, the relative rate constants with the ZSM-5 catalyst are found to be influenced by diffusion and/or shape selectivity. Disproportionation is significant with zeolite LaY but not with ZSM-5. Also, small amount of 1,2,4-trimethylbenzene were formed at low conversions over ZSM-5, indicating that shape selectivity influences the reaction products over this catalyst.

Ma and Savage, 1987 [38] employed a gradientless fixed-bed reactor to study the kinetics of o-xylene transformation over a series of cation-exchanged (H^+, Li^+, Na^+, and K^+) USY, ZSM-5 and silicalite to observe the effects of site modification on the reaction. With the USY zeolites, the decrease in the catalytic activity is in the order: H-USY > Li-USY > Na-USY > K-USY. Adsorption, diffusion, and kinetic parameters were determined in the presence of the reaction using Laplace transform techniques and the method of moments. The obtained results generally agreed with literature data.

The simultaneous isomerization of ethylbenzene and m-xylene on zeolite catalysts, including Pt/Mordenite, Pt/USY, Pt/ZSM-5, and Pd/ZSM-5, was studied by Hsu et al., 1988 [41]. The activity of the catalyst was found proportional to the temperature and in the following order: Pt/Mordenite < Pt/USY < Pd/ZSM-5 < Pt/ZSM-

5. Pd/ZSM-5 was reported to be better than Pt/USY in both isomerization selectivity and P/O ratio, although both were good enough for the reactions, in comparison with Pt/Mordenite. A kinetic model with plausible reaction paths was proposed for the isomerization. The estimated reaction rate constants and activation energies indicated that the transformation of m-xylene to o- or p-xylene might be limited by the mass-transfer rate of the diphenylmethane-type intermediate, and the formation of o-xylene from ethylbenzene could be restricted by the smaller protonated cyclopropane intermediate.

2.10 Summary

The literatures reviewed clearly indicates that although several works have been conducted with regards to xylene transformation over zeolite-based catalysts, however, some aspects, such as the other reaction pathways apart from disproportionation and isomerization reaction pathways have received less attention. Moreover, all the previously reported kinetic studies on xylene transformation have been conducted using fixed-bed reactors, which are known to have some limitations of temperature and concentration gradients.

2.11 References

[1] Sreedharan, V., Bhatia, S., Vapor phase isomerization study of m-xylene over a nickel hydrogen mordenite catalyst. Chem. Eng J., (Amsterdam, Netherlands) 36(1987), 101-9.

[2] Lanewala, M.A., Bolton, A.P., The Isomerization of the Xylenes Using Zeolites Catalysts. J. Org. Chem., 34 (1969), 3107.

[3] Chatterjee, M., Ganguli, D., Conversion of o-xylene over multicationic zeolite Y catalysts. Ind. J. Tech., 23 (1985), 80-3.

[4] Molina R., Schutz A., Poncelet G., Transformation of m-Xylene over Al-Pillared clays and Ultrastable Zeolite Y. J. Catal., 145 (1994). 79.

[5] Yang, M.G., Nakamura, I., Fujimoto, K., m-Xylene Transformation over NiS/Al2O3-USY Hybrid Catalysts: Effects of Hydrogen Spillover. Appl.Catal. A., 144 (1996), 221-235.

[6] Morin, S., Gnep, N.S., Guisnet, M., A Simple Method for Determining the Relative Significant of the Unimolecular and Bimolecular Pathways of Xylene Isomerization over HY Zeolites. J. Catal., 159 (1996), 296.

[7] Cortes, A., Corma A., The Mechanism of Catalytic Isomerization of Xylenes: Kinetic and Isotopic Studies. J. Catal., 51 (1978), 338.

[8] Sulikowski, B., Datka, J., Gill, B., Ptaszynski, J., Klinowski, J., Acidity and Catalytic Properties of Realuminated Zeolite Y. J. Phys. Chem. B, 101(1997), 6929.

[9] Morin, S., Ayrault, P., Gnep, N.S., Guisnet, M., Influence of the Framework Composition of Commerical HFAU Zeolites on their Activity and Selectivity in m-Xylene Transformation. Appl. Catal. A, (1998a), 166, 128.

[10] Pamin, K., Kubacka, A., Olejniczak, Z., Haber ,J., Sulikowski, B., Immobilization of Dodecatungstophosphoric acid on Dealuminated Zeolite Y: A Physicohemical Study. Appl. Catal. A., 194-195 (2000), 137-146.

[11] Morin, S., Gnep, N.S., Guisnet, M., Influence of Coke Deposits on the Selectivity of m-Xylene Transformation and on the Isomerization Mechanism. Appl. Catal. A., (1998b)168, 63.

[12] Cerqueira, H. S., Rabeharitsara, A., Ayrault, P., Datka, J., Magnoux, P., Guisnet, M., Influence of the ageing of zeolite coke on composition and deactivating effect. Stud. Surf. Sci. Catal., (2001), 139.

[13] Cerqueira H.S., Ayrault P., Datka J., Magnoux P., Guisnet M., m-Xylene Transformation over a USHY Zeolite at 523 and 723 K: Influence of Coke Deposits on Activity, Acidity, and Porosity. J. Catal. 196 (2000), 149-157.

[14] Kaeding, W.W., Che, C., Young, L.B., Weinstein, B., Butter, S.A., Shape Selective Reactions with Zeolite Catalysts II. Selective Disproportionation of Toluene to Produce Benzene and p-xylene. J. Catal. 69 (1981), 392.

[15] Kurschner, U., Jerschkewitz, H. G., Schreier, E., Volter, J., Shape Selectivity of Hydrothermally Treated HZSM-5 in Toluene Disproportionation and Xylene Isomerization. Appl. Catal., 57 (1990), 167-177.

[16] Shashikala J. R., Satyanarayana, C.V.V., Chakrabarty, D.K., Shape Selective Catalysis by ZSM-35 Zeolites. Dispropotination of Ethyl benzene and Isomerization of m-Xylene Appl. Catal. A: General, 69(1991), 177-186.

[17] Araujo, A.S., Domingos, T.B., Souza, M.J.B., Silva, A.O.S., m-Xylene Isomerization in SAPO-11/HZSM-5 Mixed Catalyst. React. Kinet. Catal. Lett. 73 (2001), 283-290.

[18] Yashima, T., Sakaguchi, Y., Namba, S., Selective Formation of para-Xylene by Alkylation of Toluene with Methanol on ZSM-5 Type Zeolites. Stud. Surf. Sci. Catal. 7(1982), 418.

[19] Martens, J. A., Perez-Pariente, J., Sastre, E.; Corma, A., Jacobs, P. A. Isomerization and disproportionation of m-xylene: selectivities induced by the void structure of the zeolite framework. Appl. Catal., 45(1988), 85-101.

[20] Aboul-Gheit, Ahmed K., Abdel-Hamid, Sohair M., Abdel-Hay, Farouk M., Isomerization of xylene isomers on a platinum-rhenium-H-mordenite catalyst. Appl. Catal., A: General, 93(1993), 131-40.

[21] Hong, Y., Gruver, V., Fripiat, J. J., Role of Lewis acidity in the isomerization of n-pentane and o-xylene on dealuminated H-mordenites. J. Catal. 150 (1994), 421.

[22] Benazzi, E., Silva, J. M., Ribeiro, M. F., Ribeiro, F. R., Guisnet, M., Isomerization of C_8 aromatic cut. Improvement of the selectivity of MOR and MFI catalysts by treatment with aqueous solutions of (NH4)2SiF6. Stud. Surf. Sci. Catal., 97 (1995), 393-400.

[23] Perez-Pariente, J., Sastre, E., Fornes, V., Martens, J. A., Jacobs, P. A., Corma, A., Isomerization and Disproportionation of m-Xylene over Zeolite Beta. Appl. Catal., 69 (1991), 125-37.

[24] Rakshe, B., Ramaswamy, V., Ramaswamy, A. V., Acidity and m-Xylene Isomerization Activity of Large Pore, Zirconium-Containing Aluminosilicate with BEA Structure. J. Catal., 188 (1999), 252-260.

[25] Mavrodinova, V. P., Popova, M. D., Neinska, Y. G., Minchev, C. I., Influence of the Lewis acidity of indium-modified beta zeolite in the m-xylene transformation. Appl. Catal., A: General, 210 (2001), 397-408.

[26] Laforge, S., Martin, D., Paillaud, J. L., Guisnet, M., m-Xylene transformation over H-MCM-22 zeolite 1. Mechanisms and location of the reactions. J. Catal. 220 (2003), 92-103.

[27] Laforge, S., Martin, D., Guisnet, M., m-Xylene transformation over H-MCM-22 zeolite. 2. Method for determining the catalytic role of the three different pore systems. Micropor. Mersopor. Mater., 67 (2004), 235-244.

[28] Ratnasamy, P., Bhat, R. N., Pokhriyal, S. K., Hegde, S. G., Kumar, R., Reactions of aromatic hydrocarbons over zeolite beta. J. Catal., 119 (1989), 65-70.

[29] Morin, S., Ayrault, P., El Mouahid, S., Gnep, N. S., Guisnet, M., Particular selectivity of m-xylene isomerization over MCM-41 mesoporous aluminosilicates. Appl. Catal., A: General, 159 (1997), 317-331.

[30] Jones, Christopher W., Zones, Stacey I., Davis, Mark E., m-Xylene reactions over zeolites with unidimensional pore systems. Appl. Catal., A: General, 181 (1999a), 289-303.

[31] Jones, Christopher W., Zones, Stacey I., Davis, Mark E., Reactions of m-xylene on zeolites with intersecting medium and large pores part 2: aluminum population in structures with CON topology. Micropor. Mersopor. Mater. 28 (1999b), 471-481.

[32] Guisnet, M., Gnep, N.S., Morin, S., Micropor. Mersopor. Mater. 35, 47, (2000).

[33] Corma, A., Sastre, E., Evidence of the Presence of a Bimolecular Pathway in the Isomerization of Xylene on Some Large-Pore Zeolites J. Catal. 129 (1991), 177.

[34] Mirth, G., Cejka, J., Lercher, A.J., Transports and Isomerization of Xylenes over HZSM-5 Zeolites, J. Catal. 139 (1993), 24.

[35] Collins, Dermot J., Medina, Roger J., Davis, Burtron H., Xylene isomerization by ZSM-5 zeolite catalyst.Canadian J.Chem. Eng., 61(1983), 29-35.

[36] Hanson, K. L., Engel, A. J., Kinetics of xylene isomerization over silica-alumina catalyst. AIChE J., 13(1967), 260-6.

[37] Do D.D., Enhanced Paraxylene Selectivity in a Fixed-Bed Reactor. AIChE J. 31(1985), 574.

[38] Ma, Y. H., Savage, L. A., Xylene isomerization using zeolites in a gradientless reactor system. AIChE J. 33 (1987), 1233-40.

[39] Li, Yu-Guang, Jun, Hu., Kinetics study of the isomerization of xylene on ZSM-5 zeolites: the effect of the modification with MgO and CaO. Appl. Catal., A: General 142(1996), 123-137.

[40] Hopper, J. R., Shigemura, Dennis S., Kinetics of liquid phase xylene isomerization over H-mordenite. AIChE J., 19(1973), 1025-32.

[41] Hsu, Y. S., Lee, T. Y., Hu, H. C., Isomerization of ethylbenzene and m-xylene on zeolites. Ind. Eng. Chem. Res., 27 1988), 942-7.

[42] Gendy, Tahani S., Simulation of liquid and vapor phase xylene isomerization over deactivating H-Y-zeolite. J. Chem. Tech. & Biotech., 73(1998), 109-118.

[43] Cappellazzo, O., Cao, G., Messina, G., Morbidelli, M., Kinetics of shape-selective xylene isomerization over a ZSM-5 catalyst. Ind. Eng. Chem. Res., 30 (1991), 2280-7.

[44] Gajewski, F., Sulikowski, B., m-Xylene conversion over dealuminated Y zeolites studied by the pulse method. React. Kinet. Catal. Lett., 9 (1978), 395-9.

[45] Corma A., Llopis F., Monton J.B., Influence of the Structural Parameters of Y Zeolite on the Transalkylation of Alkylaromatics. J. Catal., 140 (1993), 384.

[46] Beschmann, K., Riekert, L., Mueller, U., Shape-selectivity of large and small crystals of zeolite ZSM-5. J. Catal. 145 (1994), 243-5.

[47] Liang, W., Chen, S., Peng, S., A model for highly para-selective reactions in HZSM-5 zeolite catalyst. Chem. Eng. Sci., 50(1995),2391-6.

[48] Li, Y., Jun H., Kinetics Study of the Isomerization of Xylene on ZSM-5 Zeolites. The Effect of the modification with MgO and CaO. Appl. Catal. A: General, 142 (1996), 123.

[49] Silvestri, A. J., Prater, C. D., Kinetic studies of the selectivity of xylene isomerization over silica-alumina catalyst. J. Phy. Chem., 68 (1964), 3268-81.

[50] Bhattacharya, R.N.; Rao, H. S. Isomerisation of xylenes over a silica-alumina catalyst. J. Appl. Chem. Biotech., 25(1975), 183-94.

[51] Bhatia, S., Chandra, S., Das, T., Simulation of the xylene isomerization catalytic reactor. Ind. Eng. Chem. Res., 28 (1989), 1185-90.

CHAPTER 3

3 Experimental Section

The experimental work developed in the present study was based on the following tasks: catalyst preparation, catalyst characterization and activity evaluation. This chapter describes the experimental setup, the analytical equipment, and the procedure adopted for carrying out the study.

3.1 Catalyst Preparation

Nowadays the FCC catalysts are composite materials containing frequently more than one type of zeolite. However, the Y-zeolite remains the principal source of catalytic activity. Kaolin clay is present as a filler to dilute the activity and to provide mechanical strength. Binders, such as silica sol, are added to provide physical integrity to the catalyst particles.

Combination of materials, such as binders and fillers, is referred to as the catalyst matrix [1]. As a result, most commercial FCC catalysts contain between 15 and 40 percent zeolite, between 15 and 30 percent binder, with the balance being the filler [2].

Commercial zeolites with similar crystal sizes were used for catalyst preparation. The characteristic of the zeolites, used in this study, is described in Table 3.1. In order to prepare 100 g of FCC catalyst, 30 g of zeolite was mixed with 50 g of kaolin (filler) and

Table 3.1 Physico-chemical properties of the as-prepared H-Y and dealuminated Y zeolites

	Zeolite				
	H-Y	USY-1	USY-2	USY-3	USY-4
Steaming temperature (°C)	-	800	600	710	600
Steaming time (h)	-	6	5	3	2
Crystal size (μm)	0.9	0.9	0.9	0.9	0.9
BET surface area (m^2/g)	187	155	174	168	183
Total acidity (mmol/g)	0.545	0.033	0.09	0.14	0.22

20 g of silica sol (binder). The resulting slurry was spray dried. The formed catalyst pellet had a particle size in the range of 70-80 μm (Figure 3.1). Such a catalyst particle size was needed for evaluating catalyst activity in the riser simulator unit. Subsequently, the catalyst powder was calcined at 600 °C for 2 h in an oven to remove all volatile material. The calcined catalyst was then steamed.

3.2 Steaming

The steaming of the fresh catalyst is an operation that precedes catalyst testing. The objective of this pretreatment is to deactivate the FCC catalyst. Laboratory steaming of fresh FCC catalysts is generally performed in the presence of 100 percent steam in a fluid-bed of inert gas (nitrogen) while the temperature is increased to the desired value. Steam, obtained by vaporization of injected water, is introduced and the nitrogen flow was stopped. After a specified period of time, say 6 h, the water injection system is arrested and nitrogen gas is introduced again reducing the temperature back to an ambient value. Then the catalyst is unloaded and screened to remove fines. Steaming conditions employed in the present study are shown in Table 3.1.

3.3 Catalyst Characterizations

Several methods are used to characterize the fresh and steamed catalysts. These methods can be used to describe the changes that occur in the catalyst during the transformation process. These are related to desirable or undesirable changes in the selectivity and activity of the catalysts [3].

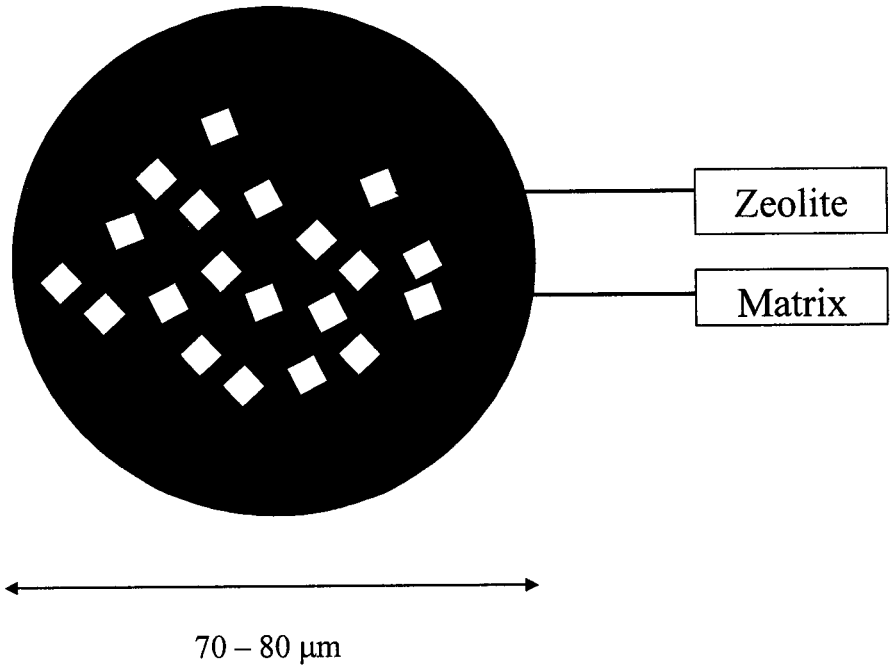

Figure 3.1 Schematic representation of catalyst particle

In general, the zeolite is designed to be hydrothermally dealuminated while being steamed in a controlled and stable manner to the desired unit cell size and surface area. Thus, catalyst characterization on the basis of surface area and unit cell size is essential to define key features (e.g degree of steaming) and to understand variabilities in catalyst performance.

3.3.1 Surface Area

The surface area of a FCC catalyst is the result of the combined contribution of the zeolite and matrix components. A high surface area is characteristic of well crystallized zeolite. Since the catalytic cracking reactions take place on the surface of the catalyst, knowledge of the specific surface area is essential.

The BET surface area was measured, in the present study, according to the standard procedure ASTM D-3663 using Sorptomatic 1800 Carlo Erba Strumentazione unit, Italy. In this unit the volume of gas adsorbed is calculated by the variation in pressure due to the adsorption of a known volume of nitrogen. To obtain a multipoint adsorption isotherm, the amount of nitrogen adsorbed at equilibrium, at its normal boiling point (-196°C), is measured over a range of nitrogen pressures below 250 mmHg. For all the samples, the BET surface area measurements were carried out after outgassing the catalyst sample at 150°C under a vacuum of 0.04 mmHg for about four hours.

3.3.2 Unit Cell Size

X-ray diffraction (XRD) was used to identify the structure, composition and amounts of crystalline materials, such as zeolite and alumina. Also, the unit cell size was determined from XRD spectra. Unit cell measurement by XRD has been standardized as

the ASTM test D-3942. Unit cell size increases with aluminum content because the Si-O-Si bond is shorter than the Si-O-Al [3]. Hence the unit cell size is very important parameter to describe the Al framework content. Several correlations have been developed to correlate Al content of the faujasite framework to unit cell size. All these correlations are generally very close to each other [3].

An explanation of the principle of the technique is illustrated in Figure 3.2. The crystalline compound forms a series of repeating planes with a spacing of a few tenths of a nanometer and each atom in the plane scatters radiation. A part of the wave front interacts with the electrons associated with each atom on the plane that re-emits a spherical wavelet [3].

The re-emitted in phase waves give a peak at the detector for a certain angle 2θ, such that the distances passed by the wavelets differ by an integral wavelength. The amplitude of the wave reflected from neighboring atoms is out of phase at any other different angle, with the wave from second neighbors being twice as much out of phase. Finally, the negative amplitude of the reflected wave from some neighbor atoms cancel the reflection from the first and so on until there is a net cancellation. Hence, the angle 2θ is a measure of the distance (d) between planes (Peters, 1993). In this method a sample of the zeolite or catalyst containing zeolite was mixed with powdered silicon. The zeolite unit cell dimension was calculated from the X-ray diffraction pattern of the mixture, using the silicon reflections as a reference.

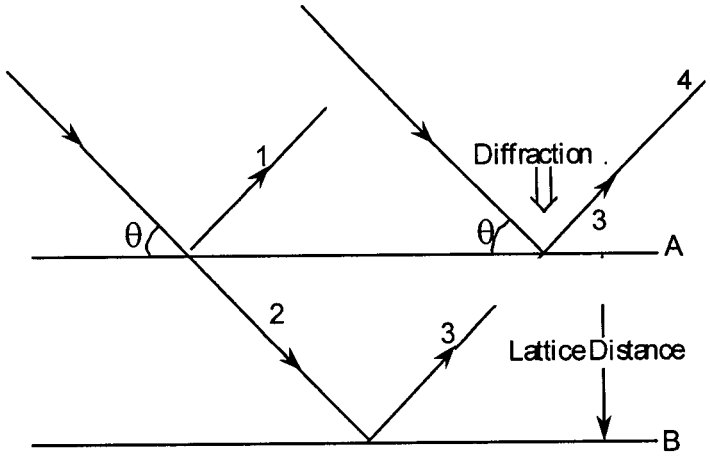

Figure 3.2 Technique of X-ray diffraction.

3.4 Catalyst Evaluation

The catalytic reaction experiments are carried out in the present study using a riser simulator as a test unit. The riser simulator is basically a mini fluidized-bed reactor operating in the batch mode with intense gas recirculation. The following section describes the experimental setup, and the experimental procedure adopted during this study.

3.4.1 Experimental Set-up

Experimental runs were carried out in a riser simulator reactor in operation at the catalysis research laboratory of CHE-KFUPM. The reactor was connected to a vacuum box through a four-port valve. The products were removed from the riser simulator at the end of the pre-set reaction period. A time/actuator assembly linked to the feed injection system controlled the four-port valve. The vacuum system was connected to a manually operated six-port sampling valve. This sampling valve was connected on-line to the gas chromatograph. Furthermore, the riser simulator reactor and the vacuum box were equipped with pressure transducers to monitor the pressure during and after the reaction periods. Both the reactor and the vacuum system were supplied with separate heating systems and both were well insulated.

The feed injecting system includes a gas tight syringe connected to switches to control the timer/actuator assembly on the four port valve and the data acquisition system. The data acquisition system allowed monitoring the pressure profiles with time from the reactor and the vacuum box.

A schematic diagram of the experimental setup is given in Figure 3.3. All main parts of the setup will be discussed in detail in the following section.

3.4.1.1 Riser Simulator

The riser simulator is a fluidized-bed reactor invented by de Lasa, 1991 [4] and it was designed and operated to provide high gas phase circulation rates as well as intense catalyst mixing. As mentioned by Pruski et al. [5] good fluidization is achieved under typical riser conditions using shaft spinning rates close to 7600rpm.

In addition to the riser simulator itself, the following components completed the reactor set up:

a) a heated injector system,

b) a 4- and 6- port valve,

c) a heated vacuum chamber,

d) pressure transducers,

e) insulated transfer lines,

f) computer controlled timers and actuators.

Figure 3.4 shows a cross-sectional view of the riser simulator. A comprehensive description of the construction and operation of this unit are given in the work by Pruski et al. [5] and Kraemer [6].

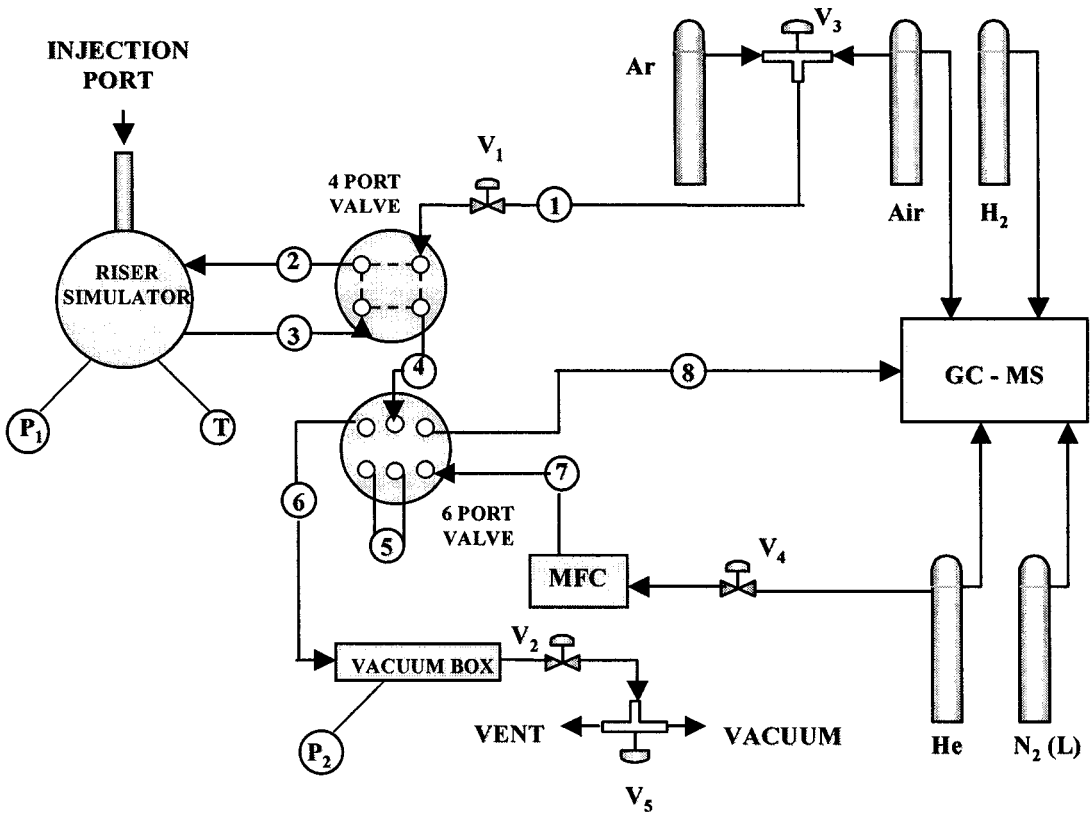

Figure 3.3 Schematic diagram of the experimental setup

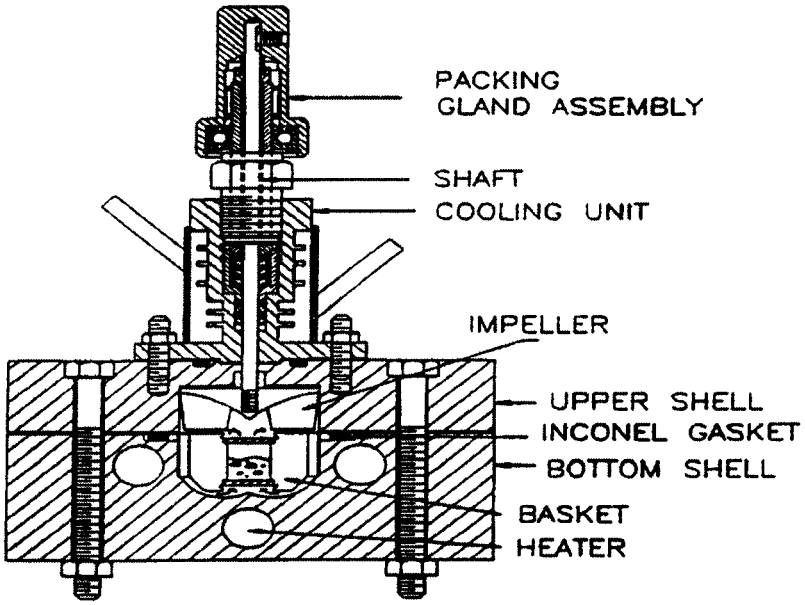

Figure 3.4 Schematic diagram of the riser simulator

3.4.1.1.1 Heated Injector System

The injector system consists of a gas tight glass syringe, which is fitted with a parallel threaded support rod and a threaded disc placed between two nuts limiting the motion of the syringe plunger. The disc is fixed at the support rod, allowing the syringe to intake, for every injection, a fixed amount of reactant from the reservoir chamber.

The injector system contained two electrically actuated micro-switches fixed at opposite ends of the sliding support rod. While one of the switches controls the data acquisition system, the other controls the timer/actuator assembly of the four-port valve. In the sample position of the three-way valve, the syringe is attached to the reactant container. The syringe fills the required amount of the reactant as soon as the plunger is pulled backwards. Meanwhile, the plunger presses against one of the switches, preventing data acquisition pressure signals.

The feed syringe is connected to its needle. Thus, when the plunger is pushed forward, the feed sample is delivered to the reactor. At this point, the micro-switch is released, hence initiating the data acquisition program. Moreover, when the plunger is fully pushed forward, it presses against another switch connected to the timer/actuator assembly of the 4-port valve. Consequently, the timer starts to count down the pre-set reaction time, upon which the timer would activate the actuator. The 4-port valve is then opened by the actuator, equalizing the pressure between the reactor and the vacuum box, thereby terminating the reaction.

3.4.1.1.2 4-Port and 6-port valves

The reactor is connected to the air/argon supply through a 1/8 inch 4-port valve. The other end of this valve is used to connect the reactor with the vacuum box. In both positions, there are always two paths available through the valve for the reaction products to move along. In the open position, the reaction products are transferred through the valve, into the reactor through an inlet port. Then, they move out of the reactor through an outlet port, back into the valve and finally reach the vacuum box. In the closed position, however, the reactor is completely isolated from the rest of the system and connected to itself through two of the four ports of the valve.

The sample injection valve (1/8" 6-port chromatographic valve) is installed between the vacuum box and the GC. For both positions, there are always two independent loops for the gases to pass through. While one path connects the vacuum box to the vent/vacuum pump, the other joins the helium carrier gas with the GC detector. The position of the valve determines the path which includes the sample loop.

3.4.1.1.3 Vacuum System

The vacuum system consists of a 485 cm^3 stainless steel cylinder fixed between the 4-port and the 6-port valves. These components together with two on-off valves, two three- way valves, and two position selector valves are placed inside a heated box. The V_1 valve (Figure 3.3) is connected between the air/argon gas supply bottles and the first "on-off" valve. This valve connects the gas bottle to the reactor and to the gas system. In addition, V_1 connects to the 4-port valve through V_2 (Figure 3.3). Finally, V_2 allows the separation of the entire system from the gas supply.

The stainless steel cylinder works as a sink for the reaction products. It has a large volume. In addition, an important pressure difference, with respect to the reactor, facilitates a quick and easy removal of reaction products as well as unreacted hydrocarbons. This rapid evacuation is needed to prevent further progress of cracking reactions after the pre-set time.

The second isolation valve V_3 is essential to control product sampling (Figure 3.3). This valve is set in closed position during post reaction evacuation period keeping the reaction products within a volume of set dimensions.

The second three-way valve (V_4) is connected between V_3 and the vacuum pump/vent line. This valve allows incorporating or removing the vacuum pump in the path of the exhaust gases going to the fume hood. The main function of vacuum pump is to reduce the pressure within the vacuum box to around 0.5 psia (almost vacuum) prior to the reaction test.

Between the second isolation valve (V_3) and the vent line/vacuum pump, there is a glass bottle. This glass bottle provides a lower pressure than the one in the vacuum box and an extra driving force for filling the sample loop of the 6-port valve.

3.4.1.1.4 Heating and Insulation

Heating tapes and insulation cover all of the connecting lines between the vacuum box and the two chromatographic valves. There are six heating tapes; each of them is connected to a Variac-type power supply. This system helps to keep the lines at high temperature, preventing hydrocarbon condensation in the lines and valves. Furthermore, the reactor is insulated to maintain close to isothermal operating conditions. Maximum temperature deviation during experiments is only of a few degrees centigrade.

3.4.1.1.5 Control Devices

a)- Temperature control: There are two independently powered controlled heater systems. One controller keeps the reaction temperature constant at around 525°C by means of four heating rods. These heaters are inserted in the bottom shell of the riser simulator. However, the top section of the riser simulator is directly heated using two smaller insertion rod heaters directly powered by Variacs.

b)- Pressure Transducers: The reactor and the vacuum box are provided with two identical Omega pressure transducers, series PX-303. Figure 3.3 shows P_1 and P_2 which represent the location of the reactor and the vacuum box transducers respectively. Each transducer is powered by its own power supply. Furthermore, these transducers have a calibrated span of 0-50 psia with 0.25% accuracy, 1 ms response time and a 0.5-5.5 Volt output signal range. The transducers are also equipped with protective pressure adjusts to take care of any sudden pressure spikes or fluctuations.

c)- Thermocouples: Several thermocouples are fixed around the riser simulator reactor to accurately monitor the temperature. Two thermocouples are connected to the reactor and the valve block. Other thermocouples are fixed at the following places:

Impeller shaft cooling jacket (20°C-40°C)

Upper reactor shell section (425°C-475°C)

Lines from the reactor to the 4-port valve (275°C-300°C)

4-port valve body (225°C-250°C)

Vacuum box (350°C-390°C)

Lines between 6-port valve and vacuum box (225°C-250°C)

6-port valve sampling loop (250°C-275°C)

Line from 6-port valve to GC (275°C-300°C)

Gas oil reservoir (50°C-75°C)

Note that the values in brackets indicate typical temperature ranges using in the various riser simulator ranges.

3.5 Analytical Equipment

3.5.1 Gas Chromatograph System

The GC system consists of a 60 meters long INNOWAX capillary column, an FID-type detector and a temperature controlled oven. While helium is used as the sample carrier gas, air and hydrogen are used as the gases for the FID detector. Furthermore, liquid nitrogen is used to facilitate the initial cryogenic operation of the GC temperature program. The liquid nitrogen cools the GC oven to -30°C. The flow of liquid nitrogen is administered by a solenoid valve actuated from the GC's internal oven temperature controller. The integrator allows strip chart recording as well as integration of the GC detector signal. The integrator is connected to the GC via the HP-IL instrument network cabling system. A detailed diagram of the experimental set-up is shown in Figure 3.3

A Mettler balance is used to accurately weigh the catalyst sample. A Hamilton gas tight syringe was calibrated for the different feed stock. Analytical weights are of precision grade or calibrated against a set of certified standard weights. Availability of this balance is of major importance for good balance calculations.

3.5.2 Coke Analyzer

Coke deposited on spent catalyst is determined, by a common combustion method. In this method, a carbon analyzer Cs-244 is used. Oxygen is supplied to the unit directly. A small amount of spent catalyst (0.25g) is used for the analysis. The coke laid

out on the sample during reaction experiments is burned completely converting the carbonaceous deposit into carbon dioxide. The moles of carbon dioxide formed are measured, and thus the coke formed is determined.

3.5.3 Procedure

All catalysts were tested at five different contact times (3, 5, 7, 10 and 15 sec). Different reaction temperature levels are also used such as 350, 400, 450, 500 and 550°C. In addition, more than three repeat runs are conducted at each experimental condition.

Regarding the experimental procedure in the riser simulator, 0.8 g of catalyst is weighed and loaded into the riser simulator basket. The system is then sealed and tested for any pressure leaks by monitoring the pressure changes in the system. Furthermore, the reactor is heated to the desired reaction temperature. The vacuum box is also heated to around 250 °C and evacuated at around 0.5 psi to prevent any condensation of hydrocarbons inside the box. The heating of the riser simulator is conducted under continuous flow of inert gases (argon) and the process usually takes a few hours until thermal equilibrium is finally attained. Meanwhile, before the initial experimental run, the catalyst is activated for 15 minutes at 620°C with air. The temperature controller is set to the desired reaction temperature, likewise the timer is equally set to the desired reaction time. At this point the GC is started and set to the desired conditions.

Once the reactor and the gas chromatograph have reached the desired operating conditions, the feed stock is injected directly into the reactor via a loaded syringe while the impeller is rotating at a speed of 5500rpm. After the reaction, the four port valve immediately opens ensuring that the reaction is terminated and the entire product stream

sent online to the gas chromatograph via a pre-heated vacuum box chamber. The products were analyzed in a gas chromatograph with FID detector and capillary column INNOWAX, containing 60 meters cross-linked methyl silicone with internal diameter of the column, 0.32 mm. After each experimental runs the catalyst is regenerated at conditions similar to initial activation.

3.6 References

[1] Veuto, P.B., Habib, E.T., Fluid Catalytic Cracking with Zeolites Catalysts. Marcel Deckker, New York, (1979).

[2] Scherzer, J. Designing FCC Catalysts with High-Silica Y-Zeolites. Appl. Catal. (1991) 75, 1.

[3] Peters, A.W., Instrumental Methods for FCC Catalyst Characterization. Fluid Catalytic Cracking: Science and Technology, Magee, J.S., and Mitchell, M.M. (editors), Amesterdam: Elservier, (1993).

[4] de Lasa, H.I. U.S. Patent 5, 102 ,628, (1991).

[5] Pruski, J.; Pekediz, A.;de Lasa, H. Catalytic Cracking of Hydrocarbons in a Novel Riser Simulator: Lump Adsorption Parameters Under Reaction Conditions. Chem. Eng. Sci. (1996), 51,1799.

[6] Kraemer, D. W. Ph.D. Dissertation, University of Western Ontario, London, Canada (1991).

CHAPTER 4

4 Xylene Isomerization over USY Zeolite in a Riser Simulator: A Comprehensive Kinetic Model

4.1 Introduction

The kinetic study of catalytic isomerization of xylenes has gained considerable interest over the years. This is as a result of the significant contribution of such studies toward the understanding of the mechanism of the reaction over acid catalysts. The parameters obtained from such studies are often used in evaluating the relative magnitudes of the different reaction paths and the ease of interconversion between the three isomers. It can also be employed in designing commercial-scale reactors from experimental studies conducted in the laboratories.

In much of the literature, fixed-bed reactors are often utilized for the xylene isomerization reaction. However, as pointed out by Ma and Savage [1], many difficulties are encountered in using the fixed-bed reactor for this reaction because of its complex nature. Temperature and/or concentration gradients usually occur within the flowing phase of the catalyst bed, which often affects the values of kinetic parameters reported from such studies. Differential reactors and pulsed microreactors have been applied to reduce the gradient difficulties, but analytical problems due to low conversion levels have been identified and as such minimization of the bulk phase gradient may not be assured. It is well-known that the reaction system for xylene isomerization over zeolite catalysts is very complicated. This is due to the presence of other side reactions, such as dealkylation, disproportionation, and transalkylation, in addition to the isomerization

reaction. Several attempts have been made in the past to obtain suitable kinetic models for the reaction [1-11]. However, the complexity of the reaction and the interplay of the diffusion and chemical reactions, which causes different reaction paths, have often posed great obstacles. Consequently, two alternate reaction schemes have been proposed for the reaction in the literature. The first one, which is based on a triangular reaction path [2-6] assumes a direct interconversion between *o*- and *p*-xylene isomers. In contrast, the second scheme assumes that the reaction proceeds via 1, 2-methyl shifts following a sequence reaction path [7-11]. Furthermore, Corma and Sastre [12] and Guisnet et al. [13] have recently shown that bimolecular isomerization can contribute to the overall isomerization process for large pore zeolites. However, the dependence of this isomerization pathway on several factors such as reaction conditions, zeolite composition, and geometrical characteristics of the zeolite catalyst [12] has made its incorporation into the kinetic model very difficult.

In an earlier work, we have studied the kinetics of m-xylene isomerization at low conversion levels over a USY zeolite catalyst [14]. A simplified kinetic model, which excludes the disproportionation of *o*- and *p*-xylene and the interconversion between the two isomers, was proposed. This work extends the previous study by taking into account the disproportionation of the three isomers and the possible interconversion between *p*- and *o*-xylenes in a more detailed kinetic model. A unique modeling technique, which involves the isomerization of each of the pure xylene isomers, will be employed in obtaining the numerous model parameters. In addition, the riser simulator, which is operated as a batch, well-mixed fluidized-bed reactor will be utilized in the present study. Employing this reactor for the reaction can alleviate the problems of temperature and

concentration gradients associated with fixed-bed and other reactor types. It can also ensure uniform coke deposition on the catalyst particle and ease the control of operating conditions such as temperature, time, and amount of air.

4.2 Kinetic Modeling

To obtain reliable and reproducible kinetic parameters, a suitable kinetic model that can adequately represent the experimental data is necessary. As a first step toward achieving this, a proper reaction scheme must be utilized. In the present study, we propose the triangular reaction scheme (Scheme 1) depicted in Figure 4.1 for the experimental data obtained based on the overall xylene isomerization process. However, this scheme involves numerous adjustable kinetic parameters and as such it may not be feasible to estimate their values simultaneously using a single fitting procedure. As a result, we explore the possibility of deriving simplified effective kinetic models from isomerization of *m*-xylene (Scheme 2), *p*-xylene (Scheme 3) and *o*-xylene (Scheme 4) respectively, as shown in Figure 4.1. The following assumptions are made in developing the simplified models:

1. The isomerization and disproportionation reactions follow simple first-order kinetics [4,7,22].
2. The reverse reactions for conversion of *p*- to *o*-xylene and *o*- to *p*-xylene are neglected in Schemes 3 and 4 respectively. This is because of the large values of C_p/C_o and C_o/C_p ratios ($\approx$80/3) obtained from these reactions, indicating that the contribution of the reverse reaction paths in both cases can be neglected.

Table 4.1 Properties of the catalyst used in this study

Unit cell size (Å)	24.28
BET Surface Area (m^2/g)	155
Crystal size (μm)	0.9
Na_2O (wt%)	Negligible

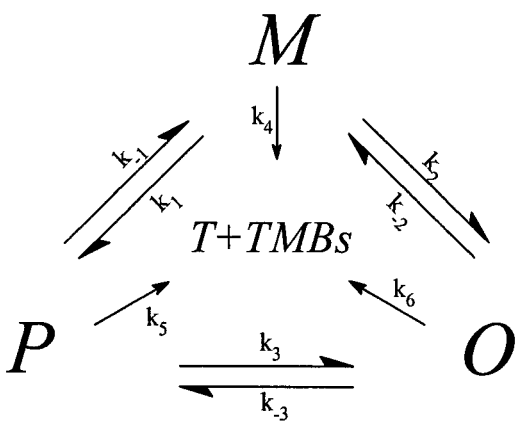

Scheme 1

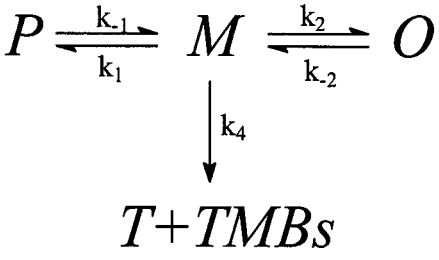

Scheme 2

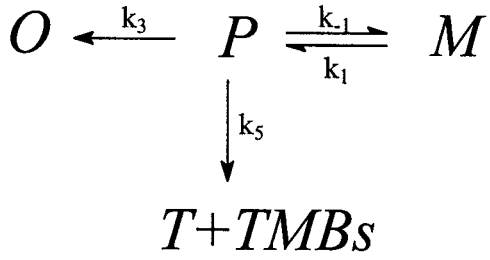

Scheme 3

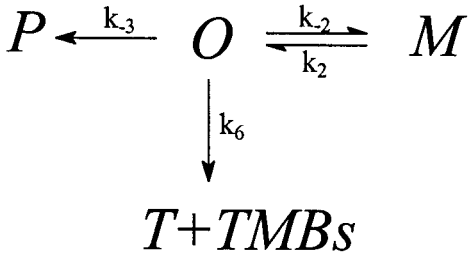

Scheme 4

Figure 4.1 Proposed reaction schemes

3. The disproportionation reaction producing toluene and trimethylbenzenes is mainly from the xylene used as the reactant [10].
4. An irreversible reaction path is assumed for the disproportionation reaction [7]. This is substantiated by the low xylene yield (max < 3%) observed when equivalent amounts of toluene and trimethylbenzenes were reacted under different reaction conditions in this work.
5. The reactor operates under isothermal conditions [15], which are justified by the negligible temperature change observed during the reactions.

The differential equations describing the kinetics of the xylene isomerization reaction based on the assumptions made above can be derived for each of the reacting species as follows:

m-xylene:

$$-\frac{V}{W_c}\frac{dC_m}{dt} = \varphi\left(k_1 + k_2 + k_4\right)C_m - k_{-1}C_p - k_{-2}C_o \tag{4.1}$$

$$\frac{V}{W_c}\frac{dC_p}{dt} = \varphi\left(k_1 C_m - k_{-1}C_p\right) \tag{4.2}$$

$$\frac{V}{W_c}\frac{dC_o}{dt} = \varphi\left(k_2 C_m - k_{-2}C_o\right) \tag{4.3}$$

$$\frac{V}{W_c}\frac{dC_d}{dt} = \varphi\, k_4 C_m \tag{4.4}$$

p-xylene:

$$-\frac{V}{W_c}\frac{dC_p}{dt} = \varphi\left(k_{-1} + k_3 + k_5\right)C_p - k_1 C_m \tag{4.5}$$

$$\frac{V}{W_c}\frac{dC_m}{dt} = \varphi(k_{-1}C_p - k_1 C_m) \tag{4.6}$$

$$\frac{V}{W_c}\frac{dC_o}{dt} = \varphi k_3 C_p \tag{4.7}$$

$$\frac{V}{W_c}\frac{dC_d}{dt} = \varphi k_5 C_p \tag{4.8}$$

o-xylene:

$$-\frac{V}{W_c}\frac{dC_o}{dt} = \varphi\left(k_{-2} + k_{-3} + k_6\right)C_o - k_2 C_m \tag{4.9}$$

$$\frac{V}{W_c}\frac{dC_m}{dt} = \varphi\left(k_{-2}C_o - k_2 C_m\right) \tag{4.10}$$

$$\frac{V}{W_c}\frac{dC_p}{dt} = \varphi k_{-3} C_o \tag{4.11}$$

$$\frac{V}{W_c}\frac{dC_d}{dt} = \varphi k_6 C_o \tag{4.12}$$

Regarding the catalyst deactivation function (φ) used in the above equations, it is well-known that carbon formation in catalytic cracking is responsible for the loss in activity and must be incorporated into kinetic models for catalytic cracking. Hopper and Shigemura [2] have shown that carbon formation, which is the primary cause for catalytic deactivation in the cracking reaction, is also considered to be the cause for deactivation in the xylene isomerization reaction. In this study the same exponential function $\varphi = \exp(-\alpha t)$ based on time on stream (TOS) will be employed in obtaining the model

parameters for the isomerization and disproportionation reactions because both take place on the same Brönsted sites [13].

The concentration of any species *i* is related to its mass fraction as follows:

$$C_i = \frac{y_i W_{hc}}{MW_i V} \tag{4.13}$$

while the influence of temperature on the model parameters can be accounted for through the following Arrhenius equations:

$$k'_i = k'_{0i} \exp(-\frac{E_i}{RT}) \tag{4.14}$$

The kinetic parameters obtained from eq 4.14 may show a mutual adverse effect of one parameter estimate (parameter correlation). Centering of some variables may often be helpful to reduce parameter interaction [25]. Agarwal and Brisk [26] showed that this reparametrization reduces the correlation between preexponential factors and activation energies. Therefore, k'_i constants were reparametrized by centering the temperature at an average reaction temperature of T_o.

$$k_i = k_{0i} \exp(\frac{-E_i}{R}[\frac{1}{T} - \frac{1}{T_0}]) \tag{4.15}$$

An important aspect in developing a reliable kinetic model for the reacting system is its thermodynamic consistency at equilibrium. This condition can be introduced in the model by enforcing that at equilibrium conditions the net rate of each reversible reaction in Schemes 1- 4 vanishes by using the following relationships [8]:

$$k_{-1} = k_1/K_{pm} \tag{4.16}$$

$$k_{-2} = k_2/K_{om} \tag{4.17}$$

where $K_{pm} = (C_p/C_m)_{eq}$ and $K_{mo} = (C_o/C_m)_{eq}$ are temperature dependent equilibrium

constants for *m*- to *p*-xylene and *m*- to *o*-xylene reactions respectively. However, an average value can be computed for both constants, because the thermodynamic equilibrium concentrations of the xylenes remain fairly constant within the temperature range of this work. The xylenes equilibrium concentrations are obtained from a published work [23].

The overall kinetic model (based on Scheme 1) can be obtained as follows:

$$\frac{dy_m}{dt} = -[(k_1 + k_2 + k_4)y_m - k_{-1}y_p - k_{-2}y_o]\frac{W_c}{V}\exp(-\alpha t) \tag{4.18}$$

$$\frac{dy_p}{dt} = [k_1 y_m + k_{-3}y_o - (k_{-1} + k_3 + k_5)y_p]\frac{W_c}{V}\exp(-\alpha t) \tag{4.19}$$

$$\frac{dy_o}{dt} = [k_2 y_m + k_3 y_p - (k_{-2} + k_{-3} + k_6)y_o]\frac{W_c}{V}\exp(-\alpha t) \tag{4.20}$$

$$\frac{dy_d}{dt} = [k_4 y_m + k_5 y_p + k_6 y_o]\frac{W_c}{V}\exp(-\alpha t) \tag{4.21}$$

Each set of equation for the simplified models (eqs 4.1-4.12) involves seven adjustable model parameters that have to be estimated before a solution is obtained. However, because the evaluation of these parameters a priori is not feasible, nonlinear regression analysis will be employed in fitting the experimental data to the model, as will be discussed in the next section.

4.3 Results

4.3.1 Experimental Data

The product distribution for the isomerization of *m*-, *p*- and *o*-xylenes over a USY zeolite catalyst is presented in Table 4.2 – 4.4 respectively. In addition, traces of benzene

and tetramethylbenzenes were also observed. However, the yields of these products were consistently very low, and as a result they were neglected in subsequent analyses. It can be seen from these tables that the yield of the various products increases steadily with both reaction time and temperature. This might suggest that the obtained product yields are below the thermodynamic equilibrium values. Also, the conversion obtained during the isomerization of *o*-xylene at 350°C is too low (< 1.5%) to be reported as kinetic data. Furthermore, it is obvious that higher conversions are obtained for the isomerization of *p*-xylene. This indicates that under the conditions of the present study, the USY zeolite used has a higher activity for the isomerization of *p*-xylene than that for both *m*- and *o*-xylenes. This is further elucidated from the estimated rate constants, as shown in the next section. It can also be observed that the amount of toluene and trimethylbenzenes formed from the isomerization of all the three isomers is quite high. This is expected, because the USY zeolite used belongs to the class of 12MR zeolites with larger pores that can accommodate the transition-state complexes required for the disproportionation reaction [28].

From the values of the fitted kinetic parameters (Table 4.5), it can be seen that the order of magnitude of the reaction rate constants for the unimolecular isomerization reaction is as follows: $k_{-1} > k_{-2} > k_1 > k_2 >> k_3 > k_{-3}$. Moreover, the rate constant for the isomerization of *p*- to *m*-xylene is initially about 3 orders magnitude greater than that of *p*- to *o*-xylene, and it decreased by half of this value with an increase in the reaction temperature. On the other hand, the rate constant for the isomerization of *o*- to *m*-xylene

Table 4.2 Product distribution at various reaction conditions for m-xylene isomerization*

temp, °C	time, sec	mass fractions (%)				
		m-X	*p*-X	*o*-X	*T*	*TMBs*
350	3	98.40	0.458	0.828	0.254	0
	5	98.02	0.491	0.869	0.352	0.098
	7	97.70	0.540	0.919	0.546	0.224
	10	96.90	0.699	1.034	0.762	0.541
	11	96.75	0.739	1.061	0.822	0.610
	13	96.63	0.800	1.097	0.654	0.690
	15	96.32	0.764	1.054	1.043	0.757
400	3	97.79	0.600	0.960	0.458	0.192
	5	96.68	0.909	1.204	0.698	0.507
	7	95.55	1.179	1.456	0.993	0.822
	10	94.92	1.220	1.500	1.263	1.038
	11	94.63	1.620	1.880	1.744	1.176
	13	92.38	1.626	1.929	2.000	2.060
	15	91.49	2.110	2.300	2.030	2.080
450	3	96.08	1.072	1.356	0.873	0.616
	5	91.76	2.154	2.317	1.804	1.790
	7	89.90	2.590	2.780	2.140	2.420
	10	88.70	2.810	3.030	2.490	2.813
	11	88.72	2.918	3.010	2.597	2.549
	13	86.94	2.810	3.093	3.381	3.520
	15	86.11	3.718	3.683	3.098	3.106
500	3	90.83	2.220	2.480	2.230	2.185
	5	87.96	2.890	3.110	2.824	2.940
	7	85.8	3.489	3.668	3.320	3.648
	10	83.56	3.733	3.858	4.209	4.162
	11	82.06	3.700	3.890	4.851	4.822
	13	80.22	4.345	4.454	5.159	5.210
	15	78.35	4.480	4.622	5.860	5.906

* reported experimental data are averages of at least three measurements

Table 4.3 Product distribution at various reaction conditions for *p*-xylene isomerization*

temp, °C	time, sec	mass fractions (%)				
		m-X	*p*-X	*o*-X	*T*	*TMBs*
350	3	0.615	98.40	0.201	0.577	0.191
	5	0.684	98.00	0.227	0.618	0.296
	7	0.792	97.65	0.256	0.730	0.364
	10	0.956	96.85	0.260	1.100	0.643
	15	1.287	95.71	0.306	1.541	0.973
400	3	0.966	97.51	0.290	0.693	0.347
	5	1.180	96.20	0.360	1.368	0.697
	7	1.845	94.74	0.413	1.636	1.089
	10	2.401	91.77	0.586	2.824	2.054
	15	3.869	87.59	0.832	3.963	3.182
450	3	1.923	94.87	0.502	1.436	0.951
	5	2.548	93.02	0.595	1.975	1.501
	7	3.591	89.71	0.893	2.964	2.355
	10	4.486	86.11	1.155	4.121	3.442
	15	6.191	80.24	1.649	5.856	5.095

* reported experimental data are averages of at least three measurements

Table 4.4 Product distribution at various reaction conditions for *o*-xylene isomerization*

temp (°C)	time (sec)	mass fractions (%)				
		m-X	*p*-X	*o*-X	*T*	*TMBs*
400	3	0.385	0.041	98.71	0.492	0.180
	5	0.565	0.062	98.16	0.600	0.354
	7	1.734	0.220	95.80	1.065	1.090
	10	1.675	0.178	95.48	1.277	1.140
	15	2.233	0.240	93.86	1.749	1.662
450	3	1.400	0.250	96.71	0.780	0.600
	5	2.094	0.374	94.92	1.281	1.136
	7	2.619	0.473	93.02	1.831	1.726
	10	4.235	0.808	89.50	2.527	2.578
	15	5.899	1.110	85.49	3.468	3.583
500	3	2.404	0.623	94.08	1.356	1.238
	5	3.508	0.827	91.31	2.030	1.925
	7	4.848	1.277	87.69	2.853	2.824
	10	5.657	1.565	84.54	3.757	3.809
	15	7.846	2.194	78.25	5.279	5.538

* reported experimental data are averages of at least three measurements

is initially 140 times greater than that of *o*- to *p*-xylene and is increased to 4 times this magnitude with an increase in the temperature. Furthermore, the rate constants for the isomerization of *m*- to *p*-xylene and *m*- to *o*-xylene are closely identical, with the former being slightly higher.

4.3.2 Reaction Rate Constants

It is of great interest to note that the rate constants for the disproportionation of xylenes are in the following order of magnitude: $k_5 > k_4 \approx k_6$ (Figure 4.2) which is consistent with the obtained experimental data. From Figure 4.2, it is also obvious that while k_5 varies significantly with the reaction temperature, k_4 and k_6 are less affected by temperature changes.

4.3.3 Apparent Activation Energies

The results in Table 4.5 show that the apparent activation energies for interconversion of *p*- to *o*-xylene is about 6-7 kcal/mol higher than the other unimolecular isomerization reactions. However, it is on average about 5 kcal/mol higher than those required for disproportionation reactions. This result is in qualitative agreement with the works of Hopper and co-workers [2,3] for the liquid-phase xylene isomerization over H-Mordenite. Another important result is the lower value of E_5 as compared to both E_4 and E_6.

Table 4.5 Estimated kinetics parameters

temp, °C	rate constant, k_i^* ($x10^8$)								
	k_1	k_{-1}	k_2	k_{-2}	k_3	k_{-3}	k_4	k_5	k_6
350	4.06	9.02	2.75	5.96	0.008	0.004	1.14	15.91	1.59
400	7.50	16.70	5.27	11.44	0.020	0.010	2.47	28.42	3.27
450	12.75	28.37	9.24	20.00	0.050	0.030	4.83	46.87	6.08
500	20.23	45.00	15.05	32.67	0.110	0.060	8.66	72.44	10.43
E_i^{**}	10.25	10.24	10.91	10.85	16.51	17.08	12.96	9.67	12.04
95% *CL*	1.6	1.6	1.4	1.4	0.8	1.0	0.8	1.1	1.4
$k_{oi}x10^3$	0.16	0.36	0.17	0.38	5.08	4.04	0.40	0.39	0.26
95%$CL10^3$	0.042	0.042	0.044	0.044	0.034	0.023	0.08	0.068	0.04

*k_{0i} (m^3/kgcat.s)

**E_i (kcal/mole)

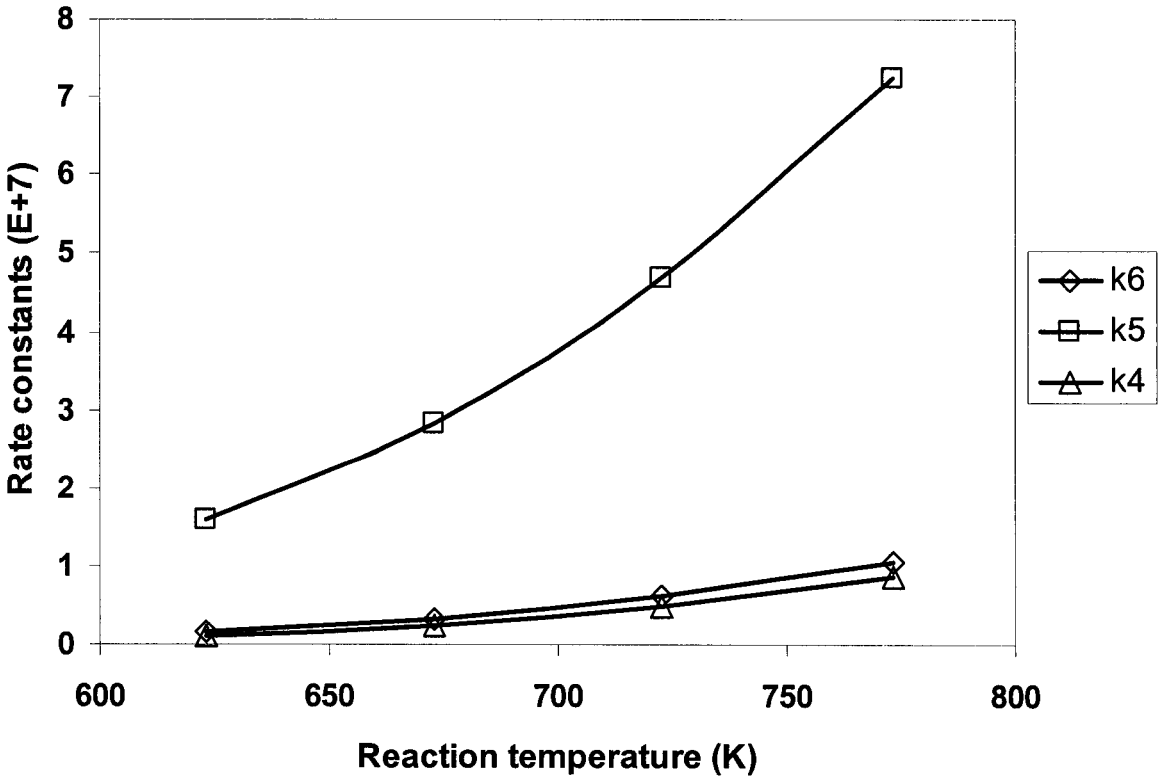

Figure 4.2 Xylene disproportionation rate constants vs. reaction temperature

4.4 Discussion

4.4.1 Reaction Rate Constants

The observed trend in the order of magnitude of reaction rate constants can easily be rationalized; the isomerization of xylenes on solid catalysts is considered to be an acid-catalysed reaction, with the acidic protons of zeolites being recognized as the active sites. As a result, the extent of interaction between the acidic sites and the adsorbed species would depend on the acid strength of the sites and the basicity of the individual molecules which is related to their dipole moment. Moreover, it has been reported in some published works that the adsorption strength of *p*-xylene is much lower than those of *o*- and *m*-xylene [7,30]. Therefore, the faster adsorption–desorption of *p*-xylene might result in an easier intramolecular 1, 2-methyl shift during the conversion of *p*-xylene compared to the other two isomers.

On the other hand, the closely identical rate constants for the isomerization of *m*- to *p*-xylene and *m*- to *o*-xylene can be explained by the similarity of the two reactions because both involve the migration of adjacent methyl groups [7]. Moreover, this is also evident from the closeness in their estimated preexponential factors (0.16×10^{-3} and 0.17×10^{-3} m^3/kg of catalyst·s, respectively). This is expected because the kinetic diameters of the transition-state complexes in *m*- to *p*-xylene and *m*- to *o*-xylene are lower than the cage opening of the USY zeolite used. Thus, the constraint of transition-state complexes in both reactions is negligible under the present conditions.

A very significant result is the much lower value of the estimated rate constant for the isomerization of *p*- to *o*-xylene (and vice versa) as compared to all others. This clearly indicates that the mutual interconversion between the two isomers in a 1, 3-methyl migration is quite difficult, in contrast to intramolecular 1, 2-methyl shifts (i.e. *m*- to *p*-xylene, *m*- to *o*-xylene, and vice versa). However, at higher reaction temperatures, this difficulty can be relatively be reduced for the conversion of *p*- to *o*-xylene in comparison to *o*- to *p*-xylene conversion, as observed by the higher dependence of the former on the reaction temperature. A similar conclusion regarding the difficulty of interconversion between *p*- and *o*-xylenes based on the estimated rate constants over H Mordenite has been previously reported [2,3]. Consequently, it has been proposed that the apparent interconversion of the two isomers can only occur via *m*-xylene as an intermediate step and not directly as a single step [9]. In addition, it can also proceed via a bimolecular transalkylation reaction with diphenylmethane as the intermediate over larger pore zeolites [12,13,32].

Figure 4.2 show that the three xylene isomers undergo disproportionation to different extents, with *p*-xylene disproportionation 10 times greater than that of *o*- and *m*-xylene. Guisnet et al. [13] reported a similar result, with the disproportionation of *p*-xylene being 9 times faster than that of *o*-xylene. In addition, it as been shown by Lanewala and Bolton [32] that a direct correlation exits between the extent of disproportionation and conversion of the xylene isomers, with a higher disproportionation accompanying *p*-xylene isomerization. This finding, which is in perfect agreement with the results obtained in the present study, indicates that the higher reactivity of *p*-xylene is simply responsible for its corresponding greater disproportionation rate. However,

Collins et al. [10] found a higher disproportionation for the less reactive *m*-xylene during xylene isomerization over HZSM5.

4.4.2 Activation Energies

It has been mentioned above that the mutual interconversion between *p*- and *o*-xylenes is quite difficult based on the estimated reaction rate constants for both reactions. This is further confirmed by the relatively larger values of apparent activation energies (E_3 and E_{-3}) required for the direct interconversion of the two isomers, again indicating the difficulty in causing 1,3-methyl shifts along the benzene ring.

As shown in Table 4.5, E_4 and E_6 are the largest which substantiate the well established fact that the activation energy required to move out a methyl group as a result of xylene disproportionation should be higher than that required for intramolecular methyl transfer by magnitudes of 3 - 4 kcal/mol [12]. However, the unexpectedly lower value of E_5 may be as a result of the formation of diphenylmethane-type transition intermediates, during the disproportionation of *p*-xylene prior to further breakdown, instead of the usual carbonium ion intermediates.

The activation energies obtained in the present work are close to those reported by Gendy[5]over a similar Y zeolite. A direct comparison with the values previously reported in the literature may not be possible considering that different catalysts were used. However, we observed that the values reported by Hsu et al. [4] and Li et al. [30] over Pt/ZSM5, and ZSM5 respectively, are similar to those obtained in this work. On the other hand, Hanson and Engel [7] and Cappallazzo et al. [5] reported substantially higher values.

4.4.3 Simplified Model Predictions

Figure 4.3 - 4.7 show the comparison between the model predictions and the experimental data at various temperatures for the simplified models. As observed in these plots, the model predictions compare favorably with the obtained experimental data for the various conditions. This provides evidence that these models could also be used to for the interpretation of kinetic data following the assumptions made. In addition, the reconciliation plots (Figure 4.6) between the experimental data and the model predictions display a normal distribution of residuals. Besides, the adequacy of the models and the selected parameters to fit the data gives 0.99, 0.98 and 0.99 regression coefficients for the isomerization of *m*-, *p*- and *o*-xylenes respectively.

4.4.4 Comprehensive Model Predictions

As mentioned earlier, the aim of this study is to develop a comprehensive model for the isomerization of *m*-xylene over USY in the riser simulator, and to obtain the various model parameters. In view of this, it is indeed imperative to check the validity of the estimated kinetic parameters using with the proposed model. Moreover, the effect of reaction conditions (such as time, temperature, and catalyst life) for conditions beyond those of the present study could be simulated. Thus, the estimated rate constants were substituted into eqs 4.18-4.21, and the equations were solved numerically using the fourth-order Runge-Kutta method. The simulated results were compared with the experimental data, as shown in Figure 4.7. It can be observed from this figure that the simulated results compares fairly well with the experimental data, except at T = 350 °C where the product yields were slightly underpredicted.

In summary, the comprehensive kinetic model proposed in the present study based on the triangular reaction network proved to be adequate for predicting *m*-xylene isomerization over USY in the riser simulator. However, it is worth emphasizing that the simplified models based on Schemes 2-4 are only applicable within a limited range of conversion, unlike the Scheme 1, which has a wider range of application and a sounder mechanistic basis.

4.5 Conclusion

The kinetics of vapor-phase isomerization of xylenes has been carried out over a USY zeolite catalyst using the riser simulator. A comprehensive kinetic model that is consistent with an overall picture of xylene reaction system based on a triangular reaction network is proposed for the reaction. Simplified effective kinetic models which are based on the isomerization of the pure xylene isomers are employed in obtaining the various kinetic parameters using the method of non-linear regression analysis. The much lower values of the estimated rate constants and the relatively higher activation energies for the isomerization of *p*- to *o*-xylene (and vice versa) confirm the great difficulty for the mutual interconversion between the two isomers. Also, the higher disproportionation

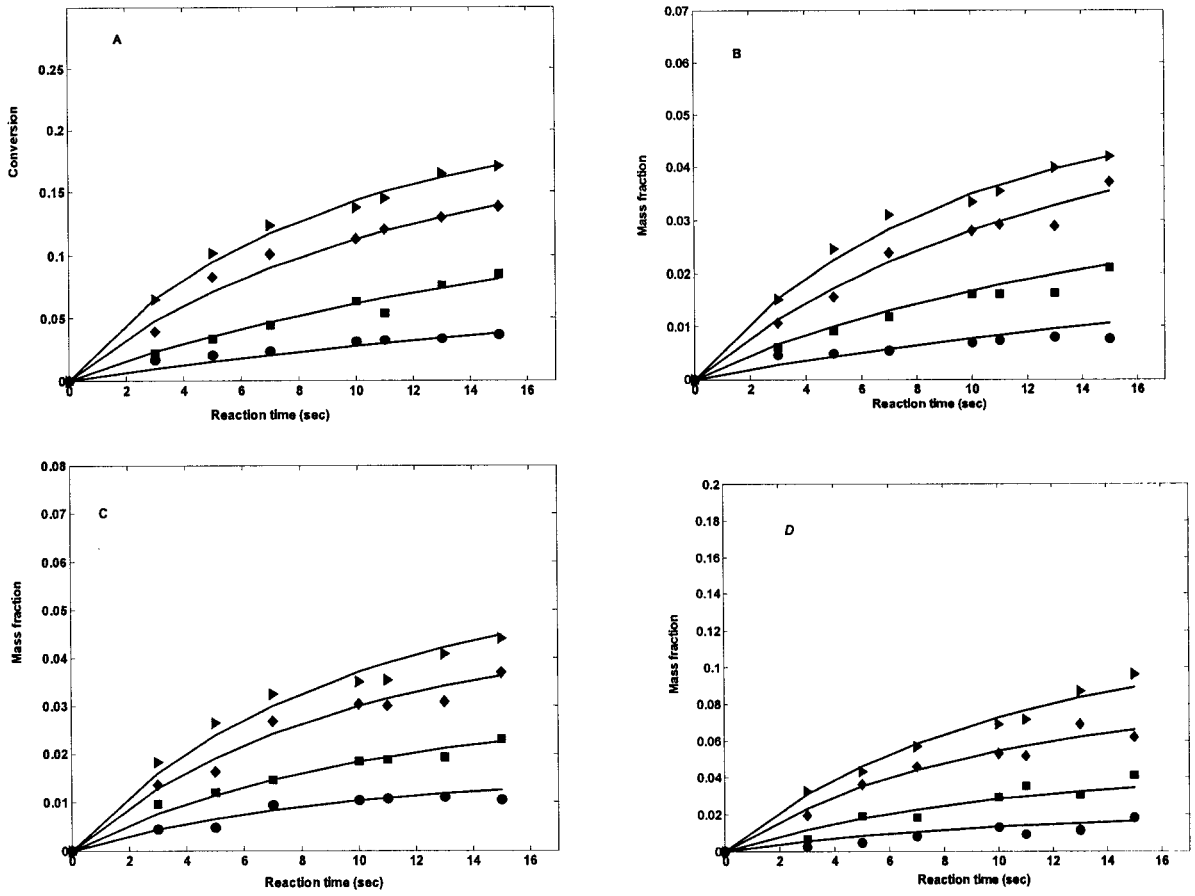

Figure 4.3 Comparison between experimental results and model predictions (—) based on *m*-xylene isomerization (scheme 2): (A) m-xylene conversion, (B) p-xylene yields, (C) o-xylene yields (D) T + TMBs yields. (●) 350°C (■) 400°C (♦) 450°C (▶) 475°C

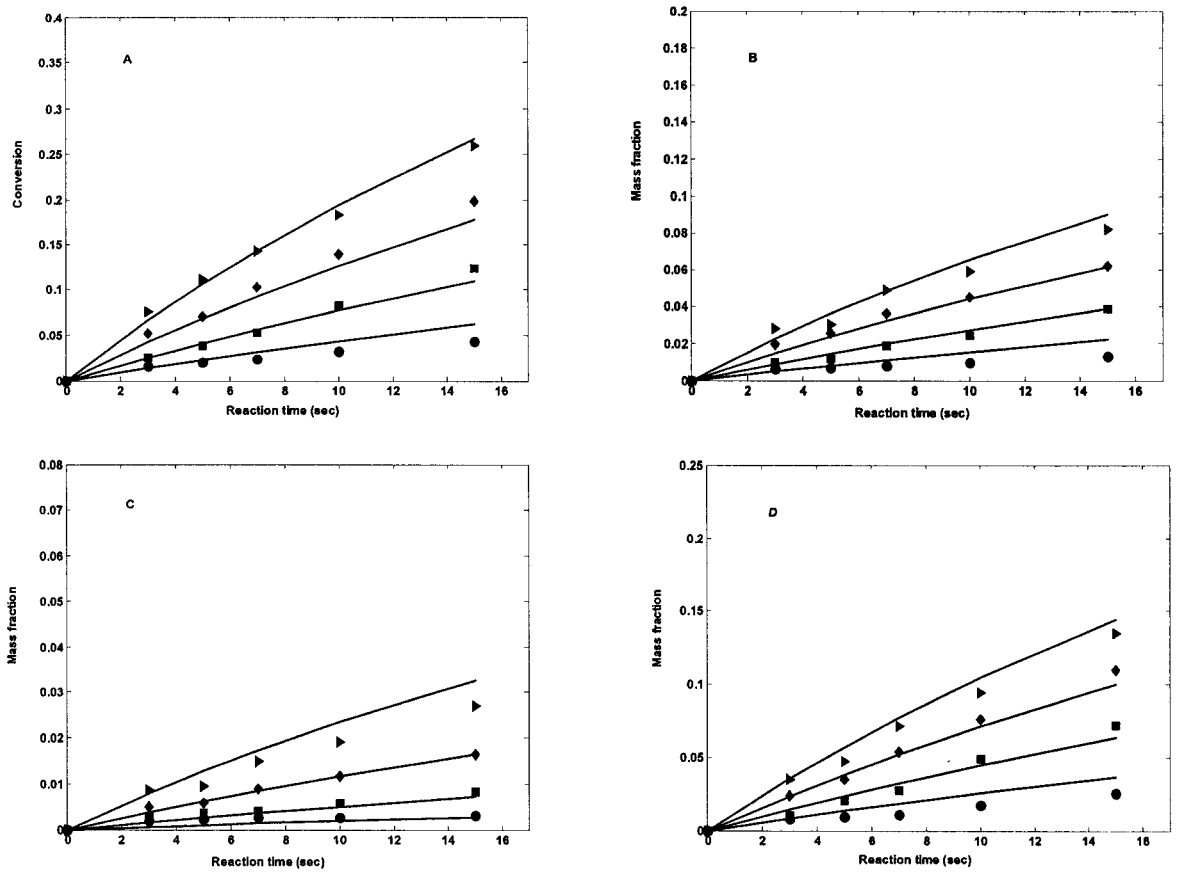

Figure 4.4 Comparison between experimental results and model predictions (—) based on *p*-xylene isomerization (scheme 3): (A) p-xylene conversion, (B) m-xylene yields, (C) o-xylene yields, (D) T + TMBs yields. (●) 350°C (■) 400°C (♦) 450°C (▶) 475°C

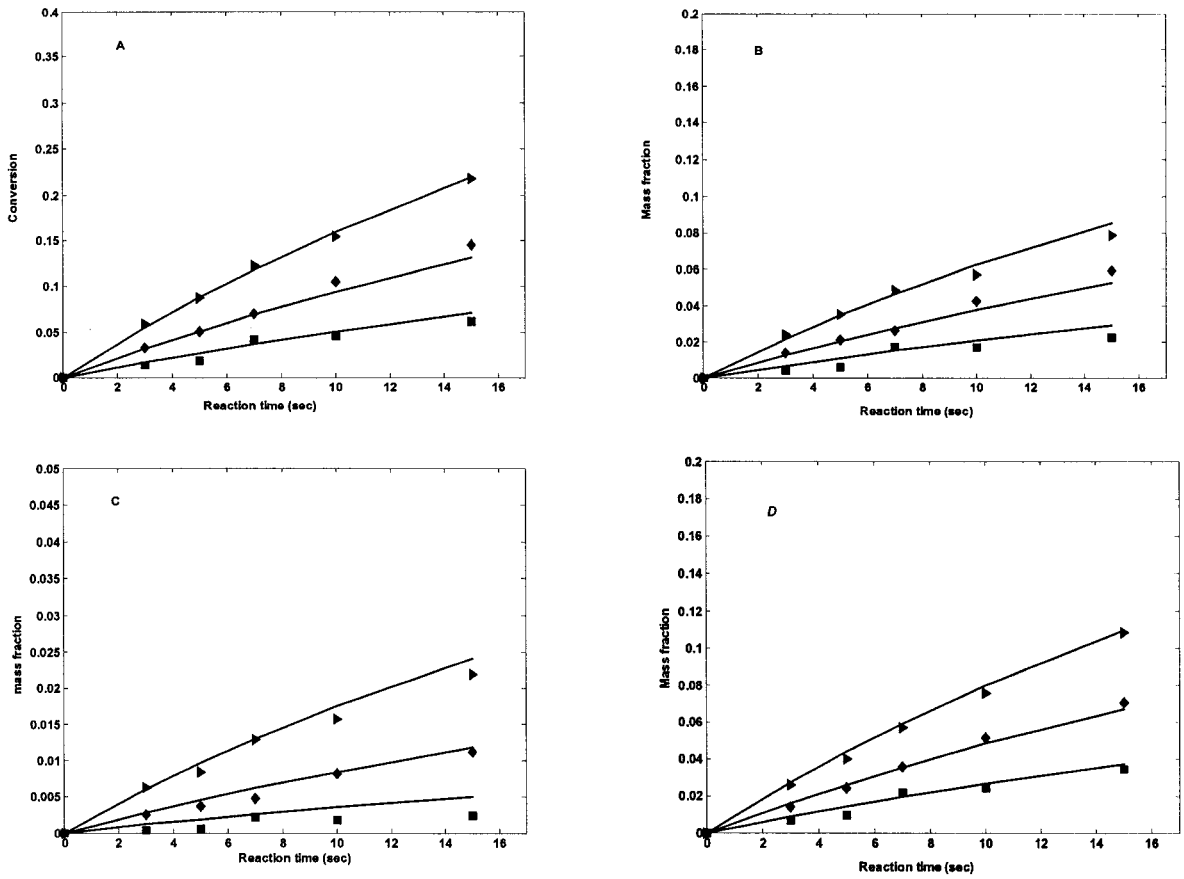

Figure 4.5 Comparison between experimental results and model predictions (—) based on *o*-xylene isomerization (scheme 2): (A) o-xylene conversion, (B) m-xylene yields, (C) p-xylene yields (D) T + TMBs yields. (●) 350°C (■) 400°C (♦) 450°C (▶) 475°C

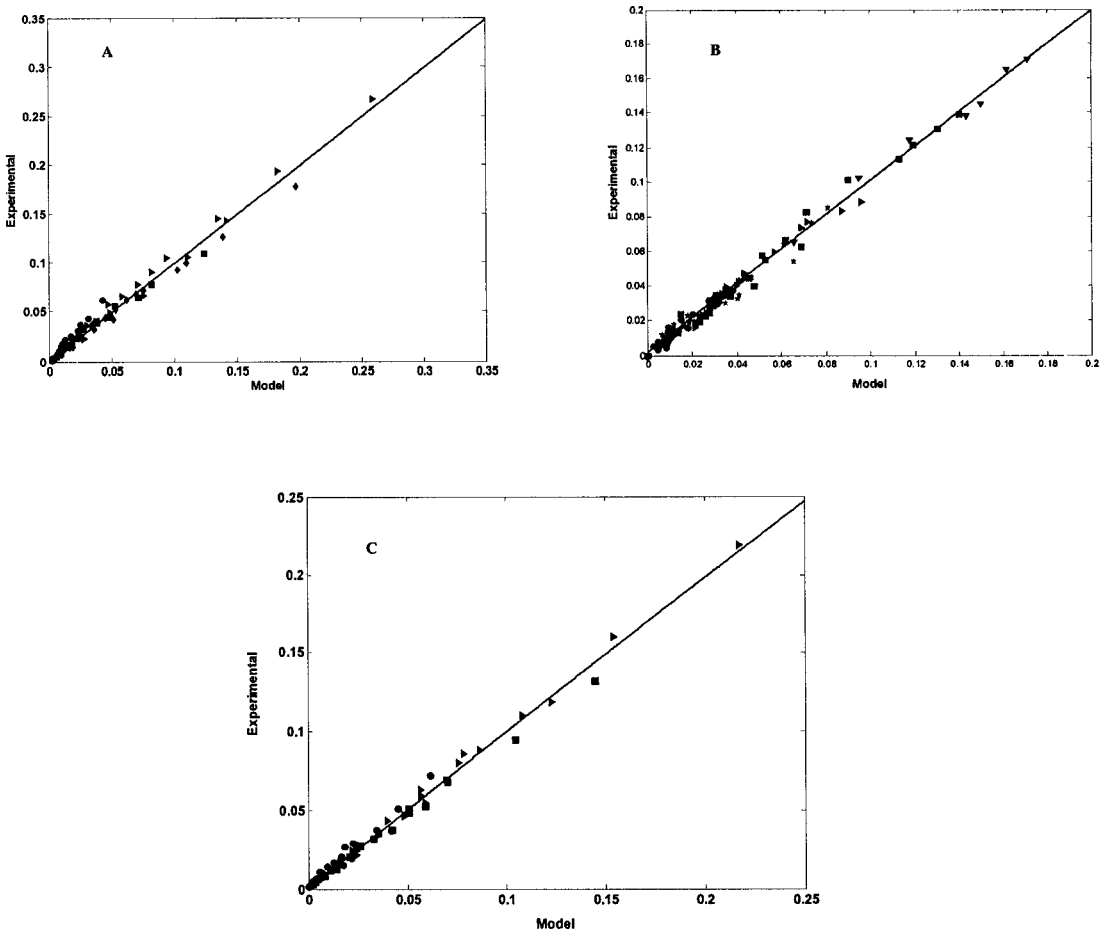

Figure 4.6 Overall comparison between the experimental results and model predictions based on p-xylene isomerization (A) Scheme 2, (B) Scheme 3, (C) Scheme 4

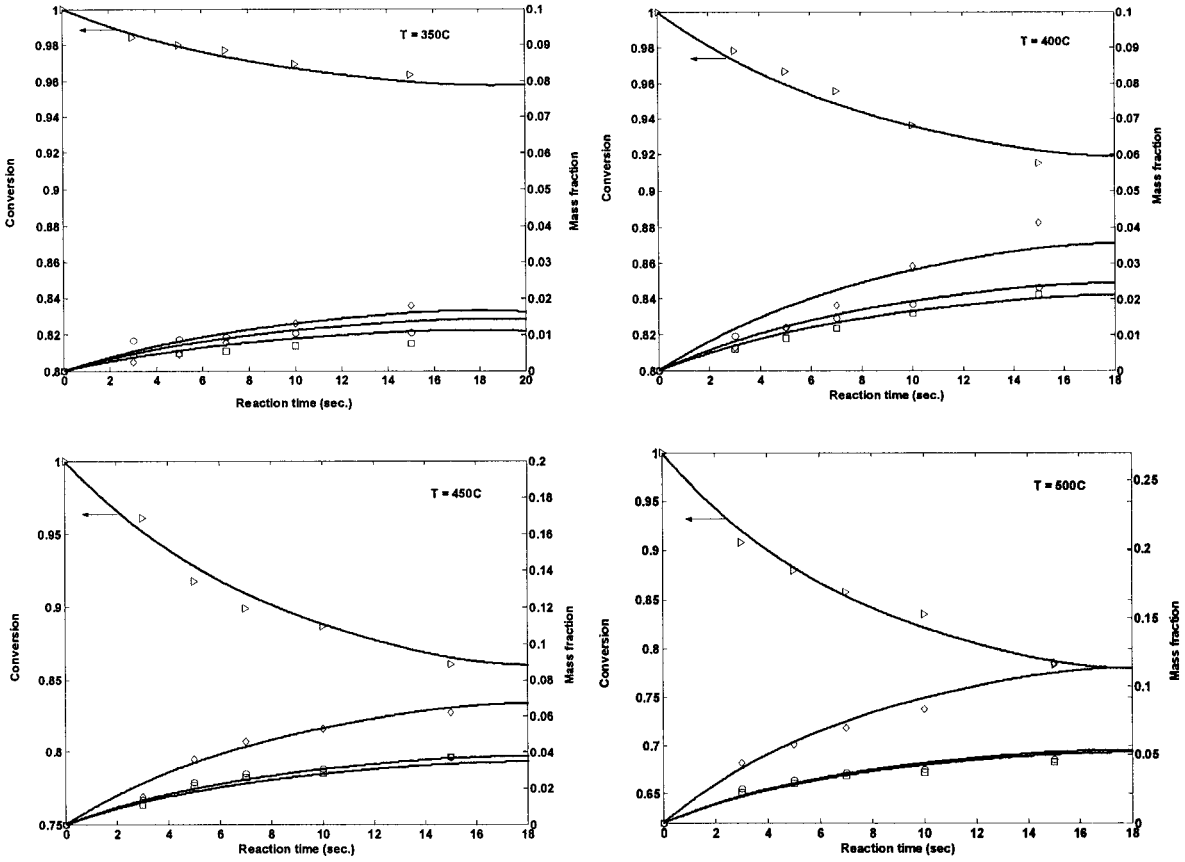

Figure 4.7 Comparison between experimental results and numerical solution (—) based on the overall kinetic model (scheme1) at various temperatures (▷) *m*-xylene conversion (□) *p*-xylene yield (○) *o*-xylene yield (◊) *T+TMBS* yield

accompanying *p*-xylene isomerization as compared to that of *o*- and *m*-xylenes can be attributed to its corresponding higher activity over the USY catalyst used. A good comparison between the experimental data and model predictions was obtained. This provides significant evidence that the riser simulator and associated modeling technique can be used as an effective tool in the investigation of the kinetics of xylene isomerization and disproportionation reactions.

4.6 References

[1] Ma, Y. H., Savage, L. A., Xylene isomerization using zeolites in a gradientless reactor system. AIChE J. 33 (1987), 1233-40.

[2] Hopper, J. R., Shigemura, Dennis S., Kinetics of liquid phase xylene isomerization over H-mordenite. AIChE J., 19(1973), 1025-32.

[3] Norman, G.H., Shigemura, D.S., Hopper, J.R., Isomerization of Xylene over Hydrogen Mordenite. A Comprehensive Model. Ind. Eng. Chem. Prod. Res. Dev., 15 (1976), 41.

[4] Hsu, Y. S.,Lee, T. Y., Hu, H. C., Isomerization of Ethylbenzene and m-Xylene on Zeolites. Ind. Eng. Chem. Res., 27 (1988), 942-7.

[5] Gendy, Tahani S., Simulation of liquid and vapor phase xylene isomerization over deactivating H-Y-zeolite. J. Chem. Tech. Biotech., 73(1998), 109-118.

[6] Collins, Dermot J., Medina, Roger J., Davis, Burtron H., Xylene isomerization by ZSM-5 zeolite catalyst. Can. J.Chem. Eng., 61(1983), 29-35.

[7] Hanson, K. L., Engel, A. J., Kinetics of xylene isomerization over silica-alumina catalyst. AIChE J., 13(1967), 260-6.

[8] Cappellazzo, O., Cao, G., Messina, G., Morbidelli, M., Kinetics of shape-selective xylene isomerization over a ZSM-5 catalyst. Ind. Eng. Chem. Res., 30 (1991), 2280-7.

[9] Cortes, A., Corma A., The Mechanism of Catalytic Isomerization of Xylenes: Kinetic and Isotopic Studies. J. Catal., 51 (1978), 338.

[10] Collins, D.J., Mulrooney, K.J., Medina, R.J., Xylene Isomerization and Disproportionation over Lanthaniun Y Catalyst. J. Catal. 75 (1982), 291.

[11] Sreedharan, V., Bhatia, S., Vapor Phase Isomerization Study of m-Xylene over a Nickel Hydrogen Mordenite Catalyst. Chem. Eng. J. 36 (1987), 101-9.

[12] Corma, A., Sastre, E., Evidence of the Presence of a Bimolecular Pathway in the Isomerization of Xylene on Some Large-Pore Zeolites J. Catal. 129 (1991), 177.

[13] Morin, S., Gnep, N.S, Guisnet, M., A Simple Method for Determining the Relative Significant of the Unimolecular and Bimolecular Pathways of Xylene Isomerization over HY Zeolites. J. Catal., 159 (1996), 296.

[14] Iliyas A., Al-Khattaf S., m-Xylene Isomerization over USY Zeolite in a Riser Simulator: A Simplified Kinetic Model. Chem. Eng. J., in press (2003).

[15] de Lasa, H.I. U.S. Patent 5, 102 ,628, (1991)

[16] Al-Khattaf, S., de Lasa, H.I., Catalytic Cracking of Cumene in a Riser Simulator: A Catalyst Activity Decay Model. Ind. Eng. Chem. Res., 40 (2001), 5398.

[17] Al-Khattaf, S., de Lasa, H.I., Diffuision and Catalytic Cracking of 1,3,5 tri-iso-propyl-benzene in FCC Catalysts. Chem. Eng. Sc. 57 (2002), 4909.

[18] Al-Khattaf, S., de Lasa, H.I., The Role of Difusión in Alkyl-benzenes Catalytic Cracking. Appl. Catal. A: General, 226 (2002), 139.

[19] Al-Khattaf, S., The Influence of Y-Zeolite Unit Cell Size on the Performance of FCC Catalysts During Gas Oil Catalytic Cracking. Appl. Catal. A: General 231 (2002), 293.

[20] Al-Khattaf, S., de Lasa, H.I., Diffusion and Reactivity of Hydrocarbon Feedstocks in FCC Catalysts. Can. J. Chem. Eng. 79 (2001), 329.

[21] Kraemer, D. W. Ph.D. Dissertation, University of Western Ontario, London, Canada (1991).

[22] Beschmann, K., Riekert, L., Isomerization of Xylene and Methylation of Toluene on Zeolite HZSM5. Compound Kinetics and Selectivity. J. Catal., 41(1993), 48-65.

[23] Stull, D.R., Westrum, E.F., Simke, G.C., "The Chemical Thermodynamics of Organic Compounds" Wiley: New York, (1969) 368.

[24] Bhatia, S., Chandra, S., Das, T., Simulation of the Xylene Isomerization Catalytic Reactor. Ind. Eng. Chem. Res. 28 (1989), 1185-90.

[25] Draper, N., Smith, H., "Applied Regression Analysis", 2nd edition; John Wiley and Sons: New York, (1981).

[26] Agarwal, A.K., Brisk, M.L., Sequential Experimental Design for Precise Parameter Estimation: 1. Use of Reparameterization., Ind. Eng. Chem. Process Des. Dev. 24 (1985), 203.

[27] Chirico, R.D., Steele, W.V., Thermodynamic Equilibrium in Xylene Isomerization. J. Chem. Eng. Data. 42 (1997), 784.

[28] Jones, C. W., Zones, S. I., Davis, M. E., m-Xylene Reactions over Zeolites with Unidimensional Pore Systems. Appl. Catal. A: General, 181 (1999), 289-303.

[29] Martens, J. A., Perez-Pariente, J., Sastre, E., Corma, A., Jacobs, P. A.m Isomerization and Disproportionation of m-Xylene: Selectivities Induced by the Void Structure of the Zeolite Framework. Appl. Catal. 45 (1988), 85-101.

[30] Li, Y., Jun, H., Kinetics Study of the Isomerization of Xylene on ZSM-5 Zeolites: the Effect of the Modification with MgO and CaO. Appl. Catal. A: General, 142 (1996), 123-137.

[31] Mirth, G., Cejka, J., Lercher, A.J., Transports and Isomerization of Xylenes over HZSM-5 Zeolites. J. Catal., 139 (1993) 24.

[32] Lanewala, M.A., Bolton, A.P. The Isomerization of the Xylenes Using Zeolites Catalysts. J. Org. Chem., 34 (1969), 3107.

[33] Ratnasamy, P., Pokhriyal, S.K., Surface Passivation and Shape Selectivity in Xylene Isomerization over ZSM-48. Appl. Catal. 55 (1989), 265.

CHAPTER 5

5 Xylene Transformation over USY Zeolite: An Experimental and Kinetic Study

5.1 Introduction

The demand for xylenes as a raw material for polyester fibers and films continues to grow, and drive the search for improved xylene isomerization processes. Most of the currently working isomerization plants are using zeolites based catalysts. It is well-known that xylenes undergo two main competitive reactions, isomerization and disproportionation over zeolite catalysts. However, it is usually desired to minimize disproportionation in favor of isomerization reaction, especially to para-isomer. Thus, three types of selectivity can be defined, isomerization, disproportionation, and distribution of trimethylbenzene isomers (TMBs) [1]. The isomerization selectivity has been shown to depend mainly on the diffusion path of xylenes, while that of trimethylbenzenes distribution and disproportionation selectivity both depend on the diffusion path, size, and shape of cavities or channel intersections [2]. Moreover, the p-xylene/o-xylene (P/O) ratio during xylene transformation has also been utilized as a tool to characterize zeolite pore structure [2-7].

Surveying the present literature on the isomerization of xylenes, it appears that systematic studies which focus on the influence of reaction parameters (reaction time, temperature, and conversion) on the three types of selectivity mentioned above are

scarce. Thus, with this in mind we explore the possibility of a systematic study on the influence of reaction parameters on the isomerization and disproportionation selectivity during the transformation of the three xylene isomers.

Regarding the kinetics of xylene transformations over zeolitic catalysts, several modeling techniques have been applied to obtain the numerous kinetic parameters of this complex reaction system. Amongst the techniques employed in the literature include: analytical methods such as Wei-Prater method [8,9,10], Laplace transform [11], and finite integral transform [12, 13]. Curve fitting method, such as Himmelblau method [14, 15], and least-squares method [16, 17] have also been applied. Recently, Iliyas and Al-Khattaf [18] proposed a new modeling procedure based on the isomerization of the each xylene isomers. The various kinetic parameters of the overall m-xylene transformation were obtained from simplified effective kinetic models.

However, in most of the previous kinetic studies on xylene transformation, the deactivation of the catalyst was not adequately accounted for, in the development of kinetic models used in such studies. Moreover, the limited papers, which incorporated a catalyst deactivation function, used the time on stream (TOS) decay model [14, 18, 19, and 20]. This deactivation function is empirically based, as it does not incorporate a mechanistic description of catalyst deactivation [21]. On the other hand, since coke deposition is the major cause of catalyst deactivation in the transformation of xylenes, the "reactant converted" decay model, proposed by Al-Khattaf and de Lasa [22] will be employed in this work. This important deactivation model has been successfully tested for modeling of 1,2,4 trimethylbenzene reactions [21], cracking of cumene [22, 23], and 1,3,5-triisopropylbenzene [24].

The second part of the present study is aimed at modeling the kinetics of xylene transformation over a USY zeolite by using the "reactant converted" catalyst deactivation model. The modeling procedure proposed in our previous work [18], will be employed to obtain the kinetic constants for the reaction. The xylene transformation will be carried out using the riser simulator. This reactor has been shown to overcome the limitation of temperature/concentration gradients associated with fixed-bed and other reactor types. Besides, utilizing the riser simulator is more relevant in testing the new catalyst deactivation model, because it ensures uniform coke deposition on the catalyst particle due to the intensed fluidization, and well-mixed characteristics of this reactor. Also, performing xylene transformation using the riser simulator is practically relevant. This is because it can adequately mimic the transformation of the C8 aromatic compounds (including the three xylene isomers) in the catalytic cracking unit of the refinery, which is similar to riser simulator used in the present study.

5.2 Kinetic Model Development

To develop a suitable kinetic model representing the overall transformation of m-xylene, we propose the reaction network shown in Scheme 1 of Figure 4.1. However, the reaction schemes 2-4 of Figure 4.1, which are based on the transformation of each of the each xylene isomers, will be employed to obtain the numerous kinetic parameters of Scheme 1. The details of this analysis can be found in Ref. 18.

The riser simulator mass balances based on the schemes 2-4 can be expressed as follows:

m-xylene (Scheme 2):

$$\frac{dy_m}{dt} = -\left[(k_1 + k_2 + k_4)y_m - \frac{k_1}{K_{pm}}y_p - \frac{k_2}{K_{om}}y_o\right]\frac{W_c}{V}\exp\left[-\lambda_m(1-y_m)\right] \quad (5.1)$$

$$\frac{dy_p}{dt} = \left[k_1 y_m - \frac{k_1}{K_{pm}}y_p\right]\frac{W_c}{V}\exp\left[-\lambda_m(1-y_m)\right] \quad (5.2)$$

$$\frac{dy_o}{dt} = \left[k_2 y_m - \frac{k_2}{K_{om}}y_o\right]\frac{W_c}{V}\exp\left[-\lambda_m(1-y_m)\right] \quad (5.3)$$

$$\frac{dy_d}{dt} = k_4 y_m \frac{W_c}{V}\exp\left[-\lambda_m(1-y_m)\right] \quad (5.4)$$

Following the same procedure, the mathematical models for the simplified kinetic schemes (Schemes 3 and 4) and the overall reaction (Scheme 1) can be developed. The concentration of any species *i* in the above equations is related to its mass fraction as follows:

$$C_i = \frac{y_i W_{hc}}{MW_i V} \quad (5.5)$$

while the influence of temperature on the model parameters can be accounted for, through the following Arrhenius equation:

$$k_i = k_{0i}\exp\left(\frac{-E_i}{R}\left[\frac{1}{T} - \frac{1}{T_0}\right]\right) \quad (5.6)$$

T_o is the average reaction temperature introduced for reparametrization of kinetic constants [26]. As mentioned earlier, the "reactant converted" decay function ($\varphi = \exp[-\lambda_i(1-y_i)]$) is employed in the mathematical models to account for catalyst deactivation.

In order to ensure thermodynamic consistency at equilibrium, the rate constants for *m*- to *p*-xylene, and *m*- to *o*-xylene reactions in the above equations are expressed as follows [13]:

$$k_{-1} = k_1/K_{pm} \tag{5.7}$$

$$k_{-2} = k_2/K_{om} \tag{5.8}$$

where $K_{pm} = (C_p/C_m)_{eq}$ and $K_{mo} = (C_o/C_m)_{eq}$ are temperature-dependent equilibrium constants for both reactions, respectively. However, an average value can be computed for both constants, because the thermodynamic equilibrium concentrations of the xylenes remain fairly constant within the temperature range of this work. The xylene equilibrium concentrations are obtained from a published work [27].

Each set of equation for the simplified models involves seven adjustable model parameters that have to be estimated before a solution is obtained. These parameters were adjusted using the weighted least-square algorithm for nonlinear parameters in a MATLAB package. The results obtained in this regard are presented and discussed in subsequent sections.

5.3 Results

5.3.1 m-Xylene Transformation

The transformation of m-xylene over the USY zeolite produces p-xylene, o-xylene, toluene, and trimethylbenzenes. The isomerization and disproportionation selectivity obtained during m-xylene reaction is shown in Figure 5.1. It can be observed from this figure that isomerization and disproportionation selectivity are almost identical.

Furthermore, the P/O ratio (Figure 5.2) is consistent with the thermodynamic predicted value of 1.09.

It has been mentioned earlier that disproportionation reaction is a major reaction pathway during the transformation of xylenes over large pore zeolites such as USY zeolite used in this study. As a result, the distribution of trimethylbenzenes can give further insight into the initial products of disproportionation reaction. Thus, Figure 5.3 presents the distribution of TMBs isomers obtained with m-xylene disproportionation. Indeed, it is obvious that 1,2,4- and 1,3,5-TMBs are primary products of m-xylene disproportionation, while 1,2,3-TMB is not. Furthermore, the plot of toluene to trimethylbenzenes (T/TMBs) mole ratio presented in Figure 5.4 depicts a high initial value, which decreases exponentially as conversion increases. Beyond 5% conversion, the ratio can be observed to remain constant at a value 20-30 % above the stoichiometric ratio of 1.0.

5.3.2 p-Xylene Transformation

The conversion of p-xylene produces m-xylene, o-xylene, toluene, and trimethylbenzenes. The initial selectivity to isomerization and disproportionation during the reaction of p-xylene appears to be similar (Figure 5.5). Whatever the reaction condition, the ratio of m-xylene/o-xylene (M/O) obtained with p-xylene transformation is much higher than the thermodynamic value of 2.0. Also, the plot of M/O ratio as a function of p-xylene conversion at different reaction temperature (Figure 5.6) shows that it varies more with reaction temperature than conversion.

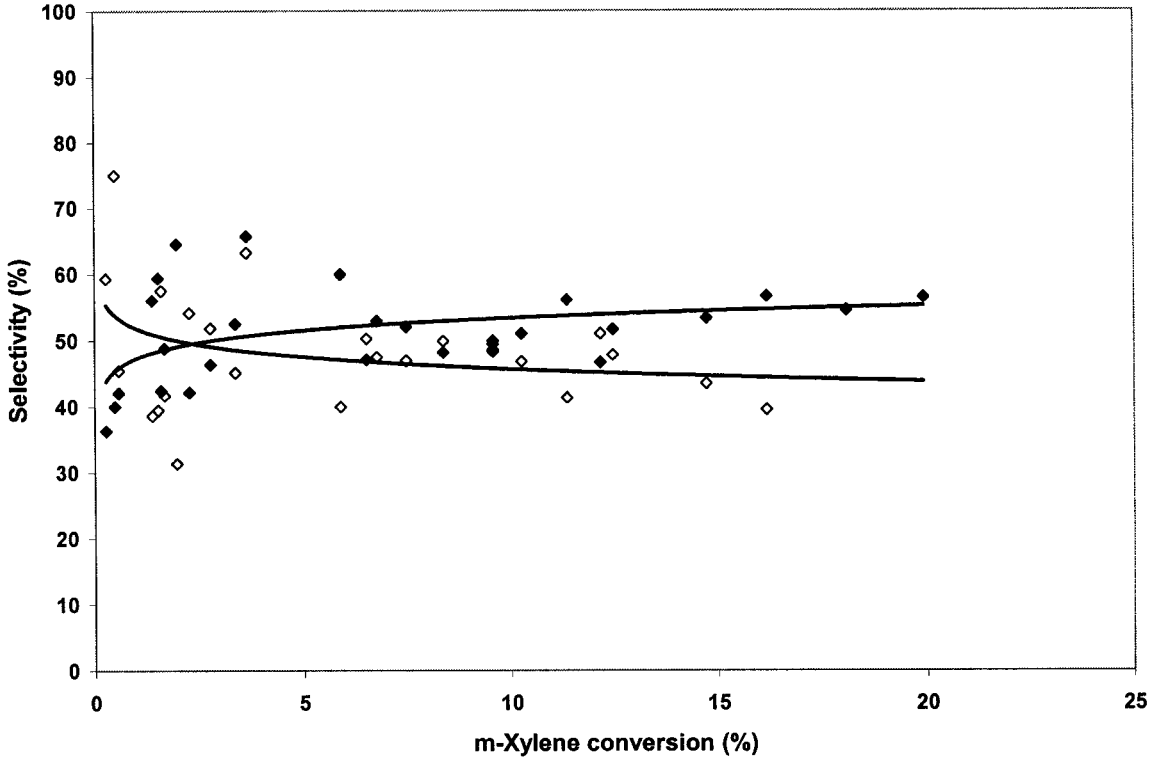

Figure 5.1 Isomerization and disproportionation selectivity during the transformation of m-xylene as a function of conversion. (◊) isomerization; (♦) disproportionation

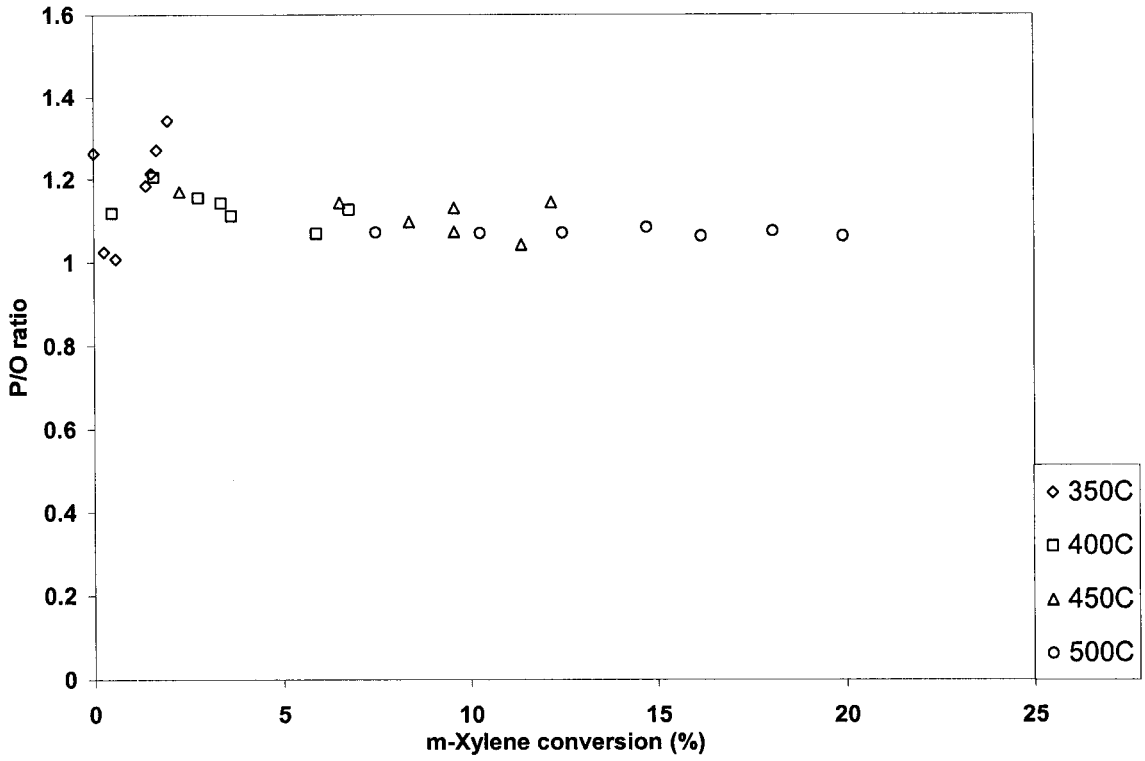

Figure 5.2 p-xylene/o-xylene (P/*O*) ratios vs. m-xylene conversion at different temperatures

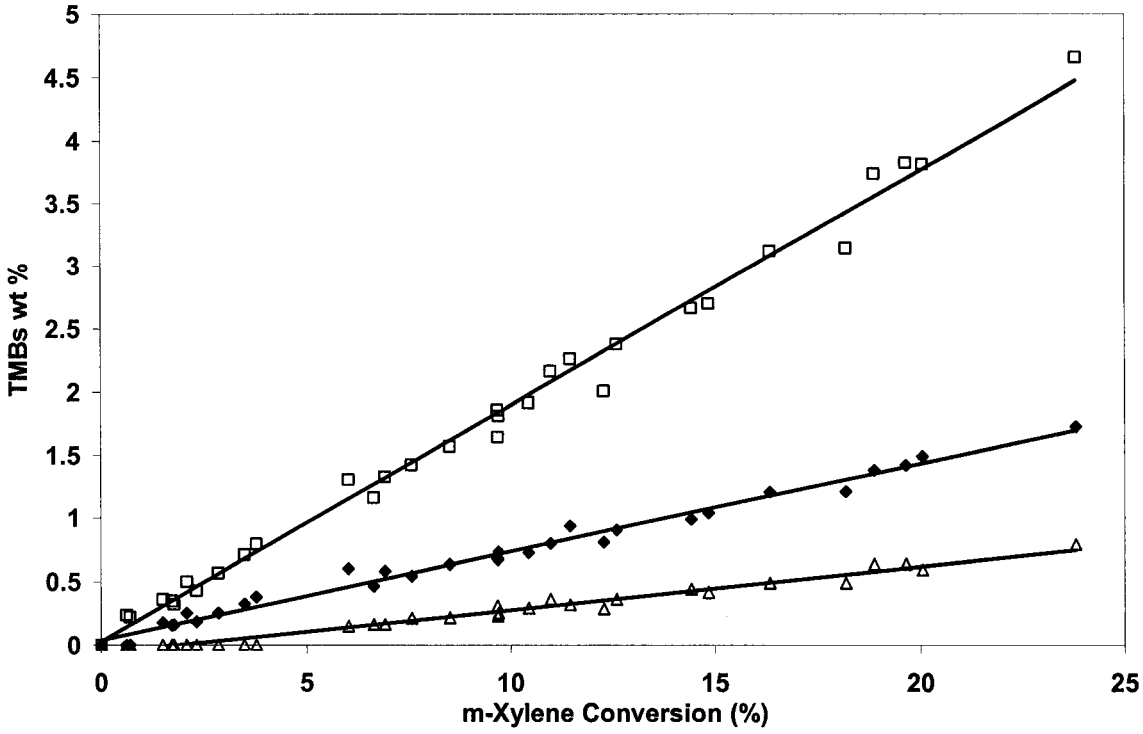

Figure 5.3 Distributions of trimethylbenzenes isomers as function of m-xylene conversion
(Δ) 1,2,3-TMB, (□)1,2,4-TMB, (♦) 1,3,5- TMB

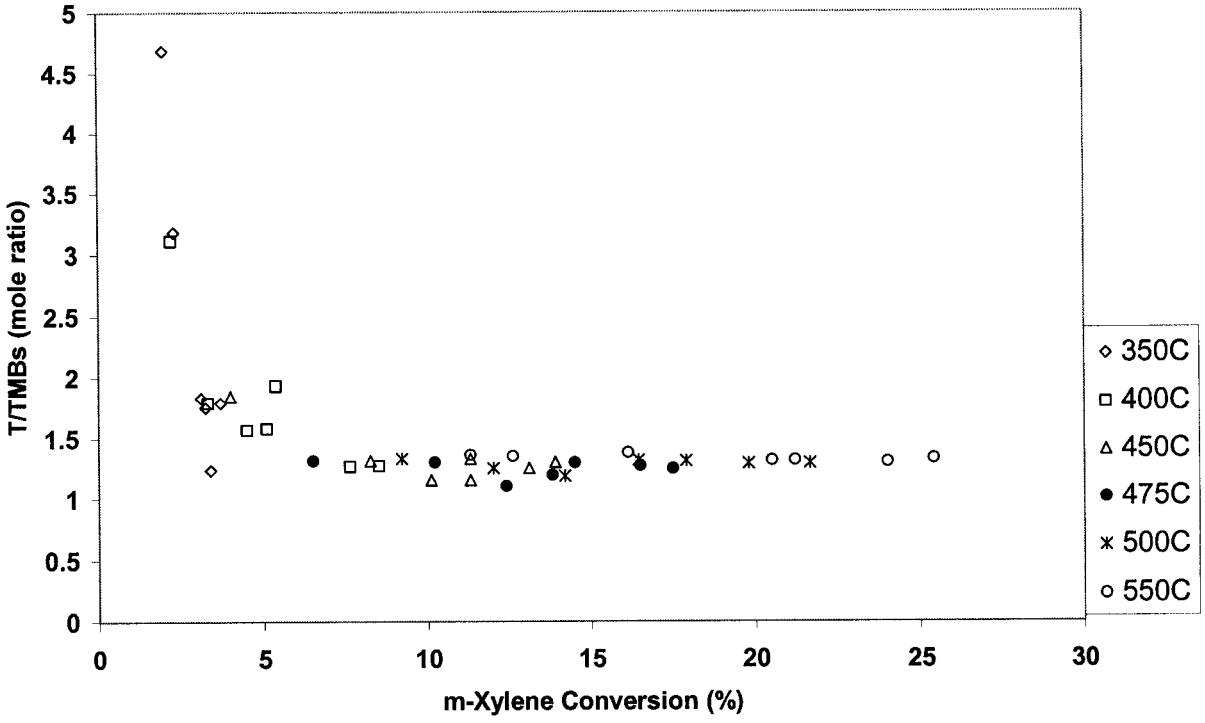

Figure 5.4 Molar ratio of toluene to trimethylbenzene as a function of m-xylene conversion at different reaction temperatures

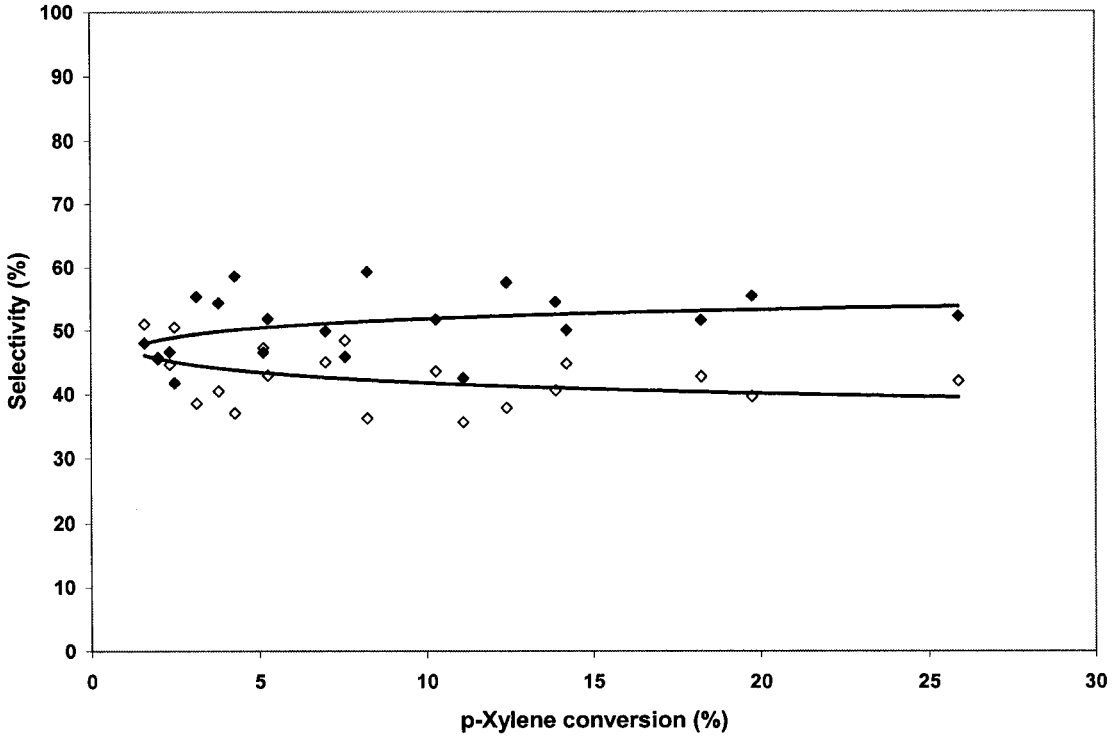

Figure 5.5 Isomerization and disproportionation selectivity during the transformation of p-xylene as function of conversion
(◊) isomerization, (♦) disproportionation

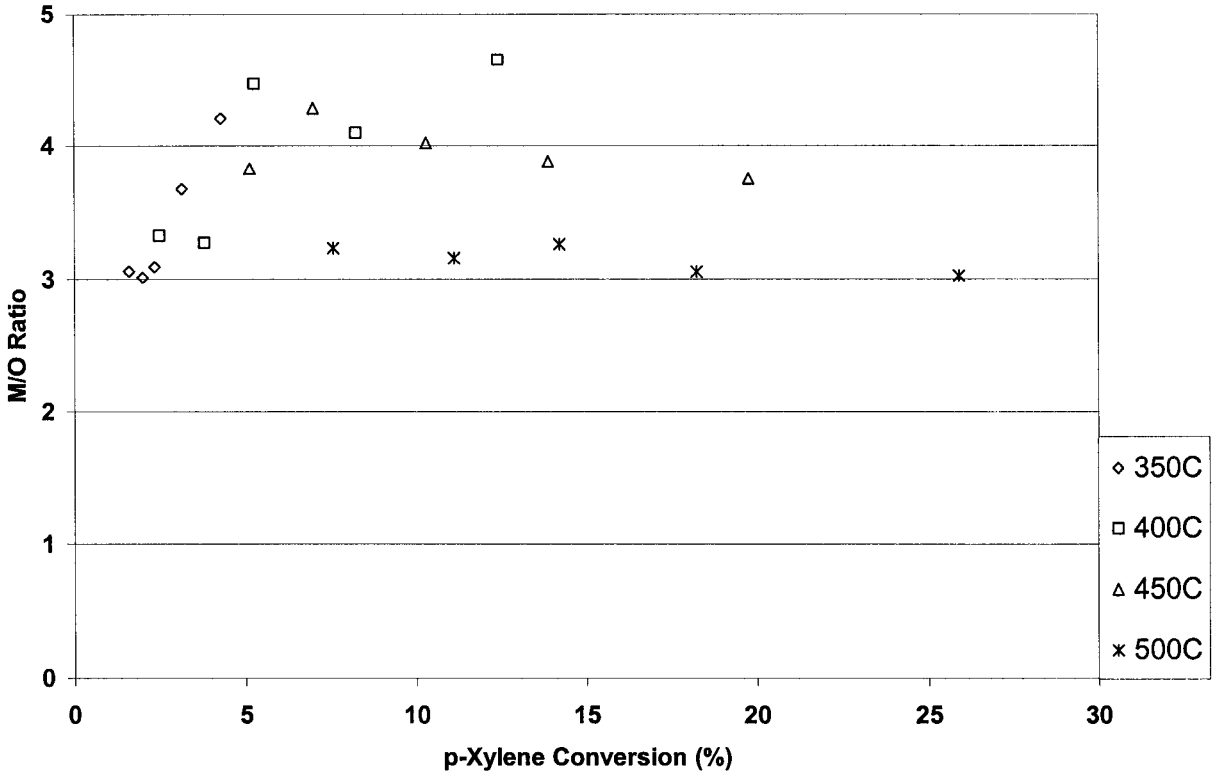

Figure 5.6 m-xylene/o-xylene (M/*O*) ratios vs. p-xylene conversion at different reaction temperatures

With p-xylene transformation, 1,3,5- trimethylbenzene approaches zero at low conversion, while 1,2,3 and 1,2,4 isomers did not appear to extrapolates to zero under similar conversion level (Figure 5.7). Moreover, the ratios of the three trimethylbenzene isomers produced approaches equilibrium value after 15% p-xylene conversion is attained. This result agrees with the work of Collins et al. [10]. The plot of toluene to trimethylbenzene (T/TMB) mole ratio versus p-xylene conversion gives a similar trend to that obtained with respect to m-xylene (Figure 5.4), although, the ratio can be observed to be constant at a slightly higher value than with m-xylene.

5.3.3 o-Xylene Transformation

Unlike m- and p-xylene, o-xylene did not react to any appreciable extent at 350°C. The trend of initial selectivity to isomerization and disproportionation (Figure 5.9), m-xylene/p-xylene (M/P) ratio (Figure 5.10), trimethylbenzenes distributions (Figure 5.11), and T/TMB mole ratio (Figure 5.12) as a function of o-xylene conversion were very similar to those obtained with p-xylene (refer to the preceding section). M/P ratio appears to be unaffected by increasing conversion level, whereas it decreases steadily with increasing reaction temperature.

5.3.4 Comparison Between the Transformations of the Xylene Isomers

Data presented in Figure 5.13 indicate that the reactivity of the xylene isomers decreases in the following order: p-xylene > m-xylene > o-xylene. Moreover, it can be observed that the xylene isomers undergo disproportionation to different extent, with higher disproportionation accompanying p-xylene than either m- or o-xylene transformations as shown Figure 5.14.

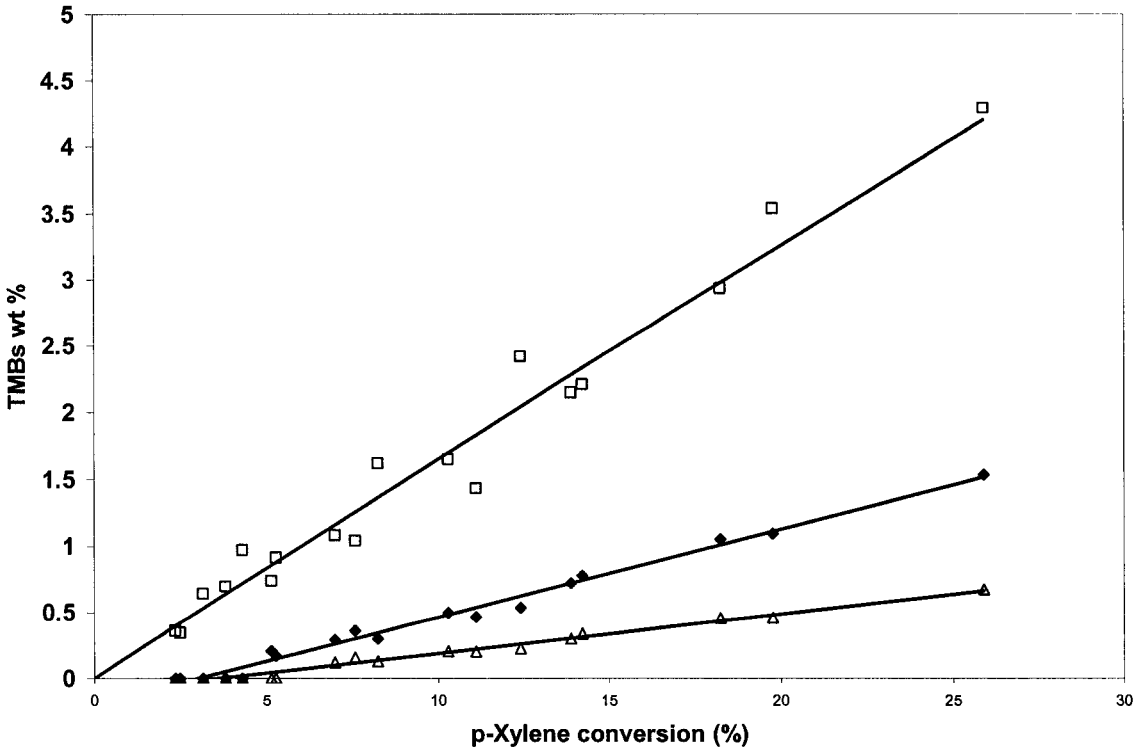

Figure 5.7 Distributions of trimethylbenzenes isomers as function of p-xylene conversion (Δ) 1,2,3-TMB, (□)1,2,4-TMB, (♦) 1,3,5- TMB

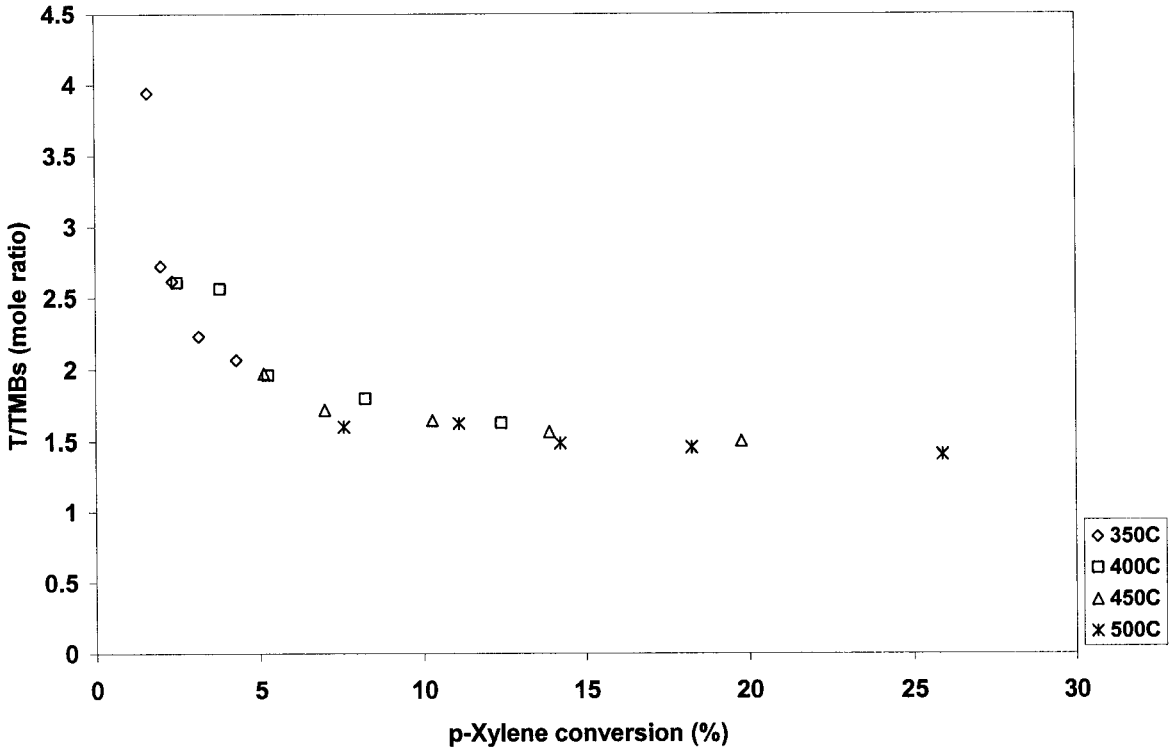

Figure 5.8 Molar ratio of toluene to trimethylbenzenes as a function of p-xylene conversion at different reaction temperatures

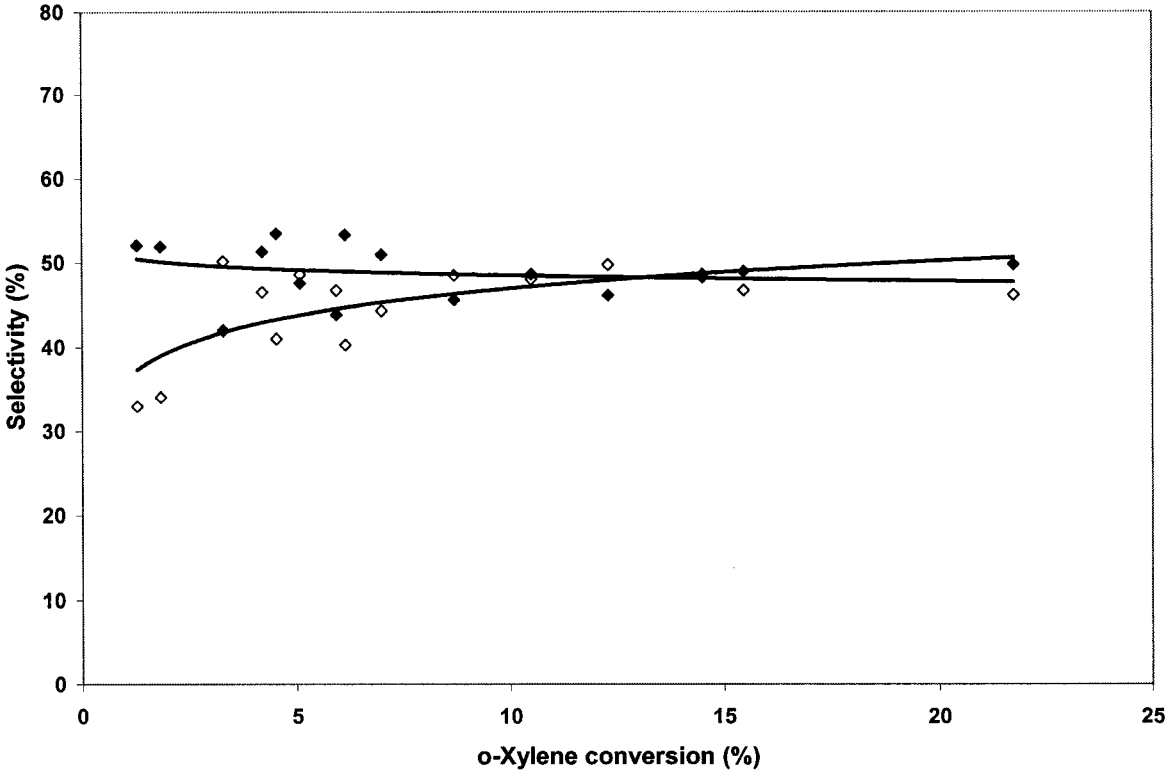

Figure 5.9 Isomerization and disproportionation selectivity during the transformation of o-xylene as function of o-xylene conversion
(◊) isomerization, (♦) disproportionation

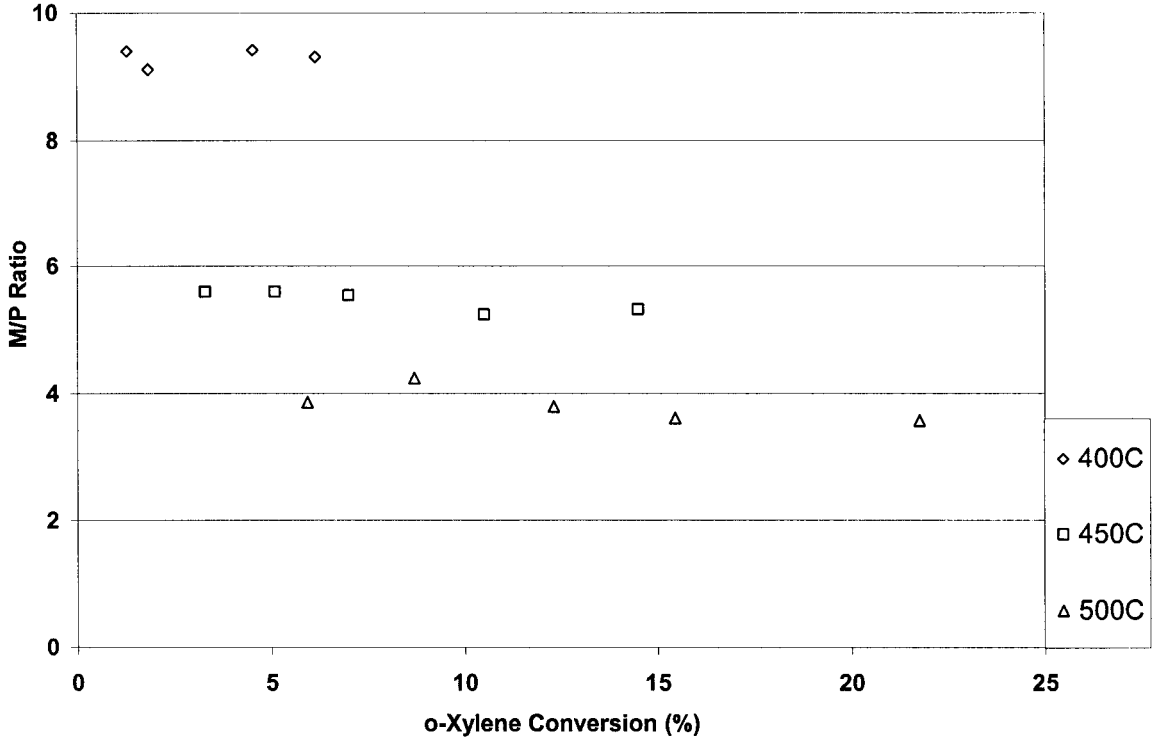

Figure 5.10 m-Xylene/p-xylene (M/*P*) ratios vs. o-xylene conversion at different temperatures

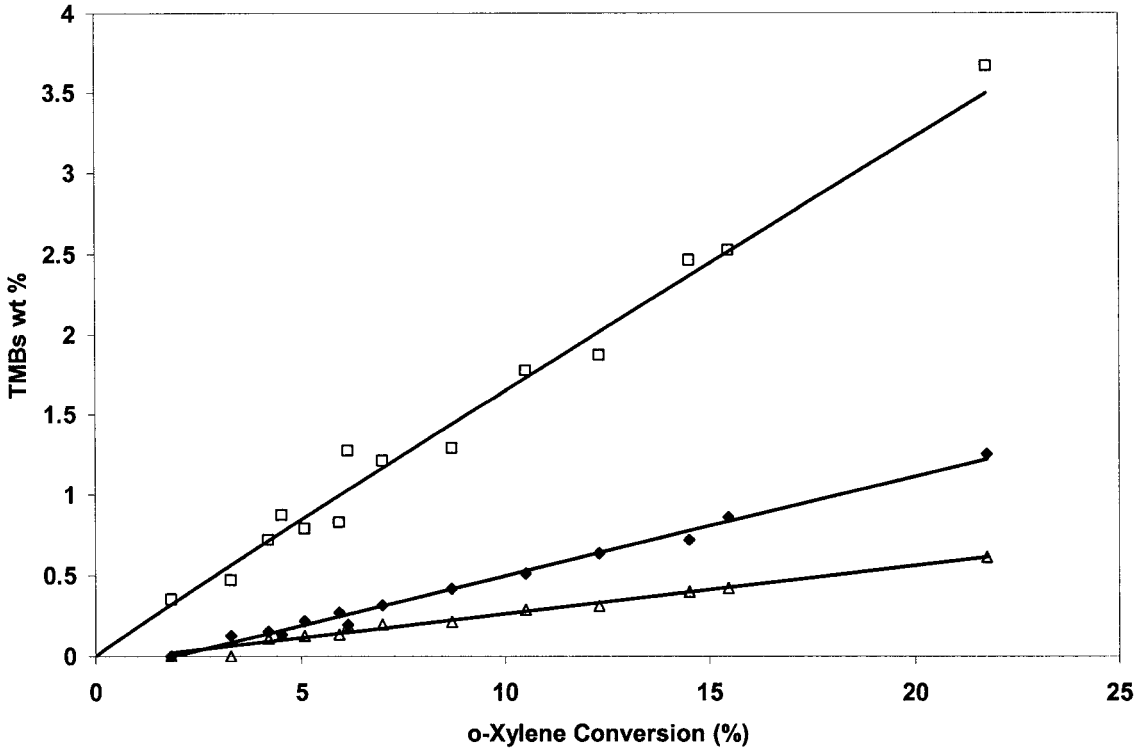

Figure 5.11 Distributions of trimethylbenzenes isomers as function of o-xylene conversion. (Δ) 1,2,3-TMB, (□)1,2,4-TMB, (♦) 1,3,5- TMB

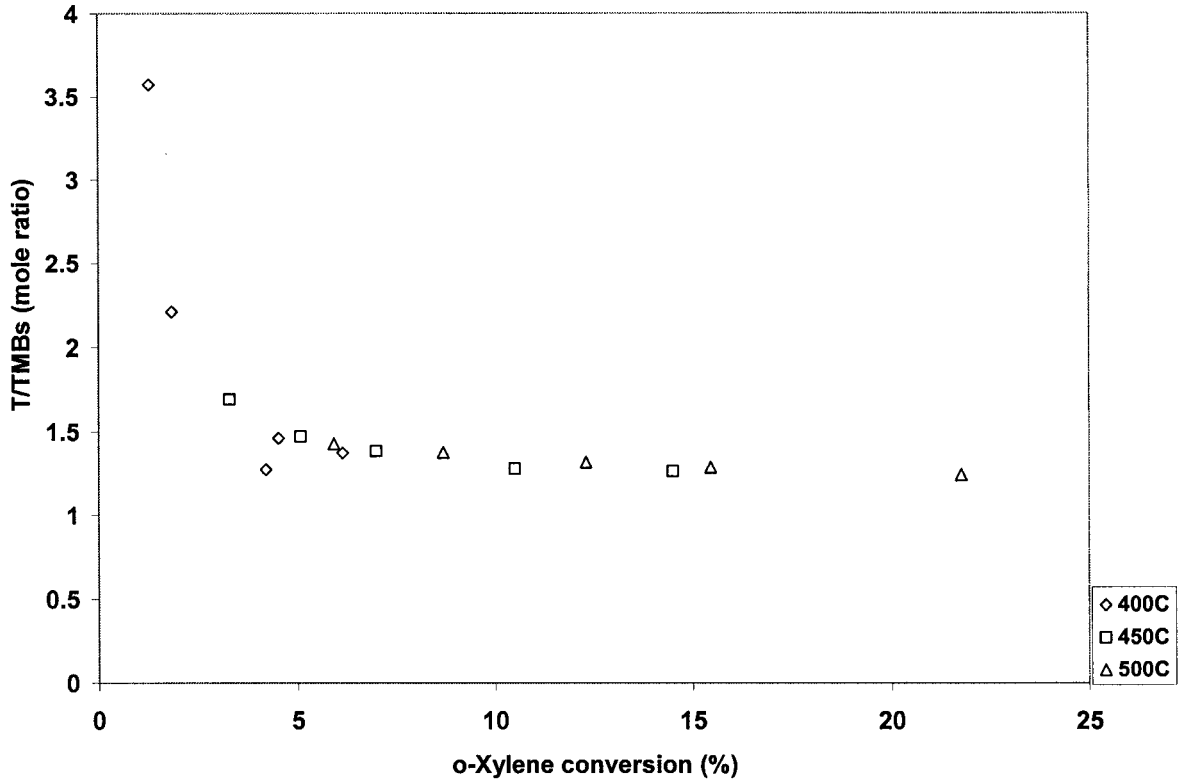

Figure 5.12 Molar ratio of toluene to trimethylbenzene against o-xylene conversion at different reaction temperatures

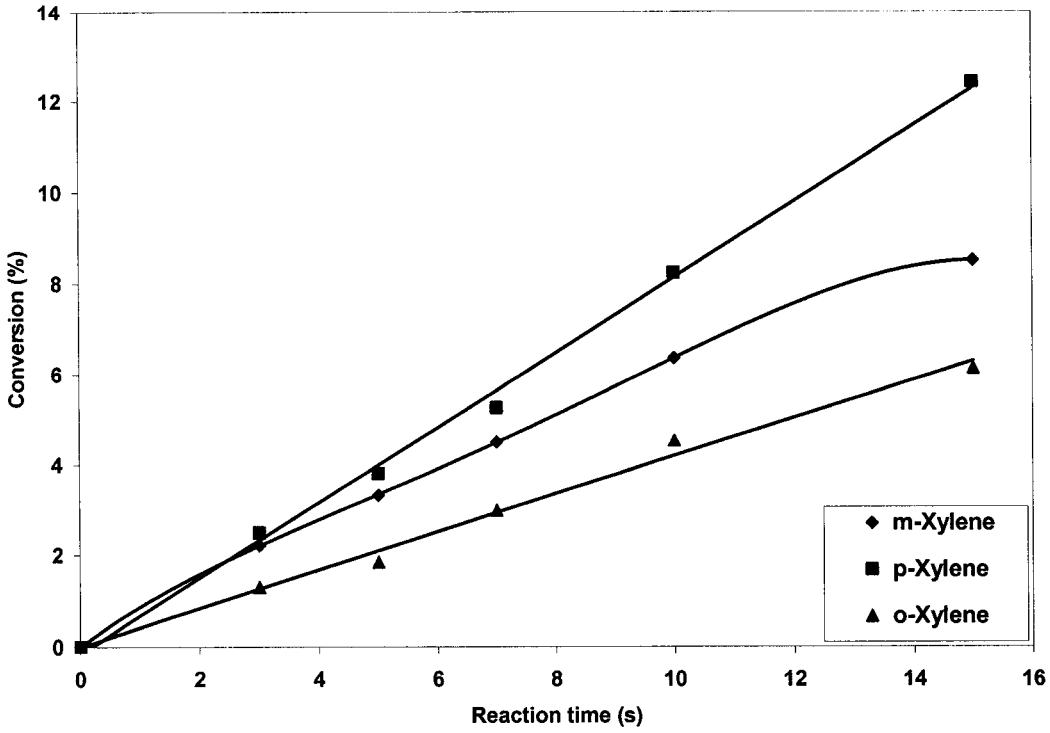

Figure 5.13 Xylenes conversion as a function of reaction time at 400°C

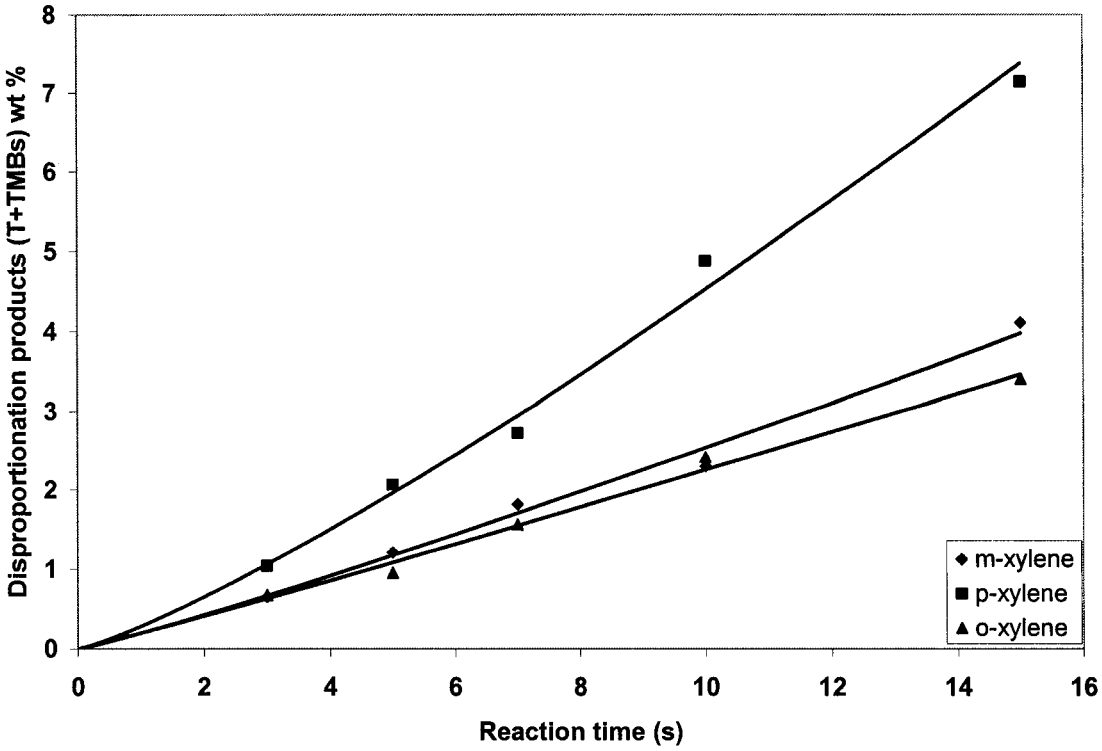

Figure 5.14 Comparison between the disproportionation products of the three xylene isomers at 400°C

5.4 Discussion

5.4.1 m-Xylene Transformation

The plot of initial selectivity to isomerization and disproportionation during m-xylene transformation shown in Figure 5.1 indicates that both the isomerization and disproportionation are primary reactions. Moreover, as the level of m-xylene conversion increases disproportionation becomes more pronounced since the produced xylenes also contributes to the overall disproportionation reactions.

It is remarkable that the slight increase in the disproportionation selectivity with increasing conversion level (Figure 5.1) differs from some previously reported trend [28-30]. Indeed, it is well-known that xylene disproportionation is a bimolecular reaction, which requires a higher concentration of acid sites. When these sites are selectively covered by coke precursors, it loses its activity. This results in the decrease of disproportionation selectivity with increasing time on stream [29]. The trend observed inthe present study could be explained due to the following; the contact time for xylene transformation in this study is much smaller (<15 s) than most of the previous studies. This reduces the deactivation of the strong active sites of USY zeolite, since trimethylbenzenes which are necessary intermediates for the formation of coke precursors cannot undergo secondary transformation. Besides, the low acidity (0.033 mmol/g) of the USY used in the present study contributes to this observation. In addition, the negligible coke deposition (< 0.1 wt %) measured for different the reaction condition over the USY catalyst [31] further substantiates the foregoing explanation. Thus, it could be said that this study focuses on the initial behavior of xylene transformation.

It is interesting to observe that the transformation of m-xylene produced almost equilibrium values of P/O ratio (Figure 5.2). This can be easily understood since the isomerization of m-xylene to produce p-and o-xylene involves 1, 2 methyl shifts which are identical reactions. Moreover, the cage opening of Y zeolite is large enough, and thus allows the produced isomers to exit the zeolite presumably without any shape selectivity. Figure 5.3 shows that with m-xylene as reactant, 1,2,4- and 1,3,5- TMB isomers are obtained as initial products, however, 1,2,3-TMB appeared as secondary product. It could be that 1,2,3- isomer is formed by secondary isomerization of 1,2,4-TMB under the conditions of this study. In contrast, all the three isomers have been reported as primary products of m-xylene disproportionation in some previous studies [10, 32], however, over metal cation exchanged Y zeolite.

5.4.2 p-Xylene Transformation

Similar to m-xylene, the transformation of p-xylene proceeds with both isomerization and disproportionation as primary reactions (Figure 5.5). This is obvious from the initial selectivity for both reactions. In addition, 1,2,4 trimethylbenzene isomer can be observed to approach zero at low conversions, indicating that it is a primary product for p- xylene disproportionation (Figure 5.7). This result is in conformity with some previously published works [10, 32].

The higher M/O ratio beyond the equilibrium ratio of 2.0 (Figure 5.6) particularly at lower reaction temperature is most probably due to the difficulty in causing direct conversion of p- to o-xylene. Moreover, the decrease in this ratio from 4.5 to around 3.1 with reaction temperature could be explained due to the ease in causing this reaction with increasing reaction temperature, as will be shown later. Indeed, it has been found that the

apparent direct interconversion between p- and o-xylene requires a higher activation energy as compared to 1,2 methyl shift [14, 18, 19]. Thus, a higher reaction temperature is needed to overcome this high energy barrier.

5.4.3 o-Xylene Transformation

The plot of initial selectivity to isomerization and disproportionation depicted in Figure 5.9, with o-xylene transformation is identical to that of p-xylene. As in the case of m- and p-xylenes, this plot clearly shows that both isomerization and disproportionation are primary products of o-xylene transformation. Moreover, employing o-xylene as reactant 1,2,4- and 1,3,5- are predicted from the directing effect of methyl groups during electrophilic substitution [10]. However, Figure 5.11 shows that only 1,2,4-trimethylbenzenes was obtained as initial product during o-xylene disproportionation. This behavior can not be associated with shape selective diffusion of the products, because USY zeolite has large pores that can accommodate the bulky trimethylbenzenes isomers. Thus, it is possible that both 1,3,5 and 1,2,3- TMBs are formed from secondary isomerization of the produced 1,2,4-isomer. Collins et al. [10] observed 1,2,4- and 1,2,3-TMBs as primary products, while Lanewala and Bolton [32] reported that only 1,2,4- and 1,3,5 are primary products of o-xylene disproportionation.

5.4.4 Comparison Between the Transformation of the Xylene Isomers

The observed trend in the reactivity of the xylene isomers (Figure 5.13) is consistent with some previous studies [1, 32]. This trend could be related to ease of protonation of carbon positions on the aromatic ring for each xylene isomers [5]. With o-xylene reactant, the close proximity of both methyl groups results in a pronounced steric

hindrance leading to the difficulty of a proton accessing the C_2 atom during intramolecular isomerization reaction. Consequently, o-xylene is the least reactive of the three isomers. On the other hand, m-xylene with a framework carbon between the two methyl groups has less effect of steric hindrance, while with p-xylene, the preferred protonation of the most accessible C_4 atom makes it most reactive. Similarly, as shown by Lanewala and Bolton [32], a direct correlation exits between the extent of disproportionation and the conversion of the xylene isomers. Therefore, the higher reactivity of p-xylene may be responsible for its corresponding higher disproportionation rate [18]. This result also agrees with the work of Morin et al. [1] for xylene isomerization over HY zeolite.

The high initial value of T/TMBs mole ratio observed with the transformation of all the three isomers (Figure 5.4, 5.8, and 5.12) could be due to the slower desorption rate of the bulky trimethylbenzenes isomers as compared to toluene under short reaction time (< 3s). However, as the reaction time increases, T/TMBs mole ratio decreases to around 1.2. The higher initial value of this ratio may be due to the increase on the desorption rate of TMBs from the pore of the USY zeolite. A similar observation regarding the slower desorption rate of TMBs as compared to toluene was also reported in previous studies [2, 33, 34]. In addition, the higher value of T/TMBs above stoichiometric ratio is probably the result of conversion of TMBs to coke molecules. The approach of the xylene isomers to their equilibrium values (ATE) is defined as [15]:

$$\frac{F_i - P_i}{F_i - E_i} x100 \qquad (5.9)$$

where F_i = feed concentration of species *i*, P_i = product concentration of species *i*, and E_i = equilibrium concentration of species *i*. Figure 5.15 present the ATE of the other two

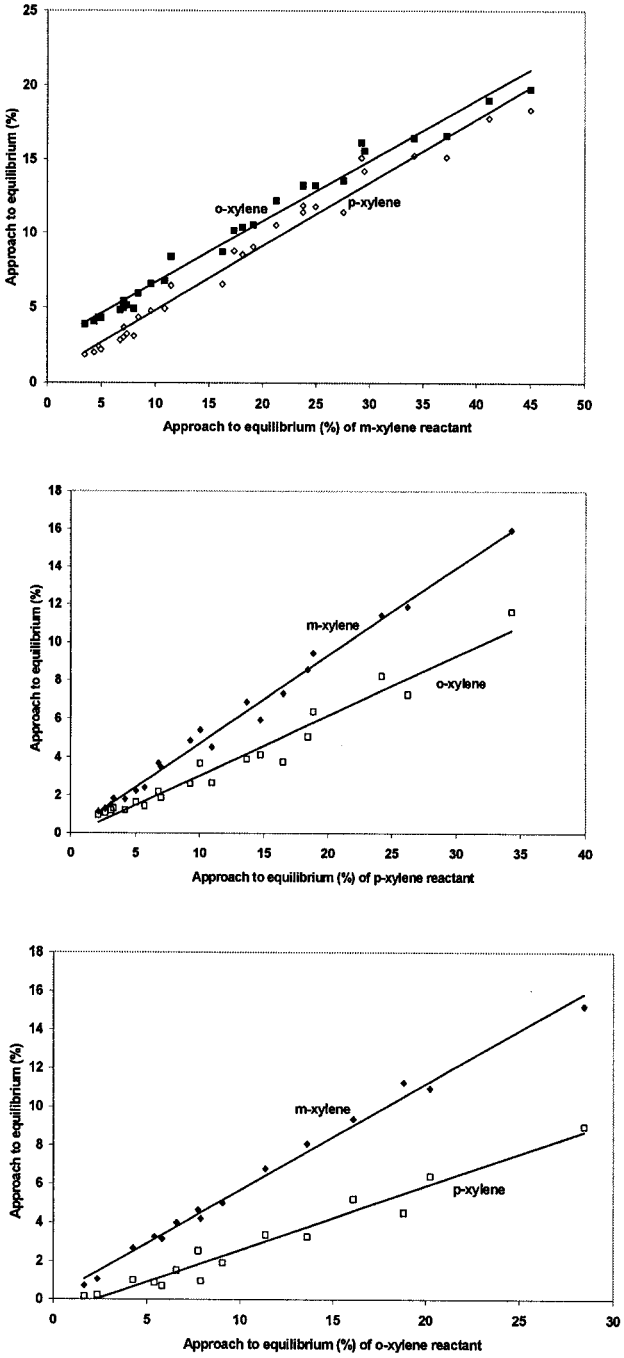

Figure 5.15 Approach to equilibrium composition (ATE) of the two xylene products as function of ATE of each xylene reactant

xylene isomers as a function of ATE of each xylene reactant. From this plot, it can be seen that p- and o-xylene approaches their equilibrium value at almost the same rate during m-xylene transformation. This suggests that the transformation of m-xylene to produce p- and o-xylene advance at identical rate, as shown by the estimated kinetic constants below. On the other hand, with the transformation of o-xylene, m-xylene approaches its equilibrium value 1.3 times faster than p-xylene, and with about 70% higher value of ATE. Similarly, m-xylene approaches equilibrium 1.1 times faster than o-xylene and with 50% higher value of ATE during p-xylene transformation. These findings, which agree qualitatively with a previous study [10] suggests that the transformation of xylenes over the USY zeolite used in this study advance in the thermodynamic controlled regime, unlike over ZSM-5 zeolite, where it proceeds in the diffusion controlled regime [9].

5.4.5 Modeling Result

The results presented in Table 5.1 substantiate earlier observation regarding the identical rate of producing p- and o-xylene during m-xylene isomerization. The values of the estimated preexponential factors for both reactions are essentially the same (0.17 m^3/kg of catalyst·s), and also their activation energies are closely similar at 13.7 and 14.1 (kcal/mol), respectively. A similar result was obtained with the time on stream deactivation model [18]. This was explained by the similarity of the two reactions, because both involve the migration of adjacent methyl groups along the aromatic ring. Moreover, the constraint of transition state complexes in conversion of m- to p-xylene, and m- to o-xylene is negligible under the present conditions.

Table 5.1 Estimated kinetic parameters

	E_1	E_2	E_3	E_{-3}	E_4	E_5	E_6
	13.7	14.1	16.7	18.1	18.7	10.3	13
95% CL	1.9	1.8	7.2	7.9	1.4	1.14	0.15
	$k_{01} \times 10^3$	$k_{02} \times 10^3$	$k_{03} \times 10^3$	$k_{-03} \times 10^3$	$k_{04} \times 10^3$	$k_{05} \times 10^3$	$k_{06} \times 10^3$
	0.17	0.17	0.059	0.038	0.38	0.41	0.25
95% CL	0.02	0.02	0.027	0.019	0.035	0.03	0.02
	λ_m	λ_p	λ_o				
	0.83	1.8	1.5				
95% CL	0.12	0.9	0.9				

k_i (m^3/ kg of catalyst·s)

E_i (kcal/mole)

It is of great interest to note that E_3 and E_{-3} have the highest values (16.7 and 18.1 kcal/mol, respectively). This clearly suggests that the mutual interconversion between p- and o-xylene, is highly temperature dependent, unlike 1,2- methyl shift with lower values of activation energy (~14 kcal/mol). This significant result is in perfect agreement with some previous studies [14, 18, 19]. Consequently, it could be proposed that under low reaction temperatures (< 450°C), the interconversion of both isomers proceed via m-xylene as an intermediate reaction step (Figure 5.16). However, as the reaction temperature is increased beyond 450°C, both isomers may attain the required energy to interconvert as shown schematically by the dashed-line in Figure 5.16B and 4.23C.

In spite of the forgoing discussion on the difficulty of direct interconversion of p- and o-xylene, it could be seen in Table 4.6 that the conversion of p- to o-xylene has a lower activation energy (E_3) and higher preexponential factor (k_{03}) than that of o-xylene (E_{-3} and k_{0-3}). This result, which also agrees with the ATE plots (Figure 4.23), could be understood, giving that p-xylene reacts to a greater extent than o-xylene over the catalyst used in this study. Also, the kinetic parameters estimated with p-xylene transformation (k_{05} and E_5) indicate a higher disproportionation with this isomer, as compared with m- and o-xylene disproportionation in agreement with data presented in Figure 5.14.

5.4.6 Comparison Between Experimental Results and Model Predictions

The overall parity between experimental data and model values for the transformations of m-, p-, and o-xylene gives a correction coefficient of 0.99, 0.98, and 0.99, respectively. Moreover, from the values of the estimated kinetic constants and their corresponding 95% confidence limits (Table 5.1), it can be argued that these parameters are accurately estimated. Although, the model tended to slightly overpredict the yield of

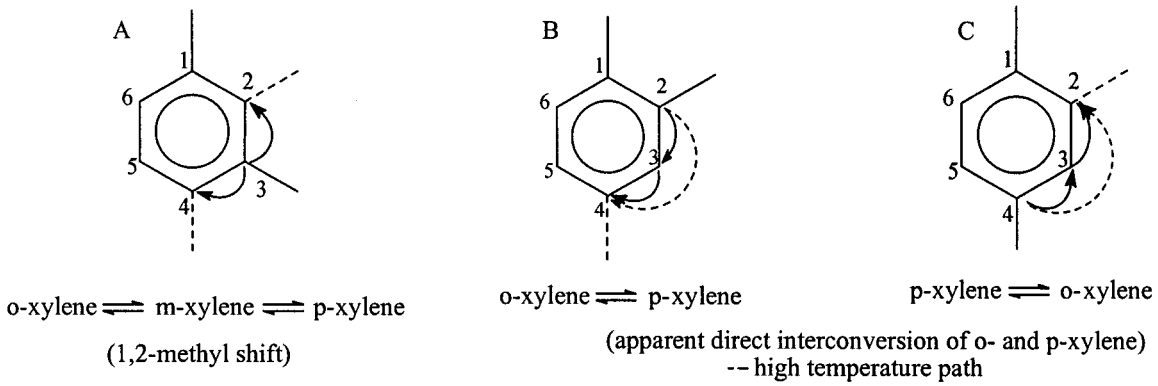

Figure 5.16 Schematic representation of apparent methyl group migration during xylene transformation

p-xylene from o-xylene transformation and vice versa. This is not surprising, because the direct interconversion of both isomers occurs only at high reaction temperatures, meanwhile, the model assumes that their direct interconversion proceed right from the onset. The separation of the two modes of conversion for both isomers i.e. via m-xylene as intermediate reaction step, and apparent direct interconversion with different temperature regime, is quite difficult in the same kinetic model.

To check the validity of the estimated kinetic parameters using with the overall kinetic model (Scheme 1), the fitted parameters were substituted into the model developed for this scheme, and the equations were solved numerically using the fourth order Runge-Kutta method. The simulated results were compared with the experimental data as shown in Figure 5.17. It can be observed from this figure that the simulated results compares fairly well with the experimental data. This provides significant evidence that the overall model could be used for the interpretation of the data obtained during m-xylene transformation in the riser simulator.

In summary, the good agreement between the model and experimental results proves that the "reactant converted" decay model can be used to successfully model the overall xylene transformation. This model correctly captures the deactivation of the catalyst as a function of the reactant concentration. Moreover, it is consistent with the well-established fact that the deactivation of USY zeolite during xylene transformation is caused by the deposition of coke on active catalyst sites.

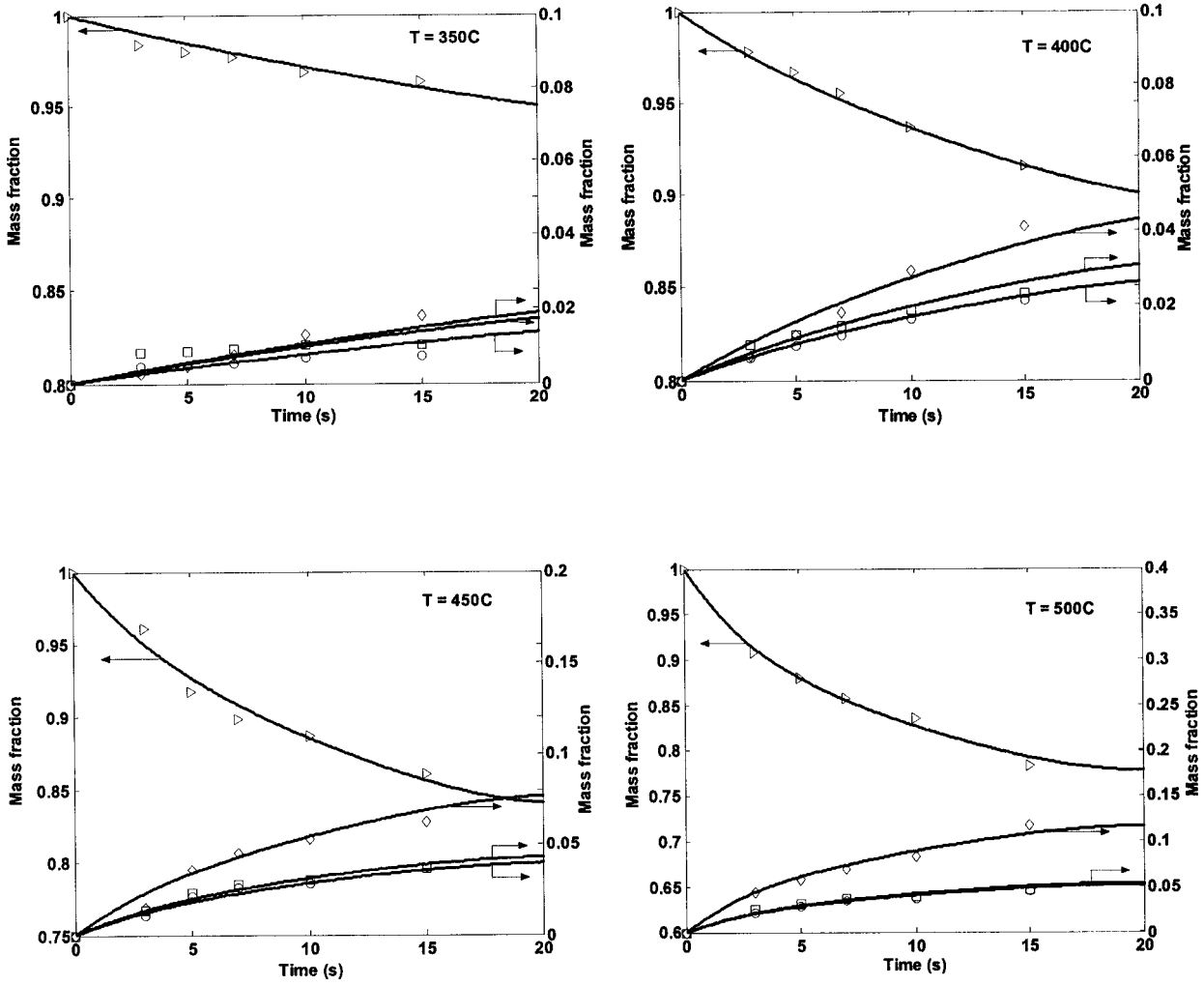

Figure 5.17 Comparison between experimental results and numerical simulations (—) based on overall m-xylene transformation (Scheme 1)
(○) p-xylene; (□) o-xylene; (◊) T+TMBs; (tilted Δ) m-xylene.

5.5 Conclusions

Experimental studies were conducted in a riser simulator to study the influence of reaction parameters on xylene transformation. The selectivity to isomerization, disproportionation, and distribution of trimethylbenzene isomers were also investigated. Initial selectivity revealed that both isomerization and disproportionation reactions advance as primary reactions. A higher initial value of T/TMBs mole ratio was observed with the three xylene reactants, and this was explained by the slower desorption rate of bulky TMBs isomers under the short reaction time of the riser simulator. p-Xylene was found to be more reactive than the others xylene isomers. This was explained by the higher accessibility of proton to C_4 atom, due to its least effect of steric hindrance.

A recently proposed catalyst deactivation model, so-called "reactant converted" decay model was tested with the transformation of xylenes. Effective, mechanistic kinetic models were developed to describe the transformation of each of the xylene isomers based on the obtained experimental results. The model parameters were estimated using non-linear regression analysis. The parameters optimized to the experimental data gave a good prediction of the overall reaction kinetics for the xylene transformations. Thus, providing significant evidence that the "reactant converted" decay model can be adequately utilized to account for the catalyst deactivation. Moreover, based on the values of the estimated activation energy, it was found that the interconversion of p- and o-xylene is highly temperature dependent, unlike 1,2- methyl shift, which is only slightly dependent on temperature.

5.6 References

[1] Morin, S., Gnep, N.S., Guisnet, M., A Simple Method for Determining the Relative Significant of the Unimolecular and Bimolecular Pathways of Xylene Isomerization over HY Zeolites, J. Catal., 159 (1996), 296.

[2] Morin, S., Ayrault, P., Gnep, N.S, Guisnet, M., Influence of the Framework Composition of Commerical HFAU Zeolites on their Activity and Selectivity in m-Xylene Transformation Appl. Catal. A, 166 (1998a), 281.

[3] Guisnet, M., Characterization of Acid Catalysts by Use of Model Reactions. Stud. Surf. Sci. Catal., 20 (1985), 283-97

[4] Perez-Pariente, J., Sastre, E., Fornes, V., Martens, J. A., Jacobs, P. A., Corma, A., Isomerization and Disproportionation of m-Xylene over Zeolite Beta. Appl. Catal., 69 (1991), 125-37.

[5] Martens, J. A., Perez-Pariente, J., Sastre, E., Corma, A., Jacobs, P. A., Isomerization and Disproportionation of m-Xylene: Selectivities Induced by the Void Structure of the Zeolite Framework. Appl. Catal. 45 (1988), 85-101.

[6] Olson, D. H., Haag, W. O., Structure-Selectivity Relationship in Xylene Isomerization and Selective Toluene Disproportionation. ACS Symposium Series 248 (1984), 275-307.

[7] Jones, Christopher W., Zones, Stacey I., Davis, Mark E., m-Xylene reactions over zeolites with unidimensional pore systems. Appl. Catal., A: General, 181 (1999), 289-303.

[8] Chutoransky, P., Jr., Dwyer, F. G., Effect of zeolite crystallite site on the selectivity kinetics of the heterogeneous catalyzed isomerization of xylenes. Adv. Chem. Ser., 121 (1973), 540-52.

[9] Collins, Dermot J., Medina, Roger J., Davis, Burtron H., Xylene isomerization by ZSM-5 zeolite catalyst. Can. J. Chem. Eng., 61 (1983), 29-35.

[10] Collins, D.J., Mulrooney, K.J., Medina, R.J., Xylene Isomerization and Disproportionation over Lanthaniun Y Catalyst. J. Catal. 75 (1982), 291.

[11] Do D.D., Enhanced Paraxylene Selectivity in a Fixed-Bed Reactor. AIChE J. 31 (1985), 574.

[12] Ma, Y. H., Savage, L. A., Xylene isomerization using zeolites in a gradientless reactor system. AIChE J. 33 (1987), 1233-40.

[13] Li, Yu-Guang, Jun, Hu., Kinetics study of the isomerization of xylene on ZSM-5 zeolites: the effect of the modification with MgO and CaO. Appl. Catal., A: General 142 (1996), 123-137.

[14] Hopper, J. R., Shigemura, Dennis S., Kinetics of liquid phase xylene isomerization over H-mordenite. AIChE J., 19 (1973), 1025-32.

[15] Hsu, Y. S., Lee, T. Y., Hu, H. C., Isomerization of ethylbenzene and m-xylene on zeolites. Ind. Eng. Chem. Res., 27 (1988), 942-7.

[16] Gendy, Tahani S., Simulation of liquid and vapor phase xylene isomerization over deactivating H-Y-zeolite. J. Chem. Tech. Biotech., 73 (1998), 109-118.

[17] Cappellazzo, O., Cao, G., Messina, G., Morbidelli, M., Kinetics of shape-selective xylene isomerization over a ZSM-5 catalyst. Ind. Eng. Chem. Res., 30 (1991), 2280-7.

[18] Iliyas A., Al-Khattaf S., Xylene Isomerization over USY Zeolite in a Riser Simulator: A Comprehensive Kinetic Model. Ind. Eng. Chem. Res., 43 (2004) 1349.

[19] Norman, G.H., Shigemura, D.S., Hopper, J.R., Isomerization of Xylene over Hydrogen Mordenite. A Comprehensive Model. Ind. Eng. Chem. Prod. Res. Dev. 15 (1976), 41.

[20] Corma A., Llopis F., Monton J.B., Influence of the Structural Parameters of Y Zeolite on the Transalkylation of Alkylaromatics. J. Catal., 140 (1993), 384.

[21] Atias, J. A., Tonetto, G.,; de Lasa, H., Catalytic Conversion of 1,2,4-Trimethylbenzene in a CREC Riser Simulator. A Heterogeneous Model with Adsorption and Reaction Phenomena. Ind. Eng. Chem. Res., 42 (2003), 4162-4173.

[22] Al-Khattaf, S, de Lasa, H.I., Catalytic Cracking of Cumene in a Riser Simulator: A Catalyst Activity Decay Model. Ind. Eng. Chem. Res. 40 (2001), 5398.

[23] Al-Khattaf, S., de Lasa, H.I., The Role of Difusión in Alkyl-benzenes Catalytic Cracking. Appl. Catal. A: General, 226 (2002), 139.

[24] Al-Khattaf, S., de Lasa, H.I., Diffuision and Catalytic Cracking of 1,3,5 tri-iso-propyl-benzene in FCC Catalysts. Chem. Eng. Sc. 57 (2002), 4909.

[25] de Lasa, H.I. U.S. Patent 5, 102 ,628, (1991).

[26] Agarwal, A.K., Brisk, M.L., Sequential Experimental Design for Precise Parameter Estimation: 1. Use of Reparameterization. Ind. Eng. Chem. Process Des. Dev. 24

(1985), 203.

[27] Stull, D.R., Westrum, E.F., Simke, G.C., "The Chemical Thermodynamics of Organic Compounds" Wiley: New York, (1969) 368.

[28] Morin, S., Gnep, N.S., Guisnet, M., Influence of Coke Deposits on the Selectivity of m-Xylene Transformation and on the Isomerization Mechanism. Appl. Catal. A: General, (1998)168, 63.

[29] Yang, M.G., Nakamura, I., Fujimoto, K., m-Xylene Transformation over NiS/Al_2O_3-USY Hybrid Catalysts: Effects of Hydrogen Spillover. Appl. Catal. A: General, 144 (1996), 221-235.

[30] Damitriu, E., Guimon, C., Hulea, V., Lutic, D., Fechete, I., Appl. Catal. A: General, 237(2002), 211.

[31] Al-Khattaf S., Iliyas A., Al-Amer A., Inui T., The Effect of Y-Zeolite Acidity on m-Xylene Transformation Reactions. Submitted to Appl. Catal. A: General, (2004).

[32] Lanewala, M.A., Bolton, A.P., The Isomerization of the Xylenes Using Zeolites Catalysts. J. Org. Chem., 34 (1969), 3107.

[33] Laforge, S., Martin, D., Paillaud, J. L., Guisnet, M., m-Xylene transformation over H-MCM-22 zeolite 1. Mechanisms and location of the reactions. J. Catal. 220 (2003), 92-103.

[34] Nakazaki, Y., Goto, N., Inui, T., J. Catal. 136 (1992), 141.

CHAPTER 6

6 Effect of Y Zeolite Acidity on m-Xylene Transformation Reactions

6.1 Introduction

Xylenes are important starting materials for some industrial processes like the production of synthetic fibers, plasticizers and resins. The major sources of these aromatic hydrocarbons are the reforming and catalytic cracking units of the refinery, which have a higher ratio of low-valued m-xylene. A convenient way to upgrade the low-valued m-xylene consists of its transformation to o- and p-xylene. In this context, the transformation of m-xylene has been studied over different types of zeolite [1-8].

There is interest in ultrastable Y-type zeolites for m-xylene transformation, partly because of their increased chemical and thermal stability, with respect to other zeolites. Y-zeolite is made ultrastable by the removal of aluminum from the framework. The dealumination can be accomplished through the use of steam [9], acid leaching [10], or by chemical treatment with hexaflourosilicate or silicon tetrachloride [11-13]. However, the most common procedure is hydrothermal treatment at elevated temperatures under controlled atmosphere (steaming). The resulting material, USY (ultrastable Y) zeolites, being modified in the framework Si/Al ratio, structure and acidity, usually exhibits improved reactivity, selectivity and coking behavior for a catalytic reaction, which is of great interest to the petroleum industry.

m-Xylene isomerization (I) and/or disproportionation (D) have been used to correlate the intrinsic properties of zeolites [14], their diffusion characteristics [15], protonic acidity [1,5], pore geometry [16] and architecture [17], frame work composition [3] on one hand, and their activity and selectivity [18] on the other hand. Both the isomerization and disproportionation reactions have been reported to be catalyzed by Brönsted acid sites [1-6]. Disproportionation being a bimolecular reaction has been established to require higher concentration of acid sites [1,3,7]. However, these reactions do not produce benzene and gases.

Paring reaction was first proposed by Sullivan et al. [19] in the early sixties for the hydrocraking of hexamethylbenzene over a $NiS\text{-}Al_2O_3\text{-}SiO_2$ catalyst. It involves a sequence of reactions to apparently pare methyl groups from polymethylated aromatics. The pared methyl groups join together to form longer side chains, and subsequently these chains splits off to form low chain olefins without disrupting the parent aromatic ring. Moreover, some researchers have employed the mechanism of paring reaction to explain the obtained products during the disproportionation of 1,2,4-trimethylbenzene [20], isomerization of 1-cyclohexyloctane mixed with dodecane [21], and formation of ethyltoluene during the isomerization of trimethylbenzenes [8].

Several studies have been conducted on the effect of Y-zeolite acid properties on isomerization and disproportionation of m-xylene reactions [1,5,7]. However, studies correlating the intrinsic properties of Y-zeolite to other reaction pathways, apart from isomerization and disproportionation are somewhat limited. With this in mind, we report in the present work, the effect of acid properties of Y-zeolite on products selectivity and reaction pathways during m-xylene transformation in a fluidized-bed reactor, with

emphasis on other reaction pathways. As prepared H-Y zeolite modified through systematic hydrothermal treatment to obtain varying concentration of acid sites were employed for the study. The resulting samples were characterized by different techniques, such as XRD and TPD order to correlate the catalytic behavior of the zeolites to their intrinsic properties. Mechanisms will be proposed for the formation of the various products. Furthermore, the stability and deactivation of the sites responsible for the proposed pathways will be investigated for the H-Y and the highly steamed USY zeolite.

6.2 Results and Discussion

6.2.1 Catalyst Characterization

The physico-chemical properties of the catalyst used in this study are presented in Table 3.1. It is well-known that steam treatment has a marked effect on both stability and the crystallinity of the H-Y zeolite. The XRD patterns (Figure 6.1) of the H-Y zeolite and dealuminated zeolites indicate high crystallinity with a slight decrease in the peak intensity depending on the severity of the steam treatment. Similarly, the specific surface area decrease with increase in steaming temperature due to the presence of extra-framework aluminium in the pores and channels as well as the formation of mesopores.

The NH_3-TPD spectra of the parent H-Y and the dealuminated Y zeolites catalysts are shown in Figure 6.2, while the amounts of desorbed ammonia (total acidity) are summarized in Table 3.1. H-Y catalyst showed two main desorption peaks at 265 and 390 ^{o}C and had a long tailing. The HT component (high temperature peak, >300 ^{o}C) of TPD spectra of H-Y is most likely to be associated with the water desorption as a result of dehydroxylation of surface hydroxyl groups. The HT peak is shifted to lower temperature

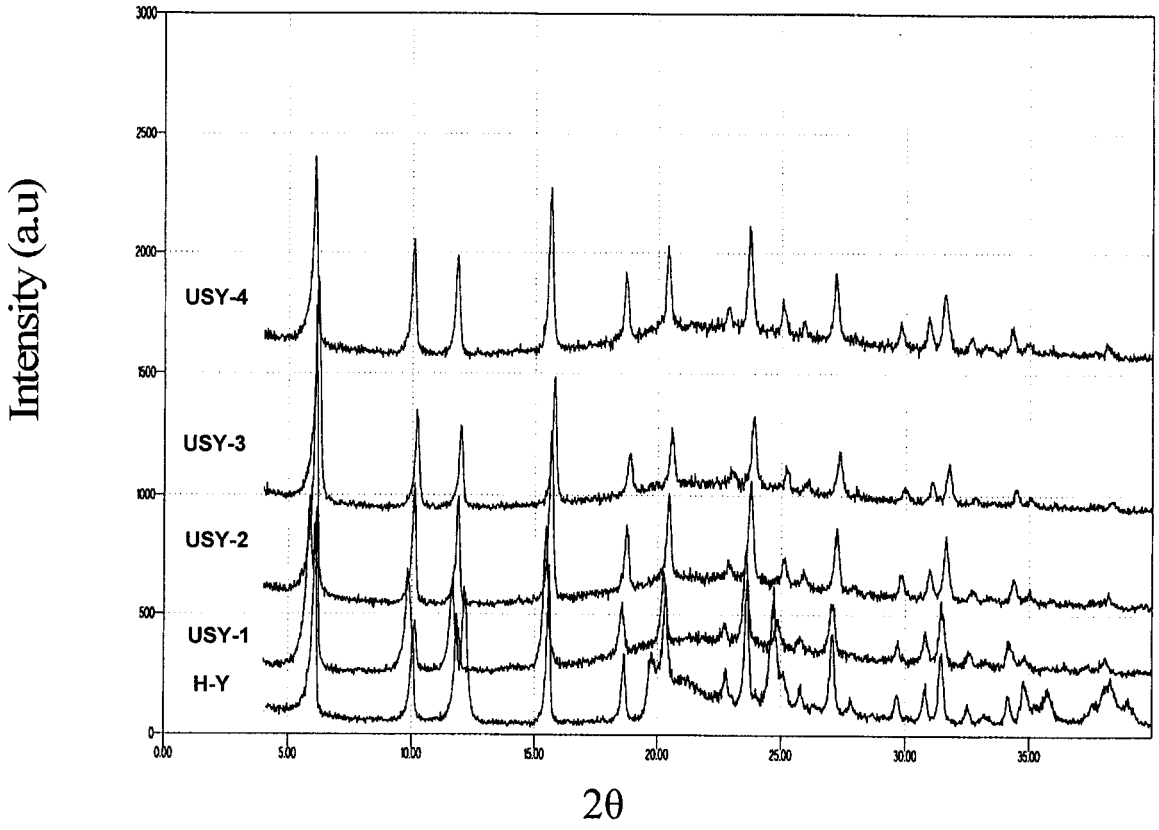

Figure 6.1. XRD Spectra of H-Y and the USY zeolites

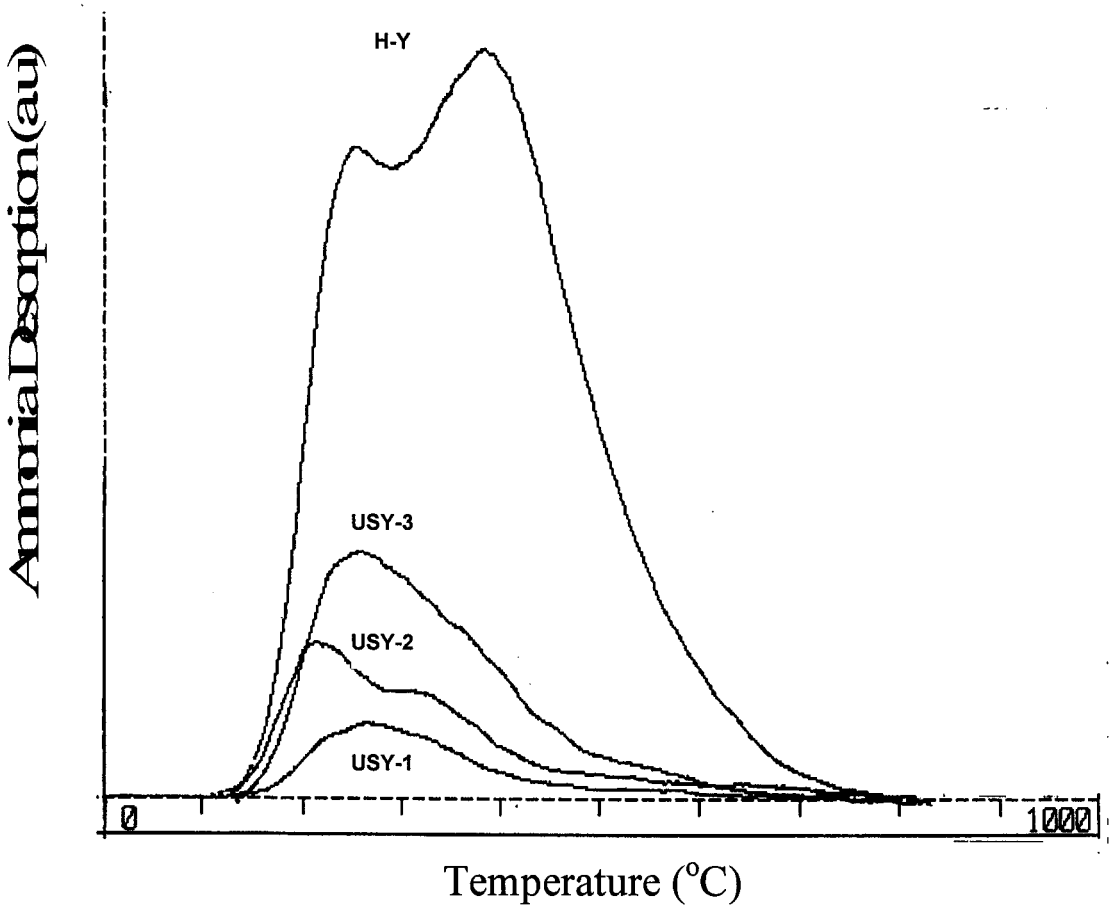

Figure 6.2 Temperature programmed desorption of ammonia over the different catalysts

in USY-2 at 310 °C and is not distinct for USY-3 catalyst. Also, the area of HT peak decreases with increasing steaming temperature.

6.2.2 Products Distribution

The degree of m-xylene conversion as a function of total number of acid sites for the catalysts under study, are compared at 450°C as shown in Figure 6.3. The activity of the catalysts taken in terms of conversion passes through a maximum for all the reaction times studied. Among the examined catalysts, the highest conversion of m-xylene was obtained over moderately dealuminated catalyst (USY-3). H-Y and USY-4 showed nearly the same initial activity, but the former deactivates faster.

The products distribution during the transformation of m-xylene over the parent and the dealuminated Y zeolites are compared in Figure 6.4A and B at constant conversion levels of 2 and 10 % respectively. It is clear from these plots that toluene has the highest yield over the catalysts at both conversion levels, except with USY-1, which gave a slightly lower yield of toluene than some other products. On the other hand, the yields of TTMBs seemed to be the lowest at 10 % conversion. Furthermore, the yields of p- and o-xylene are closely identical over all the catalysts, with the highest value being around 24% for each isomer over USY-1 catalyst.

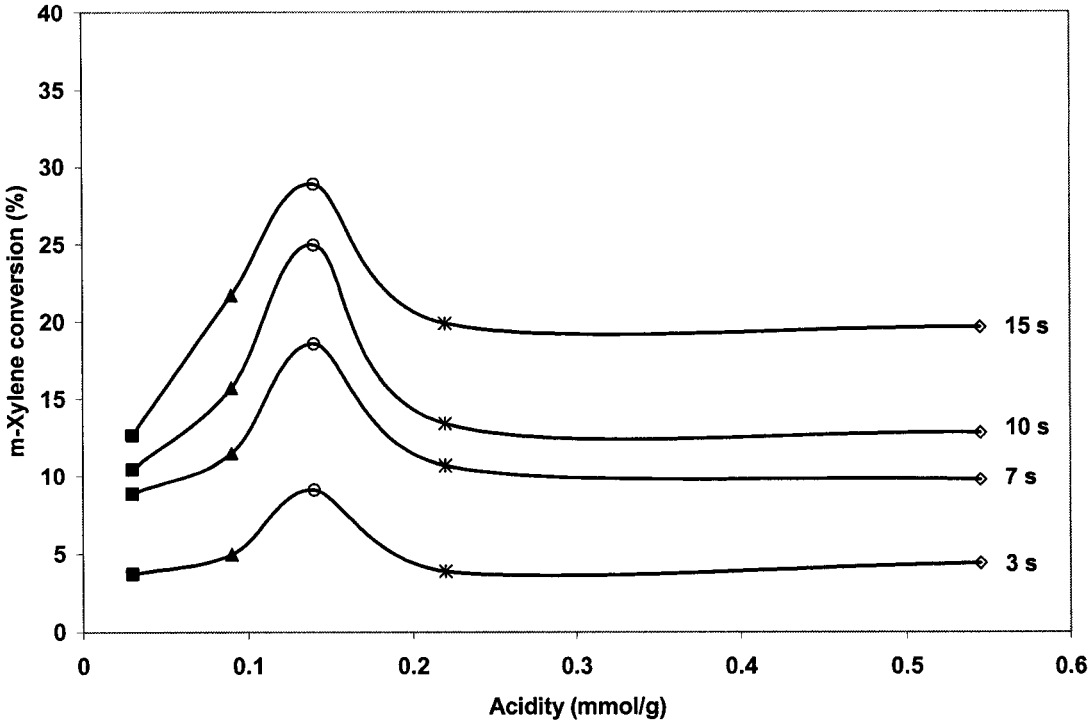

Figure 6.3 m-Xylene conversion over the different catalysts versus total acidity at various reaction times (A) 400 °C (B) 450 °C ; (■) USY-1, (▲) USY-2 (○) USY-3, (*) USY-4 (◊) USY-4

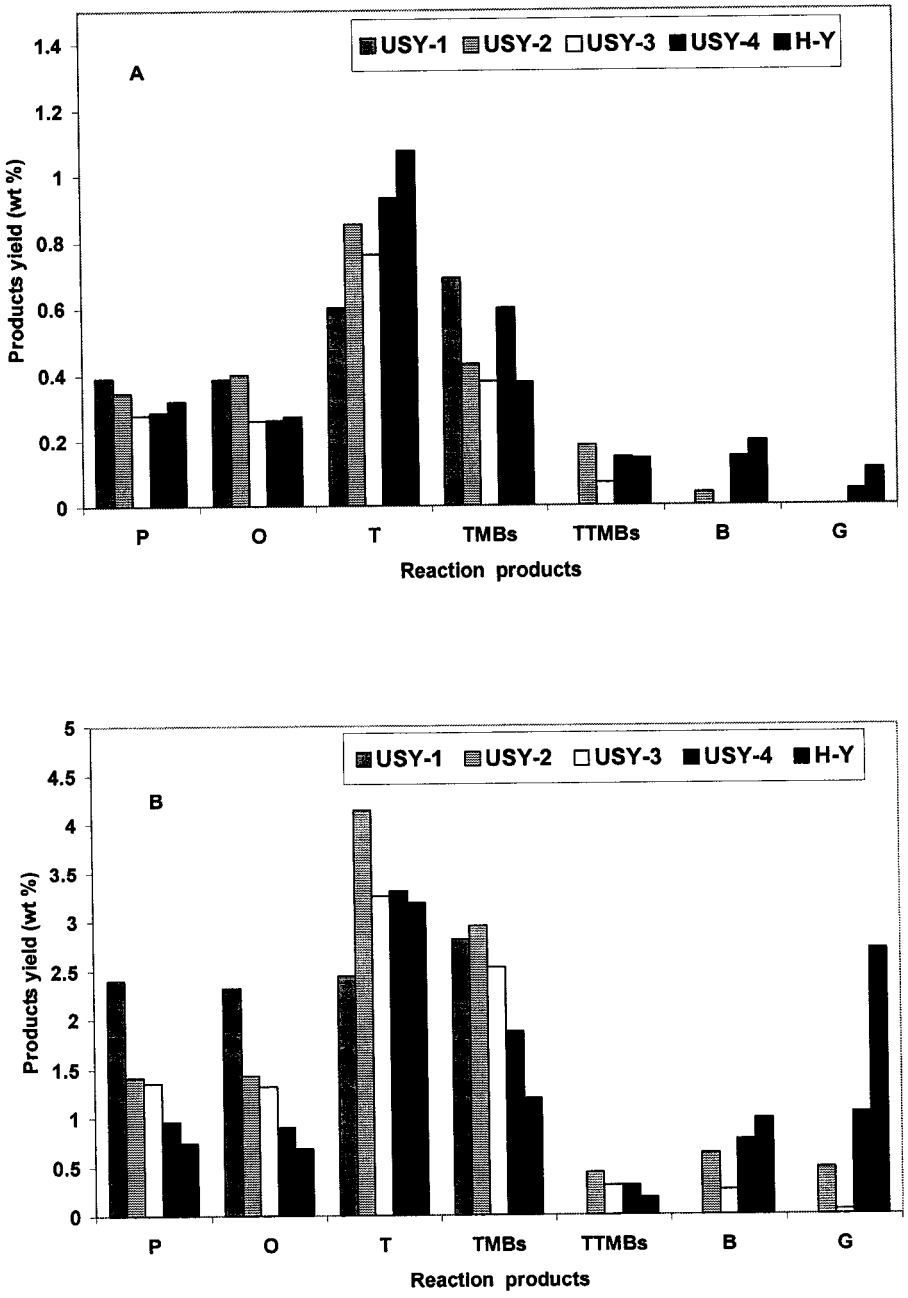

Figure 6.4 . Products distribution of m-xylene transformation over the different catalysts. (A) 2 % conversion, (B) 10 % conversion

It is worth mentioning that TTMBs, benzene, and C_2 - C_4 gases were not observed over USY-1 catalyst at all conversion levels, and were formed with relatively low yields over the highly active USY-3 catalyst. In contrast, significant amounts of benzene and C_2 - C_4 products were obtained over the parent H-Y as compared to the dealuminated catalysts. However, H-Y catalyst appeared to give the lowest selectivity toward TMBs particularly at higher reaction temperatures. This is better depicted by the plot of product yields versus reaction temperature over this catalyst (Figure 6.5). As shown in this figure, substantial decrease in the yields of TMBs can be noticed with increasing reaction temperature. This decrease suggests that it undergoes secondary reactions. Moreover, the simultaneous increase in the yields of benzene and C_2 - C_4 gases over this catalyst further indicate that these are probably the products of such secondary reactions.

Pamin et al. [5] and Sulikowski et al. [6] attributed the secondary formation of benzene to simple dealkylation reaction. However, as observed by Roger et al. [20] methyl groups do not dealkylate readily over acid catalysts. Moreover, this step needs hydrogen and forms methane, which was not reported in these studies. On the other hand, Laforge et al. [8] suggested that the produced benzene during the conversion of m-xylene over H-MCM-22 is likely the result of the transalkylation between m-xylene and toluene. However, when toluene and m-xylene were reacted under the conditions used in the present study, an appreciable amount of benzene was not observed, and toluene seemed unreactive. Thus, it can be concluded that benzene is not formed from this route. Consequently, it is possible that over the highly acidic catalyst, an alternative pathway, so-called paring reaction is initiated in addition to the well-known isomerization and

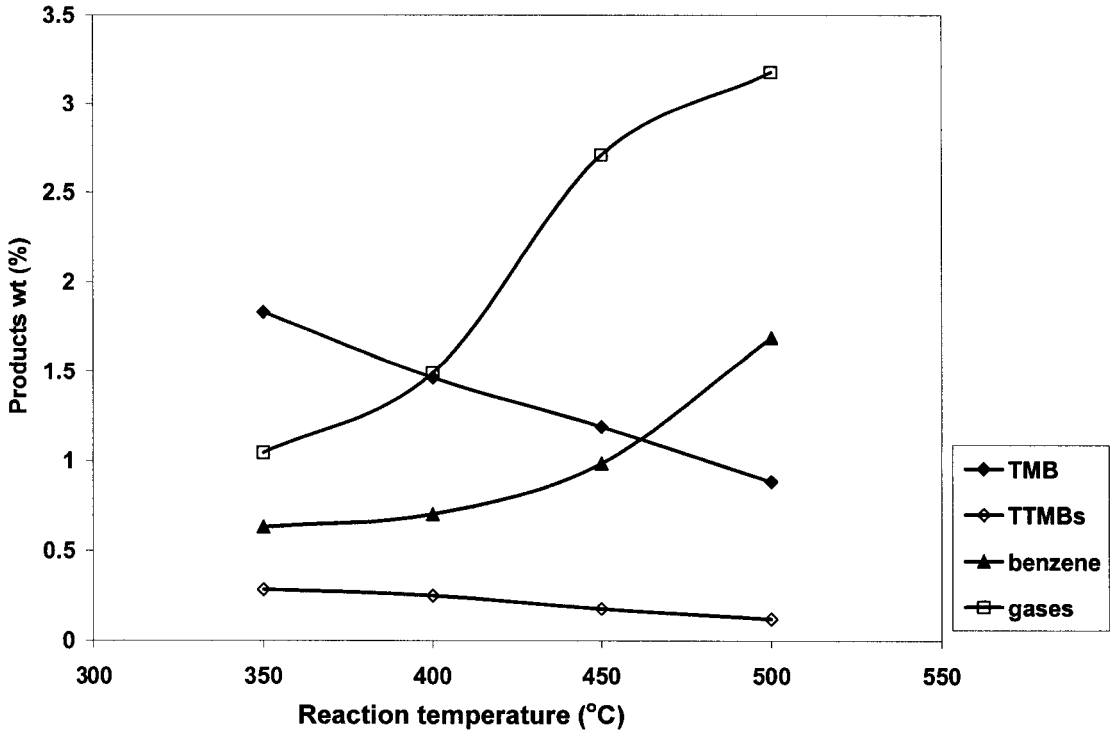

Figure 6.5 Products yield versus reaction temperature over H-Y catalyst at 10% conversion

disproportionation pathways, as shown by path 3 of Figure 6.6. Regarding paring reaction pathway, it is proposed that the high concentration of strong acid sites on the parent H-Y (Figure 6.6) and the mildly dealuminated catalysts (USY-4) initiates paring reaction of the produced TMBs, following the mechanism shown in Fig. 7 [29]. A similar conclusion regarding the formation of benzene via paring reaction was reached by Roger et al. [20] in their study of 1,2,4 trimethylbenzene conversion over H-ZSM5 zeolite. Moreover, since TMBs is formed via disproportionation route of the three xylene isomers, thus, it is further proposed that they all undergo a similar paring reaction pathway. Moreover, the surplus toluene observed in the present study may have been formed from the alternate step of paring reaction. In addition, due to the high coke formation over H-Y, an appreciable amount of hydrogen will be formed as a consequence. These might further lead to the formation of gases and benzene.

6.2.3 Selectivity to Reaction Pathways

The comparison of the products distribution over the different catalysts gives additional information about other possible reaction pathways in the course of m-xylene transformation. As shown in Figure 6.6, m-xylene may undergo paring reaction in addition to the isomerization and disproportionation reactions over highly acidic zeolite catalyst. The selectivity of m-xylene along these reaction pathways reflects, at least to a first approximation, the intrinsic properties of the catalysts, particularly the strength and concentration of acid sites. It may also provide indirect information on the relative stability and deactivation of the sites responsible for these reactions [1]. Thus, the selectivity of m-xylene transformation toward isomerization, disproportionation

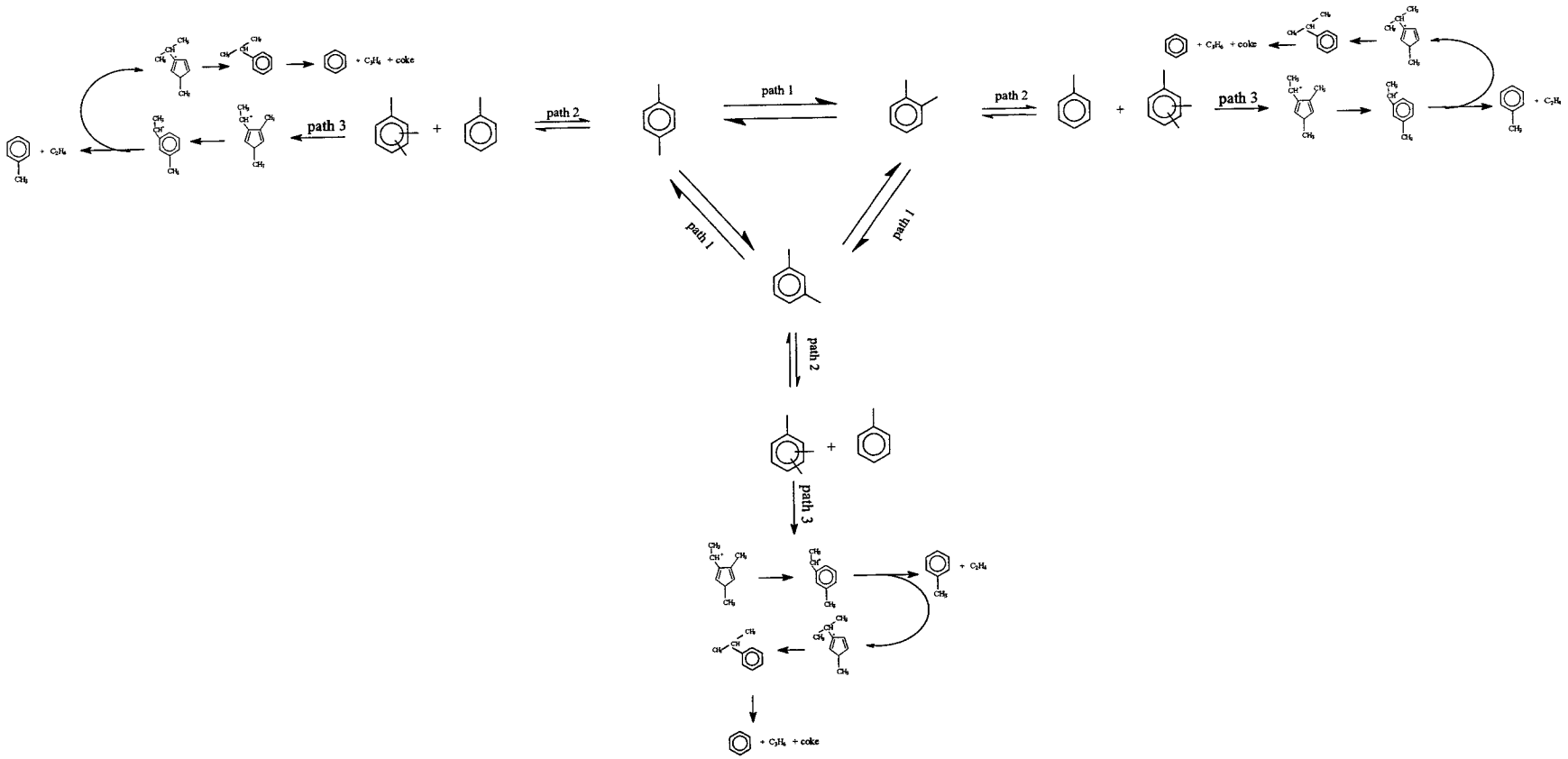

Figure 6.6 Proposed overall reaction scheme and paring reaction mechanism during m-xylene transformation.

and paring pathways are plotted in Figure 6.7 – 6.9 respectively at 450 °C, as a function of reaction time for the parent and dealuminated catalysts. The highly dealuminated (USY-1) catalyst showed the highest isomerization selectivity, which is around 50% higher than the parent H-Y catalyst (Figure 6.7). From this result, it is evident that the low concentration of acid centers in the USY-1 catalyst catalyzes above all, the isomerization reaction. This is in agreement with the well-established fact that isomerization being a monomolecular reaction requires weaker acidic sites.

Indeed it has been established that increase in concentration of Brönsted sites facilitates disproportionation reaction. Since disproportionation is a bimolecular reaction, it requires higher amount of acid sites for its catalysis [7]. Following this, one would expect that the parent H-Y catalyst should give the highest disproportionation selectivity, since it has the highest concentration of Brönsted acid sites. However, Figure 6.8 shows that the mildly dealuminated catalyst (USY-4) appeared to be the most active catalyst for m-xylene disproportionation, with selectivity values being about 45 % greater than parent H-Y catalysts at 7 s reaction time. This is probably due to secondary transformation of TMBs, a major disproportionation product to coke precursors and paring reaction, as evident from the relatively higher amount both secondary products over this catalyst. Moreover, the high coke formation over the H-Y catalyst results in the decrease in the density of these sites. Thus, suggesting that bimolecular reaction, such as disproportionation reaction is more sensitive to this effect than isomerization.

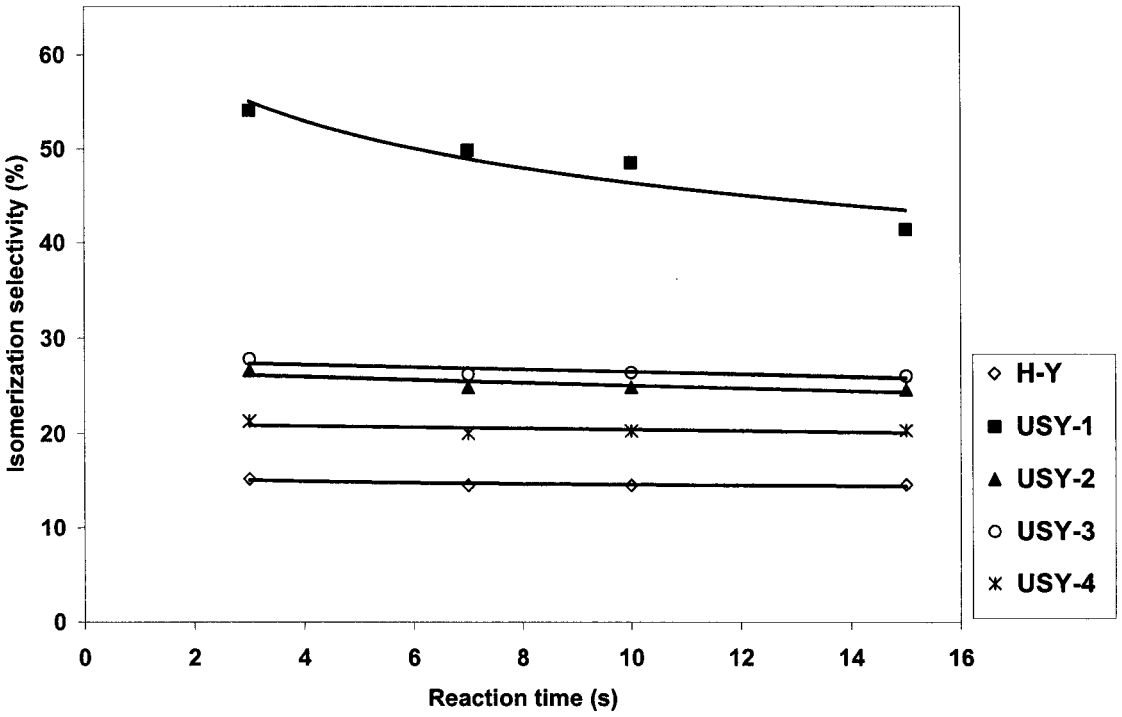

Figure 6.7 Isomerization selectivity as a function of reaction time at 450 °C

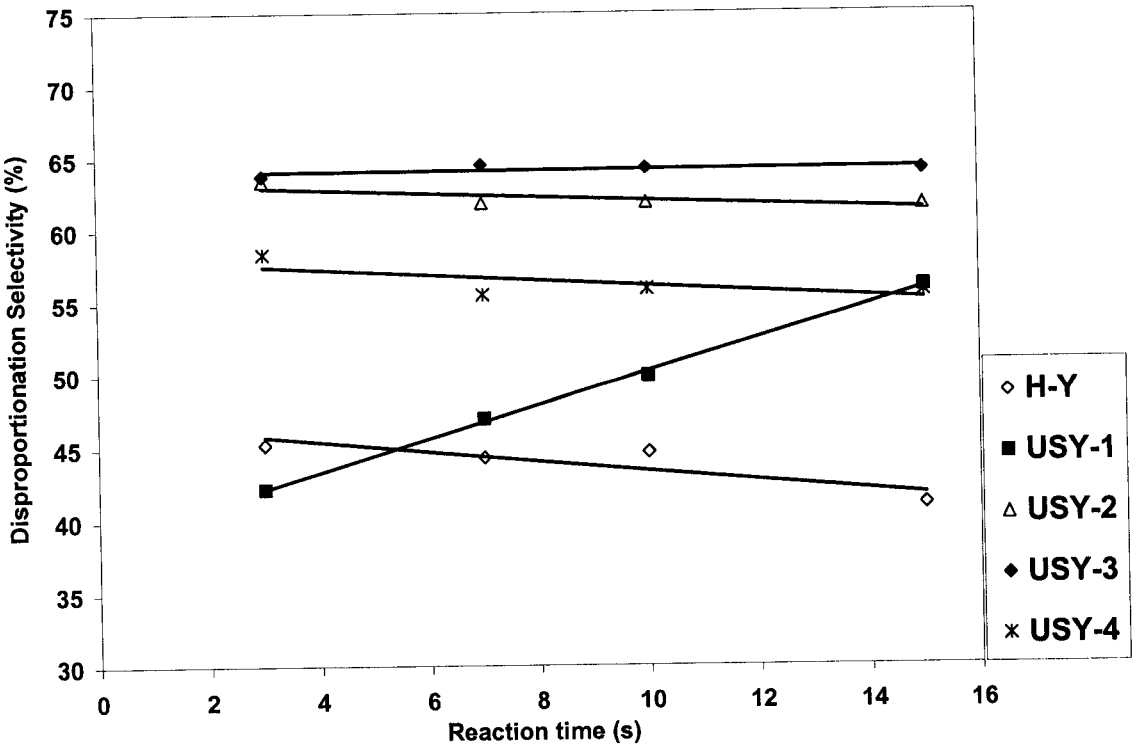

Figure 6.8 Disproportionation selectivity as a function of reaction time at 450 °C

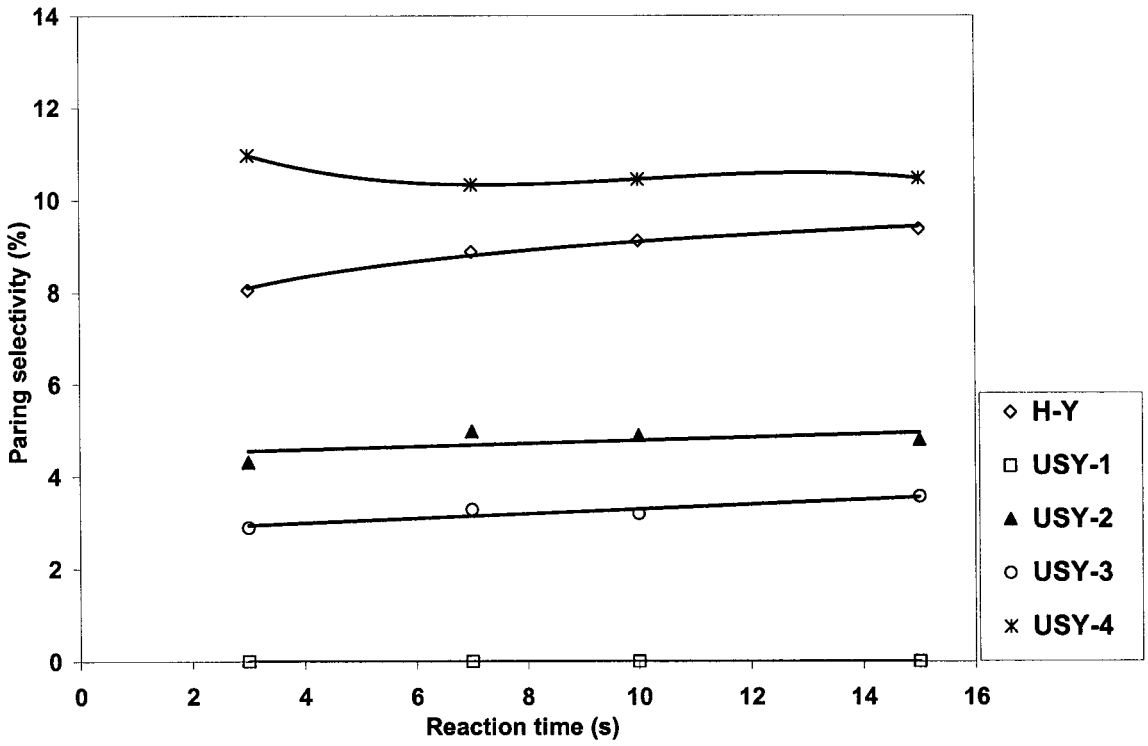

Figure 6.9 Paring selectivity as a function of reaction time at 450 °C

Furthermore, it is clear from Figure 6.8 that disproportionation selectivity increases with time over the highly dealuminated catalyst (USY-1), remains constant with partially dealuminated catalysts, and decreases with the parent H-Y catalyst. The increase in disproportionation selectively over USY-1 is consistent with the measured negligible coke deposition over this catalyst. This could be explained by fact that TMBs, which are necessary intermediates for the formation of coke precursors, did not undergo any appreciable secondary transformation over USY-1 catalyst (Table 6.1). In contrast, the observed decrease in the disproportionation selectivity with reaction time over H-Y supports earlier explanation regarding the selective deactivation of this reaction pathway.

It can be noticed that the selectivity to paring reaction differed greatly depending on the catalysts, as shown in Figure 6.9. The highest selectivity to this reaction pathway was observed over the parent H-Y catalyst, while USY-1 shows no selectivity towards paring pathway. In line with earlier discussion, the high amount of acid sites of H-Y catalyst results in its high selectivity towards paring pathway. On the other hand, the decrease in the amount of acid centers with increasing level of dealumination explains the lower selectivity of the USY zeolites toward this pathway, particularly with highly dealuminated (USY-1) catalyst, which shows no selectivity towards this reaction.

6.2.4 Influence of Temperature and Conversion

In an attempt to study the role of temperature and reaction on the different ratios, a plots of disproportionation/paring (D/Pa) and p-xylene/o-xylene (P/O) ratios are made under various conversion and temperature levels as shown in Figure 6.10 and 6.11, respectively.

Table 6.1 Coke deposited on the catalysts at various conditions

temp. °C	time (s)	total coke deposited (wt %)	
		USY-1	*H-Y*
400	3	0.044	0.63
	7	0.035	1.00
	10	0.039	1.30
	15	0.059	1.66
450	3	0.065	0.67
	7	0.051	1.17
	10	0.050	1.44
	15	0.041	1.72
500	3	0.041	0.59
	7	0.046	1.09
	10	0.075	1.35
	15	0.056	1.77

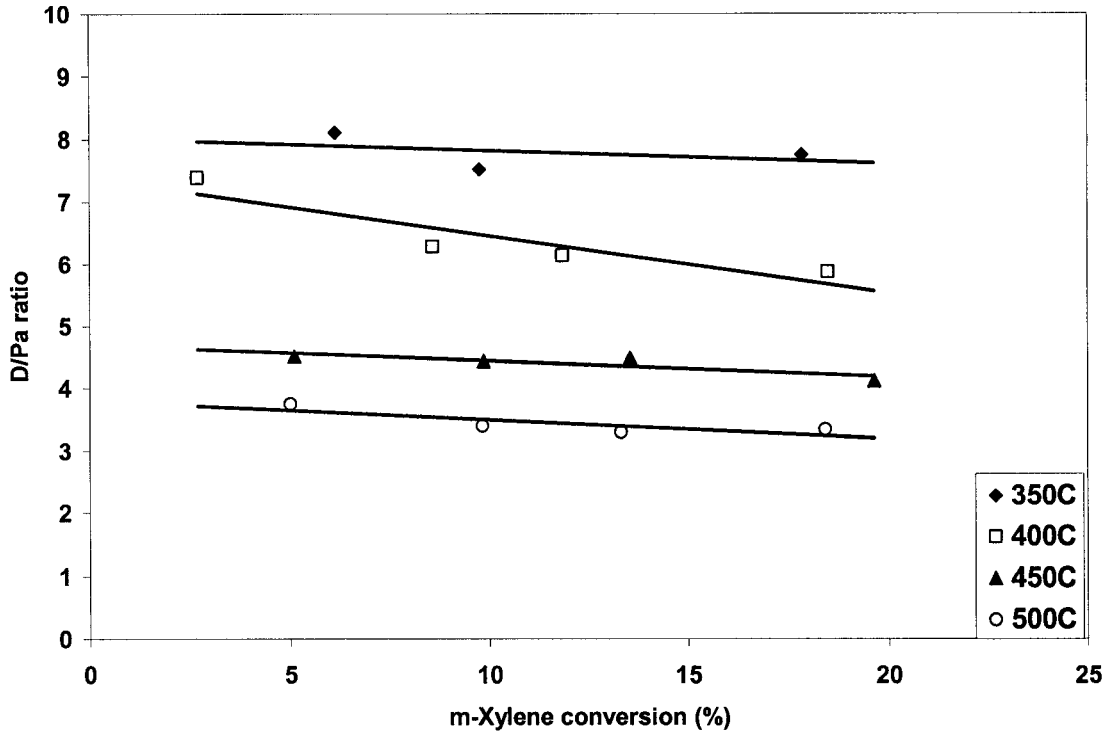

Figure 6.10 Disproportionation/paring (D/Pa) ratio as a function of m-xylene conversion over H-Y catalyst at 450 °C

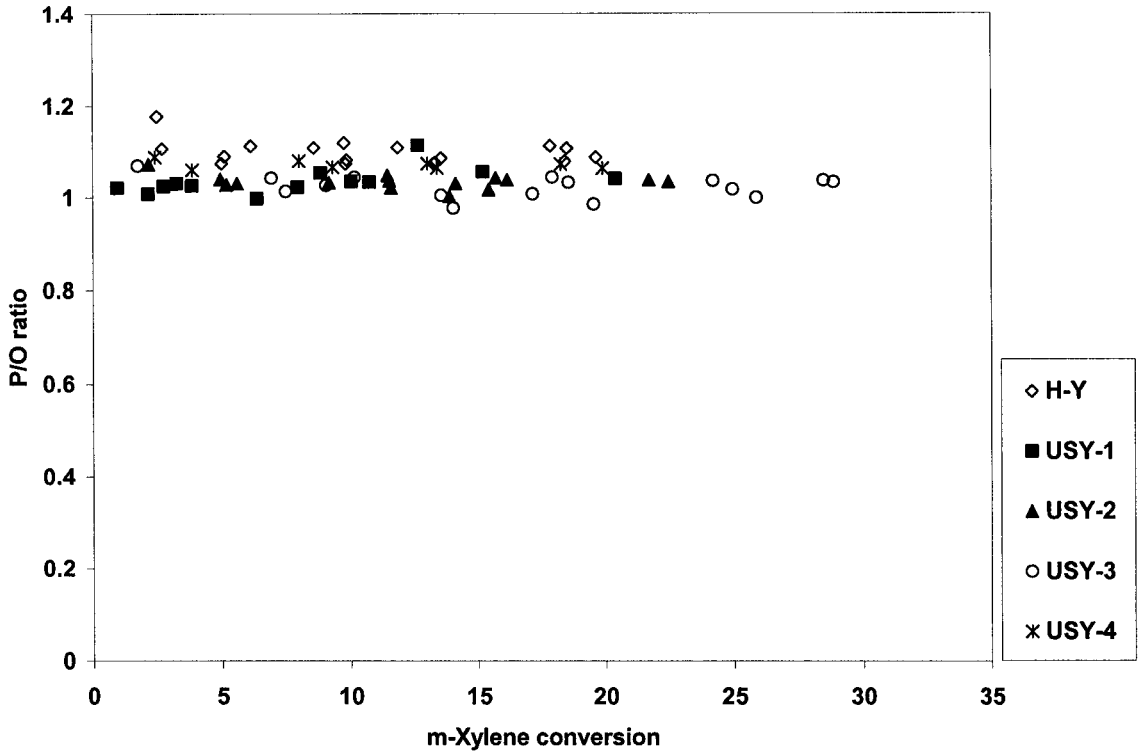

Figure 6.11 p-Xylene/o-xylene (P/O) ratio as a function of m-xylene conversion.

A significant result was obtained with regard to the variation of D/Pa ratio versus reaction temperature. As depicted in Figure 6.10, it is clear that reaction temperature has a pronounced influence on D/Pa ratio. An increase in temperature from 350 to 500 °C results in a corresponding decrease in D/Pa ratio by 80 % over the parent H-Y catalyst. A similar result was observed over the partially dealuminated catalysts (USY-2 and USY-4). This phenomenon indicates that the energy of activation is higher for paring as compared to disproportionation reaction. As a consequence, disproportionation dominates at lower temperatures, while paring at higher temperatures, as indeed found experimentally. In contrast to temperature, conversion has a negligible effect on D/Pa ratio over the catalyst examined and under the reaction conditions used.

The result presented in Figure 6.11 indicates that under the conditions of this study, all the catalysts exhibits a P/O ratio close to the thermodynamic predicted value of 1.09 [1]. This result confirmed the absence of shape selectivity over the Y zeolite used, since the pore size of this zeolite is larger than the molecular diameter of the bulky o-xylene, and thus both isomers can move freely within the pores of the zeolite.

6.2.5 Influence of Acidity

The effect acidity on P/O and D/I ratio was investigated at 2 and 10 % conversion levels, as presented in Figure 6.12. Indeed, the data presented in this figure indicate that under the conditions of this study, alteration of total acidity has no significant effect on P/O ratio. This result suggests that P/O selectivity during m-xylene transformation over large pore zeolite, such as the Y zeolite used in this work is not affected by either acid strength or acid site density. Thus, weak as well as strong acid sites should give the same

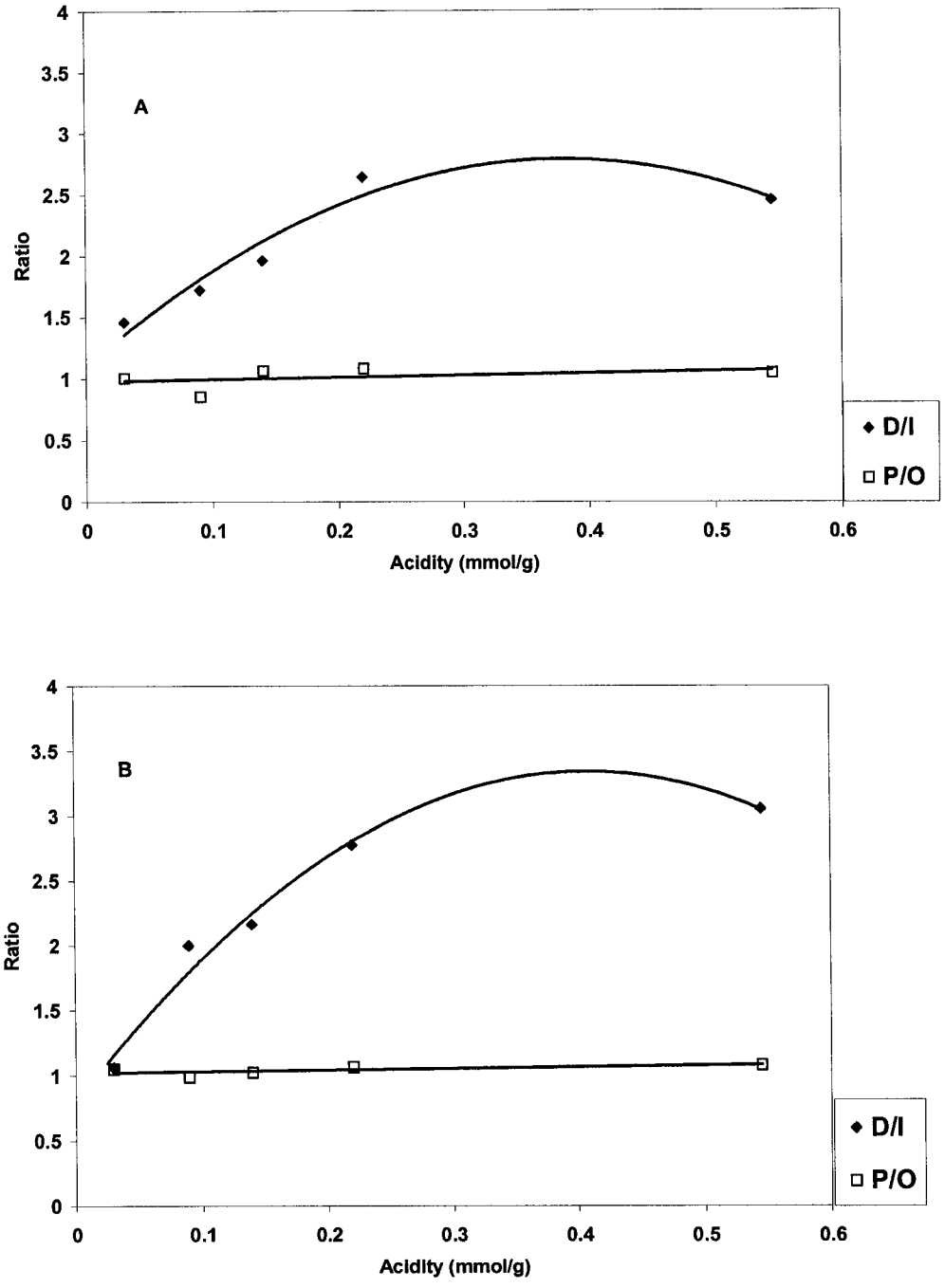

Figure 6.12 D/I and P/O ratios versus total acidity at (A) 2 %; (B) 10 % m-xylene conversions

P/O ratio. As mentioned earlier, P/O ratio is mainly a function of size of the pore channel, and as such has been used as criteria in determining the shapes and dimensions of intracrystalline cavities of zeolites [15, 16]. In contrast to P/O ratio, D/I ratio gave a volcano-shaped curve with respect to change in acidity, in agreement with earlier explanation regarding the dependence of isomerization and disproportionation reactions on acidity.

6.2.6 Coke Deposition

Zeolite deactivation during the conversion of organic compounds is mainly due to coke (carbonaceous compounds) deposition, which may cause site coverage or pore blockage. In order to study the extent of deactivation rate during m-xylene conversion, the amount of coke deposited on the parent H-Y and the highly dealuminated Y zeolite (USY-1) were measured under different reaction conditions of the present work. Both catalysts were chosen as they represent the most and least deactivated catalyst, respectively. Table 6.1 shows that carbon deposition on the as prepared H-Y catalyst is initially 15 times greater than that of USY-1 catalyst and increases by twice this value with increasing time on stream. Similarly, the amount of coke deposited on H-Y catalyst increases with reaction temperature, while temperature has a mild effect of coke deposition on USY-1 catalyst.

The more pronounced coke deposition measured over the as prepared H-Y zeolite as compared to USY-1 could be due to its stronger acid sites. It been reported that coke is formed preferentially on stronger acid sites which results in their faster deactivation rate than on weaker acid sites [7]. It is also probable that some of the expelled aluminium atoms which remain in the non framework positions following the steaming of Y zeolite

may inhibit the formation of the bulky intermediates during coke formation. Thus contributing to the low coking rate observed for the highly delaminated catalyst.

6.3 Conclusions

The transformation of m-xylene was successfully investigated over as-prepared H-Y zeolite and a series of USY zeolites dealuminated to different extent. It was found that the zeolite acidity plays an important role in the conversion, products selectivity and reaction pathways during transformation of m-xylene. The moderately dealuminated catalyst at 710 °C (USY-3) showed relatively higher activity than the parent H-Y and the other USY catalysts under the reaction condition studied. The sequence of the activity of the catalyst in the transformation of m-xylene decreases in the following order: USY-3 > USY-2 > USY-4 ≈ H-Y > USY-1. This could be explained from the difference in their framework and extraframework aluminum content and the strength and density of their acid sites.

Paring reaction is proposed as a secondary reaction pathway with m-xylene transformation over the as-prepared H-Y zeolite and the partially dealuminated catalysts. The increase in the selectivity towards paring reaction with increase zeolite acidity suggests that high concentration of strong acid sites facilitates this reaction pathway. On other hand the low concentration of acid centers in USY-1 catalyzes above all isomerization pathway. Also, the pronounced decrease in disproportionation/paring (D/Pa) ratio with reaction temperature indicates higher activation energy for paring as compared to disproportionation reaction.

The mild influence of acidity on p-xylene/o-xylene (P/O) ratio confirms earlier proposition in the literature that the pore diameter of Y zeolite is large enough, thus,

allowing the xylenes to move freely without shape selectivity. This is obvious from the obtained P/O ratio, which corresponds to the thermodynamic equilibrium value of 1.09. A higher coke deposition was measured over H-Y as compared to the USY zeolites. This again could be related to its higher concentration of strong acid sites. Moreover, the presence of extraframework aluminium species in USY zeolites may prevents the formation of the bulky coke intermediates, thus, reducing their deactivation rate.

6.4 References

[1] Molina R., Schutz A., Poncelet G., Transformation of m-Xylene over Al-Pillared clays and Ultrastable Zeolite Y. J. Catal., 145 (1994), 79.

[2] Morin, S., Gnep, N.S, Guisnet, M. A Simple Method for Determining the Relative Significant of the Unimolecular and Bimolecular Pathways of Xylene Isomerization over HY Zeolites J. Catal., 159(1996), 296.

[3] Morin, S., Ayrault, P., Gnep, N.S, Guisnet, M., Influence of the Framework Composition of Commerical HFAU Zeolites on their Activity and Selectivity in m-Xylene Transformation. Appl. Catal., 166 (1998), 281.

[4] Jones, C. W., Zones, S. I.; Davis, M. E., m-Xylene Reactions over Zeolites with Unidimensional Pore Systems. Appl. Catal., A: General, 181 (1999), 289-303.

[5] Pamin, K., Kubacka, A., Olejniczak, Z., Haber ,J., Sulikowski, B., Immobilization of Dodecatungstophosphoric acid on Dealuminated Zeolite Y: A Physicohemical Study Appl. Catal. A., 194-195 (2000), 137-146.

[6] Sulikowski, B., Datka, J., Gill, B., Ptaszynski, J., Klinowski, J., Acidity and Catalytic Properties of Realuminated Zeolite Y. J. Phys. Chem. B, 101 (1997), 6929.

[7] Yang, M.G., Nakamura, I., Fujimoto, K., m-Xylene Transformation over NiS/Al2O3-USY Hybrid Catalysts: Effects of Hydrogen Spillover. Appl. Catal. A., 144 (1996), 221-235.

[8] Laforge, S., Martin, D., Paillaud, J. L., Guisnet, M., m-Xylene Transformation over H-MCM-22 Zeolite 1. Mechanisms and Location of the Reactions. J. Catal., 220 (2003), 92-103.

[9] Stach, H., Lohse, U., Thamm, H., Schirmer, W., Adsorption Equilibria of Hydrocarbons on Highly Dealuminated Zeolites. Zeolites, 6 (1986), 74-90.

[10] Gola, A., Rebours, B., Milazzo, E., Lynch, J., Benazzi, E., Lacombe, S., Delevoye, L., Fernandez, C., Effect of Leaching Agent in the Dealumination of Stabilized Y Zeolites. Micro. Meso. Mater., 40 (2000), 73-83.

[11] Cruz, J. M., Corma, A., Fornes, V., Framework and Extra-Framework Aluminum Distribution in Diammonium Silicon Hexafluoride-Dealuminated Y Zeolites: Relevance to Cracking Catalysts. Appl. Catal., 50 (1989), 287-93.

[12] Lonyi, Ferenc., Lunsford, J. H., The Development of Strong Acidity in Hexafluorosilicate-Modified Y-type Zeolites. J. Catal., 136 (1992), 566-77.

[13] Kubelkova, L., Seidl, V., Novakova J., Bednarova S., Jiru. P., Properties of Y-type Zeolites with Various Silicon/Aluminum Ratios Obtained by Dealumination with Silicon Tetrachloride. Distribution of Aluminum and Hydroxyl Groups and Interaction with Ethanol. J. Chem. Soc. Farad. Trans. 1: Physical Chemistry in Condensed Phases, 80 (1984), 1367-76.

[14] Martens, J. A., Perez-Pariente, J., Sastre, E., Corma, A., Jacobs, P. A., Isomerization and Disproportionation of m-Xylene: Selectivities Induced by the Void Structure of the Zeolite Framework. Appl. Catal., 45 (1988), 85-101.

[15] Olson, D. H., Haag, W. O., Structure-Selectivity Relationship in Xylene Isomerization and Selective Toluene Disproportionation. ACS Symp. Ser., 248 (1984), 275-307.

[16] Kaeding, W.W., Che, C., Young, L.B., Weinstein, B., Butter, S.A., Shape Selective Reactions with Zeolite Catalysts II. Selective Disproportionation of Toluene to Produce Benzene and P-xylen. J. Catal., 69 (1981), 392.

[17] Jones, C. W., Zones, S. I., Davis, M. E., m-Xylene Reactions over Zeolites with Unidimensional Pore Systems. Appl. Catal., A: General 181 (1999), 289-303.

[18] Morin, S., Gnep, N.S., Guisnet, M., Influence of Coke Deposits on the Selectivity of m-Xylene Transformation and on the Isomerization Mechanism. Appl. Catal. A.: General 168 (1998), 63.

[19 Sullivan, R. F., Egan, C. J., Langlois, G. E., Sieg, R. P., Hydrocracking of Aromatic Hydrocarbons. J. Am. Chem. Soc. 83 (1961), 1156-60.

[20] Roger, H. P., Bohringer, W., Moller, K. P., O'Connor, C. T. Rediscovery of the Paring Reaction: the Conversion of 1,2,4-trimethylbenzene over HZSM5 at Elevated Temperature. Stud.Surf. Sci. Catal., 130A (International Congress on

Catalysis, 2000, Pt. A), 281-286.

[21] Arroyo, J. A., Thybaut, J. W., Marin, G. B., Jacobs, P. A., Martens, J. A., Baron, G. V., Reaction Pathways of 1-Cyclohexyloctane in Admixture with Dodecane on Pt/H-ZSM-22 Zeolite in Three-Phase Hydroconversion. J. Catal., 198 (2001), 29-40.

[22] de Lasa, H.I. U.S. Patent 5, 102 ,628, (1991).

[23] Iliyas A., Al-Khattaf S., Xylene Isomerization over USY Zeolite in a Riser Simulator: A Comprehensive Kinetic Model. Ind. Eng. Chem. Res., 43 (2004), 1349.

[24] Al-Khattaf, S, de Lasa, H.I., Diffuision and Catalytic Cracking of 1,3,5 tri-iso-propyl-benzene in FCC Catalysts. Chem. Eng. Sc., 57 (2002), 4909.

[25] Al-Khattaf, S., de Lasa, H.I., The Role of Difusión in Alkyl-benzenes Catalytic Cracking. Appl. Catal. A, 226 (2002), 139.

[26] Al-Khattaf, S., The Influence of Y-Zeolite Unit Cell Size on the Performance of FCC Catalysts During Gas Oil Catalytic Cracking. Appl. Catal. A: General, 231 (2002), 293.

[27] Al-Khattaf, S., de Lasa, H.I., Diffusion and Reactivity of Hydrocarbon Feedstocks in FCC Catalysts. Can. J. Chem. Eng. 79 (2001), 329.

[28] Kraemer, D. W. Ph.D. Dissertation, University of Western Ontario, London, Canada (1991).

[29] Tsai, T., Liu, S., Wang, I., Disproportionation and Transalkylation of Alkylbezenes over Zeolite Catalysts. Appl. Catal., A: General 181 (1991), 355.

CHAPTER 7

7 Conclusions and Recommendations

7.1 Conclusions

The kinetics of vapor-phase isomerization of xylenes has been successfully carried out over a USY zeolite catalyst using a fluidized-bed reactor. A new fitting procedure has been developed to obtain the numerous kinetic parameters of the xylene transformations. This procedure involves using simplified, effective kinetic models based on the isomerization of the pure xylene. The developed method is used with the well-known time on stream and reactant converted decay models. In each case, the lower values of estimated pre-exponential factors and the higher activation energies confirm that the mutual interconversion between p- and o-xylene occurs with great difficulties. A good comparison between the experimental data and model predictions is obtained. This provides significant evidence that the riser simulator and the developed modeling technique can be used as an effective tool in investigating the kinetics of xylene isomerization and disproportionation reactions.

Experimental studies are conducted in a riser simulator to study the influence of reaction parameters on xylene transformation. Initial selectivity revealed that both isomerization and disproportionation of xylenes advance as primary reactions. A higher

initial value of toluene/trimethylbenzenes (T/TMBs) mole ratio is observed with the three xylene reactants, and this could be explained by the slower desorption rate of bulky TMBs isomers under the short reaction time of the riser simulator. p-Xylene was found to be more reactive than the others xylene isomers. This is explained by the higher accessibility of proton to C_4 atom, due to its least effect of steric hindrance.

The transformation of m-xylene is successfully investigated over as-prepared H-Y zeolite and a series of USY zeolites dealuminated to different extent. It is found that the zeolite acidity plays an important role in the conversion, products selectivity and reaction pathways during transformation of m-xylene. The moderately dealuminated catalyst at 710 ^{o}C (USY-3) showed relatively higher activity than the parent H-Y and the other USY catalysts under the reaction condition studied. The sequence of the activity of the catalyst in the transformation of m-xylene decreases in the following order: USY-3 > USY-2 >USY-4 $\approx$ H-Y > USY-1.This could be explained from the difference in their framework and extraframework aluminum content and the strength and density of their acid sites.

Paring reaction is proposed as a secondary reaction pathway with m-xylene transformation over the as-prepared H-Y zeolite and the partially dealuminated catalysts. The increase in the selectivity towards paring reaction with increase zeolite acidity suggests that high concentration of strong acid sites facilitates this reaction pathway. On other hand the low concentration of acid centers in USY-1 catalyzes above all isomerization pathway. Also, the pronounced decrease in disproportionation/paring (D/Pa) ratio with reaction temperature indicates higher activation energy for paring as compared to disproportionation reaction.

The mild influence of acidity on p-xylene/o-xylene (P/O) ratio confirms earlier proposition in the literature that the pore diameter of Y zeolite is large enough, thus, allowing the xylenes to move freely without shape selectivity. This is obvious from the obtained P/O ratio, which corresponds to the thermodynamic equilibrium value of 1.09. A higher coke deposition was measured over H-Y as compared to the USY zeolites. This again could be related to its higher concentration of strong acid sites. Moreover, the presence of extraframework aluminium species in USY zeolites may prevents the formation of the bulky coke intermediates, thus, reducing their deactivation rate.

7.2 Recommendations

The work presented in this thesis is based mainly on Y zeolites, since they are used as fluid catalytic cracking catalysts, which are the best choice to meet the objectives of the study. However, it is well-known that ZSM-5 zeolite gives a higher selectivity of the most valuable xylene isomer (p-xylene). In this regard, it is recommended that a similar study is performed over ZSM-5 catalyst. Investigating the transformation of xylenes over ZSM-5 zeolite while utilizing the short contact time strategy of the riser simulator will even be a more interesting research exercise. This is because it is envisaged that short reaction time peculiar to the riser unit will prevent the secondary isomerization of the produced p-xylene, thus increase p-xylene selectivity.

The selective deactivation of the external surface of ZSM-5 zeolite by treatment with bulky molecules e.g. 1,3,5 triisopropylbenzene can also be carried out. This technique may improve the selectivity of p-xylene based on the reason given above. Moreover, metal could be dispersed on ZSM-5 to minimize the selectivity to undesired reactions e.g. disproportionation.

The kinetics of xylene transformation over ZSM-5 catalysts could be studied in the riser simulator, since this has not reported in the open literature. However, as intercrystalline diffusion limitation is unavoidable over this zeolite due to its smaller channel opening than some xylene isomers, it is highly recommended that the intrinsic kinetic parameters should be estimated, instead of apparent kinetic parameters. In this regard, adsorption, diffusion, and reaction should be considered in the kinetic model.

NOMENCLATURE

C_i	concentration of species *i*, (kmole/m^3)
CFL	confidence limit
C_d	concentration of disproportionation products (*T* + *TMBs*) (kmole/m^3)
E_i	apparent activation energy for the i^{th} reaction (kJ/mole)
K_{om}	thermodynamic equilibrium constant for the conversion of *m*- to *o*-xylene
k_i	apparent rate constant for the i^{th} reaction (m^3/ kg of catalyst·s)
k_{oi}	pre-exponential factor for the i^{th} reaction (m^3/ kg of catalyst·s)
K_{pm}	thermodynamic equilibrium constant for the conversion of *m*- to *p*-xylene
MW_i	molecular weight of species *i* (kg/kmole)
r	correlation coefficient
R	universal gas constant (kJ/kmole K)
t	reaction time (s)
T	toluene
T_o	average temperature of the experiment
TMBs	trimethylbenzenes
V	riser simulator volume
W_c	catalyst mass (kg of catalyst)
W_{hc}	mass of hydrocarbon injected into the riser simulator
y_d	mass fraction of disproportionation products
φ	apparent deactivation function
λ	catalyst deactivation constant for RC model
α	catalyst deactivation constant for TOS model
subscript	
m	meta-xylene
o	ortho-xylene
p	para-xylene

VITA

Name:	**AbdulJelil Iliyas**
Nationality:	**Nigerian**
Date of Birth:	**11th October, 1977**
Place of Birth:	**Zaria, Nigeria**
Education:	**B. Eng. Chemical Engineering from Ahmadu Bello University, Zaria, Nigeria. November, 2000.**
	M.S. Chemical Engineering from King Fahd University of Petroleum & Minerals, Dhahran, Saudi Arabia. May, 2004